NASA CR 72891
Report MDC Q0446
May 1971

Cathode Studies of a Radiation Cooled MPD Arc Thruster

J.C. Kroutil
D.W. Esker
A.V. Sedrick

Prepared for
National Aeronautics and Space Administration
NASA Lewis Research Center
Contract NAS3-13664

MCDONNELL DOUGLAS RESEARCH LABORATORIES

MCDONNELL DOUGLAS CORPORATION

This report was prepared as an account of Government sponsored work. Neither the United States, nor the National Aeronautics and Space Administration (NASA), nor any person acting on behalf of NASA:

A.) Makes any warranty or representation, expressed or implied, with respect to the accuracy, completeness, or usefulness of the information contained in this report, or that the use of any information, apparatus, method, or process disclosed in this report may not infringe privately owned rights; or

B.) Assumes any liabilities with respect to the use of, or for damages resulting from the use of any information, apparatus, method or process disclosed in this report.

As used above, "person acting on behalf of NASA" includes any employee or contractor of NASA, or employee of such contractor, to the extent that such employee or contractor of NASA, or employee of such contractor prepares, disseminates, or provides access to, any information pursuant to his employment or contract with NASA, or his employment with such contractor.

Requests for copies of this report
should be referred to:

National Aeronautics and Space Administration
Scientific and Technical Information Facility
P.O. Box 33
College Park, Maryland 20740
Attn: NASA Representative RQT-2448

NASA CR 72891
Report MDC Q0446
May 1971
Copy No. 82

Cathode Studies of a Radiation Cooled MPD Arc Thruster

by

J.C. Kroutil, D.W. Esker and A.V. Sedrick

Flight Sciences Department
McDonnell Douglas Research Laboratories
McDonnell Douglas Corporation
St. Louis, Missouri 63166

Prepared for
National Aeronautics and Space Administration
May 1971
Contract NAS3-13664

Technical Management
NASA Lewis Research Center
Cleveland, Ohio 44135
Electromagnetic Propulsion Division
D.J. Connolly, Project Manager

Foreword

The work described in this report was performed by McDonnell Douglas Corporation under Contract NAS3-13664 for the Lewis Research Center of the National Aeronautics and Space Administration. The contract period was January 6, 1970 through February 19, 1971. Dr. D.J. Connolly of NASA was Project Manager for the program.

The principal investigator was D.W. Esker and Messers. J.C. Kroutil and A.V. Sedrick were coinvestigators. The work as accomplished in the Flight Sciences Department.

Other personnel who contributed to the program were N.L. Vignati and E.E. Fischer.

Contents

Abstract

There were 137 cathode-insulator modifications of the McDonnell Douglas Corporation (MDC) X-7 radiation cooled MPD arc thruster tested in a power range of 9.8 to 46.4 kW using ammonia as the principal propellant. Thrust performance was obtained with arc currents from 200 to 800 A, magnetic fields from 0.06 to 0.173 tesla, and mass flow rates from 4.6 to 102 mg/sec. The resulting specific impulses ranged from 472 to 11,426 sec with thrust efficiencies ranging from 4.2 to 86.7%. Specific impulse values above 10,000 sec could only be maintained for short periods, and in some cases could not be reproduced.

In addition to ammonia, the following propellants were tested: argon-ammonia, nitrogen, nitrogen-hydrogen, helium, neon, and xenon.

Summary

This report describes the design modifications, performance and duration testing of the MDC X-7 arc thruster. There were 137 tests made of various cathode-insulator configurations with ammonia as propellant. The modifications consisted of varying the cathode and insulator geometry with the intent to control the arc attachment at the cathode. The best performing configuration was tested further (25 tests) with argon, nitrogen, nitrogen-hydrogen, helium, neon, and xenon propellants.

Parametric test plan

Solid conical, hollow (with and without flow through the cathode hollow section) and buffered cathodes of both solid conical and hollow configuration were investigated. A special triple cathode configuration was tested in an effort to increase the total arc current.

The interelectrode insulator geometry was varied to remove the insulator from the high temperature region of the arc discharge to reduce insulator erosion.

Various propellant feed arrangements were studied with flow control through and around the cathode. The ratio of flow rates was controlled by two separate feed systems. Addition of propellant flow around the hollow cathode usually caused the arc attachment to move from the cavity to the outside diameter of the cathode. Addition of argon to the flow of ammonia through the hollow cathode aided inner arc attachment; however, a 75% volume concentration of argon was required.

Tests of modifications

There were 137 cathode-insulator assembly modifications of the X-7 thruster tested and evaluated. Most of the tests were made with a nozzle throat diameter of 1.778 cm and a few tests with 2.54 and 3.175 cm throats. Arc current levels up to 800 A were tested, and the arc input power ranged from 9.8 to 46.4 kW. An independently controlled magnetic field was varied from 0.06 to 0.173 tesla. The propellant flow rate was varied from 4.6 to 102 mg/sec. The test chamber background pressure was maintained at less than 0.015 Torr for all tests.

Evaluation of the modifications was based mainly on thrust performance measurements. Motion pictures of the cathode-insulator region during operation were taken to aid the understanding and evaluation of performance. The thrust performance measurements obtained from these tests resulted in a specific impulse range of 472 to 11,426 sec with thrust efficiencies ranging from 4.2 to 86.7%.

The configuration showing the best performance was the HC9-A cathode. This cathode was tested more thoroughly in three 10-hour runs. Further tests were conducted with the following propellants:

nitrogen, nitrogen-hydrogen, helium, neon, and xenon.

Two independently controlled propellant feed systems were used so that the flow through and around the cathode could be varied. Addition of secondary flow around the cathode was detrimental in that generally it caused a gross instability.

Delivery of hardware

Ten cathode-insulator assemblies, five anode-radiation flange assemblies, and two complete MDC X-7 radiation cooled MPD thruster assemblies with magnets were delivered to the Lewis Research Center during the contract period.

1 Introduction

The purpose of this investigation was the modification and improvement of the MDC X-7 radiation cooled magnetoplasmadynamic thruster to better understand and control the current attachment. This thruster (Fig. 1.1) was developed by MDC previously under NASA Contract NAS3-11518. Section 2.1 gives a description of the X-7 thruster. The X-7 thruster was operated continuously for a period of over 500 hours, with an arc power input of about 32 kW.

During the development testing of the X-7 thruster and especially over the 500 hour lifetest, it became apparent that improvements, performance and reliability were closely related to the location of arc attachment on the cathode electrode. Thruster operation in several voltage modes at constant current was clearly identified with different distributions of current attachment. The high voltage mode was associated with current attachment at a small area on the tip of the cathode. The thruster operated with low erosion and high voltage but with low efficiency. In the low voltage mode, the current attached near the base of the cylindrical region of the conical cathode. The erosion in this mode was high since the insulator was close to the high temperature discharge. Thruster performance was highest in the low voltage mode.

The cathode was found to be a critical component of the thruster. Basically three modification and improvement schemes were investigated. The principal scheme used was the modification of the cathode-insulator geometry.

Previous studies by Burkhart[1] of NASA suggest that voltage mode control can be obtained by the relative amount of propellant fed through the center and around the outside of the cathode; hence at MDC dual flow was investigated. In addition to ammonia as the principal propellant, nitrogen, nitrogen-hydrogen mix, helium, neon, and xenon propellants were investigated.

The various modifications were judged on the basis of their thrust performance, as well as on the basis of their ability to operate for extended periods without changing the voltage-current, efficiency, and specific impulse characteristics. Direct visualization and motion pictures were also used as performance monitors.

1.1 Objective

The general objective of this study was the modification of the cathode-insulator assembly to control cathode attachment of the current, and erosion of the thruster insulator and cathode. The work was accomplished in three basic tasks:

(a) **Plan parametric tests and design the necessary hardware** – A systematic procedure was established for making a parametric study of the cathode arc attachment and thruster voltage modes. The best means of controlling the arc attachment was determined. Then the optimum current attach-

ment pattern for performance and thruster life was determined. The parametric study included variation of the following areas: cathode and insulator geometry, propellant feed arrangement, and propellants.

(b) **Fabricate the necessary hardware and perform the tests** – Each cathode-insulator assembly modification was tested and evaluated. The most promising configuration of the first tests was tested more thoroughly in three 10-hour tests. The primary propellant was ammonia. The most promising configuration also was tested on nitrogen, neon, and xenon propellants. The tests were conducted in a vacuum facility at a pressure of < 0.025 Torr. Performance data and current attachment data were recorded for each test. The mode of operation and its stability were also noted.

(c) **Fabricate and deliver hardware to the NASA Lewis Research Center (LRC)** – Ten cathode-insulator assemblies of the configuration selected by the LRC Project Manager, and two complete thrusters including water-cooled magnets were delivered to NASA Lewis Research Center. The thrusters were of the X-7 design except that the cathode-insulator assemblies were those developed under this contract and specified by the LRC Project Manager from among those tested. Delivery was made before 19 February 1971. Five anode-radiation flange assemblies were also fabricated without any addition in cost and shipped on 7 May 1971.

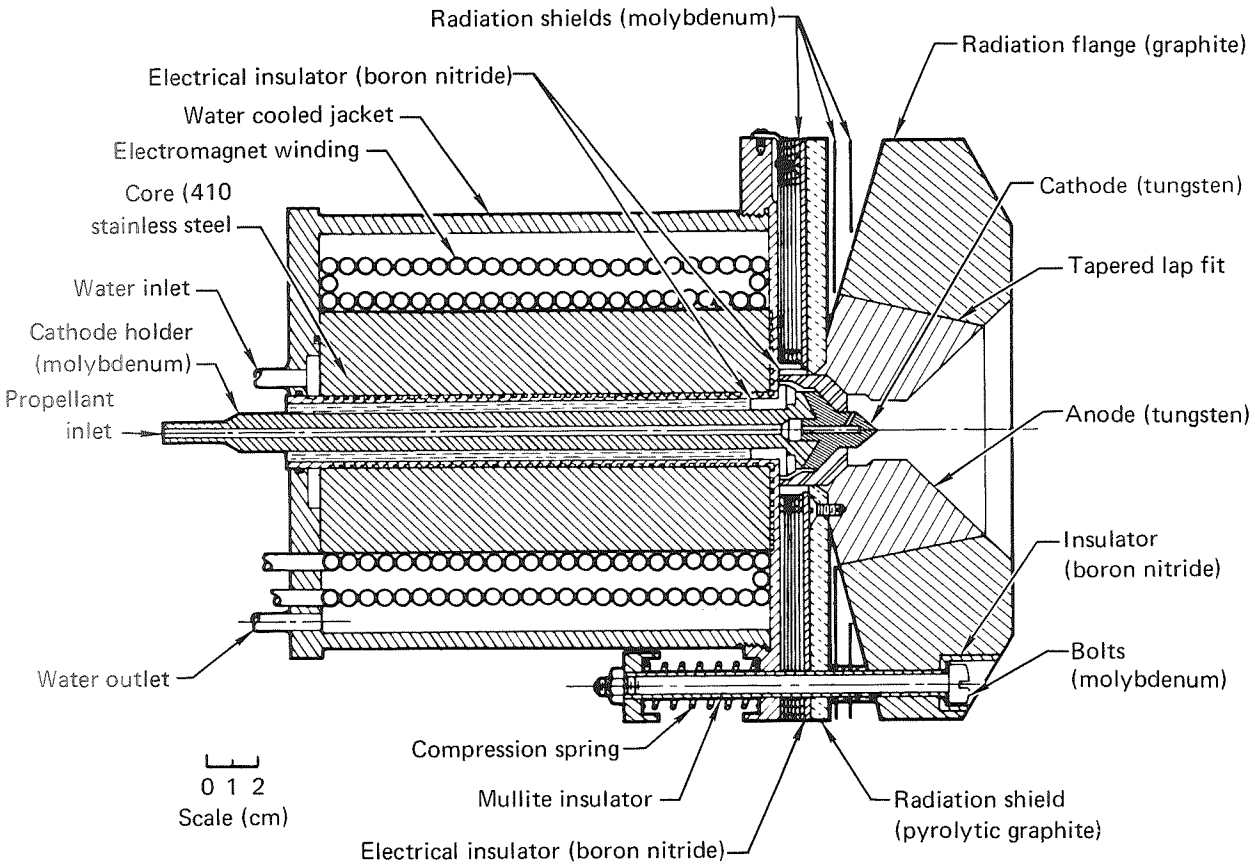

Fig. 1.1 MDC X-7 thruster

2 Experimental apparatus

All experiments were performed in a 0.91 m diam, 4.0 m long vacuum chamber. Background pressure was a function of mass flow, with a typical value of 10^{-2} Torr with an ammonia flow rate of 0.040 g/sec, as measured with a vacuum gauge (NRC Alphatron Model 520).

The operating parameters for any given design were within the following ranges:

Propellant mass flow rate	4 to 102 mg/sec
Arc current	200 to 800 A
External magnetic field at the cathode tip	0.06 to 0.173 tesla
Arc input power	9.8 to 46 kW

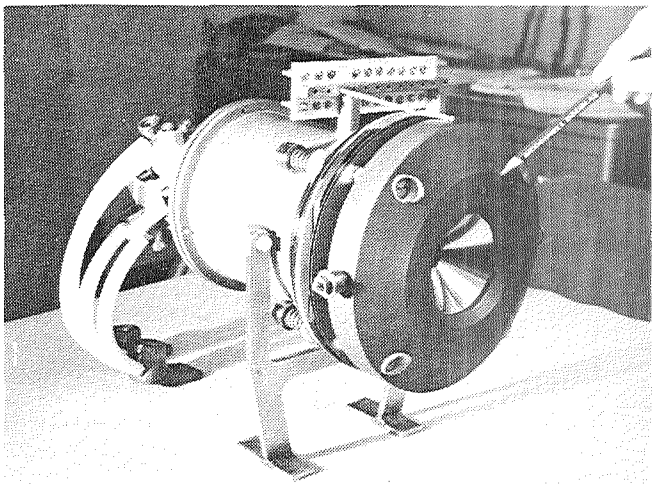

Fig. 2.1 X-7 Thruster assembled

2.1 Thruster configuration

The thruster used in this study was the MDC X-7, developed under Contract NAS3-11518. Its design and operating characteristics are reported in Ref. 2.

The X-7 thruster is a radiation-cooled device capable of steady state operation at 40 kW of input power. The cross section of the X-7 thruster with the water-cooled magnet is shown in Fig. 1.1. Figure 2.1 is a photograph of the same device.

The anode structure consists of an inner 2% thoriated tungsten annulus surrounded by a graphite radiation flange. The interface contact between the tungsten and graphite was made by a spring loaded, lapped taper joint. The cathode was a 1 cm diam pointed rod about 2.5 cm long, and was made of 2% thoriated tungsten. The upstream end had two lapped surfaces, which provided the gas seals between the boron nitride electrical insulator and the cathode, and between the molybdenum cathode holder and the cathode. A water-cooled electromagnet with a magnetic stainless steel core was used to stimulate a permanent magnet field distribution. The magnet was located at the rear and concentric with the anode assembly. Radiation shields were interposed in the magnet and the anode assembly to reduce the heat transfer to the magnet to approximately 100 W at 40 kW of arc power.

2.2 Thrust measurement

Thrust measurements were obtained by a single pendulum thrust stand. This stand, shown schematically in Fig. 2.2, has a pendulum 1.78 m in length and is suspended by two thin stainless steel flexures. Cooling water and propellant lines are brought through the top of the stand by rubber hoses. Electrical power for the thruster and magnet is connected to the stand by mercury pots and is brought to the thruster through coaxial bus bars. Power is supplied by four 60 kW welding rectifiers (Miller Model SR-1500-F1). The pendulum bar and mounting plate are water-cooled to reduce thermal drift. Deflection of the pendulum is determined by a LVDT (Daytronic DF 160) and the output is indicated on a strip chart recorder (Honeywell Electronik 16). A calibration of thrust as a function of deflection is obtained by a pulley and known weight arrangement. A thrust "killer" or flow deflection bucket is attached to the stand and can be swung in front of the thruster to turn the exhaust flow 90 deg from the thrust direction. Thrust was measured by blocking the exhaust with the "killer" for a period of 10 to 15 sec and recording the change in deflection of the pendulum. Use of the "killer" technique has been previously reported[3] and is particularly useful for radiation-cooled thruster work where thermal drift of the stand is usually encountered.

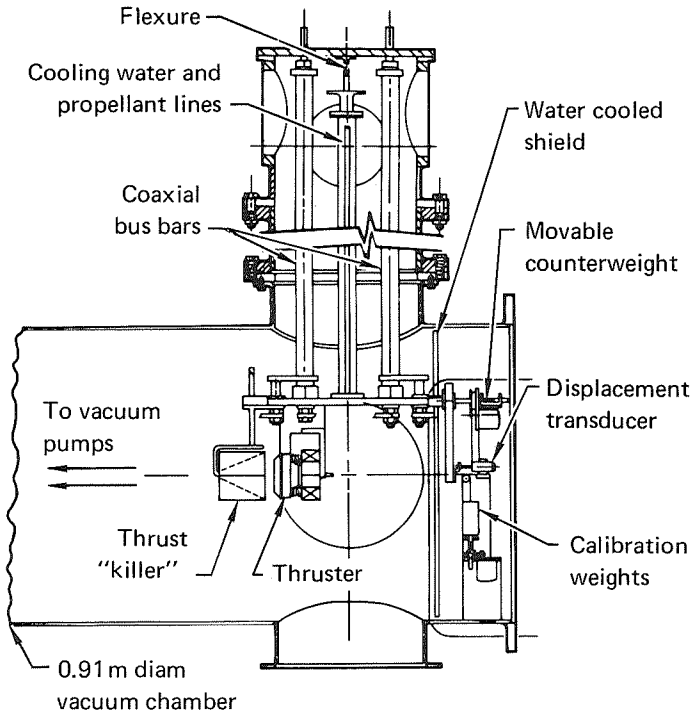

Fig. 2.2 | Thrust stand

2.3 Thruster Measurements

Current and voltage to the thruster and magnet were measured by standard dc current shunts and a voltmeter (Weston Model 901). Propellant mass flow rates were measured by sonic flow nozzles. Magnetic field measurements were made using a Bell 240 incremental gaussmeter with an A2401 probe.

Experimental measurements of thrust, arc current, voltage, and propellant mass flow rate were used to determine the specific impulse and thrust efficiency from Eqs. (2.1) and (2.2).

$$I_{sp} = \frac{T}{\dot{m}\, g} \quad , \tag{2.1}$$

$$\eta = \frac{T^2}{2\dot{m}\, P_a} \quad , \tag{2.2}$$

where T = thrust,
P_a = arc power,
$\dot{m}$ = mass flow rate, and
g = acceleration of gravity.

2.4 Cathode photography

Motion picture photography was used to record the current attachment on the various cathodes during operation. The motion pictures were taken with a 16 mm Hy-Cam rotating prism camera (Model K2S20E) which provided high resolution, full frame pictures. The camera has a speed range of 12 to 5000 pictures per second. A speed of 24 pictures per second was used during all tests. Figure 2.3 is a schematic of the vacuum chamber and shows the camera location. This camera location gave the maximum visibility of all cathode-insulator configurations. The cathode of the buffered configuration could not be seen from the side window.

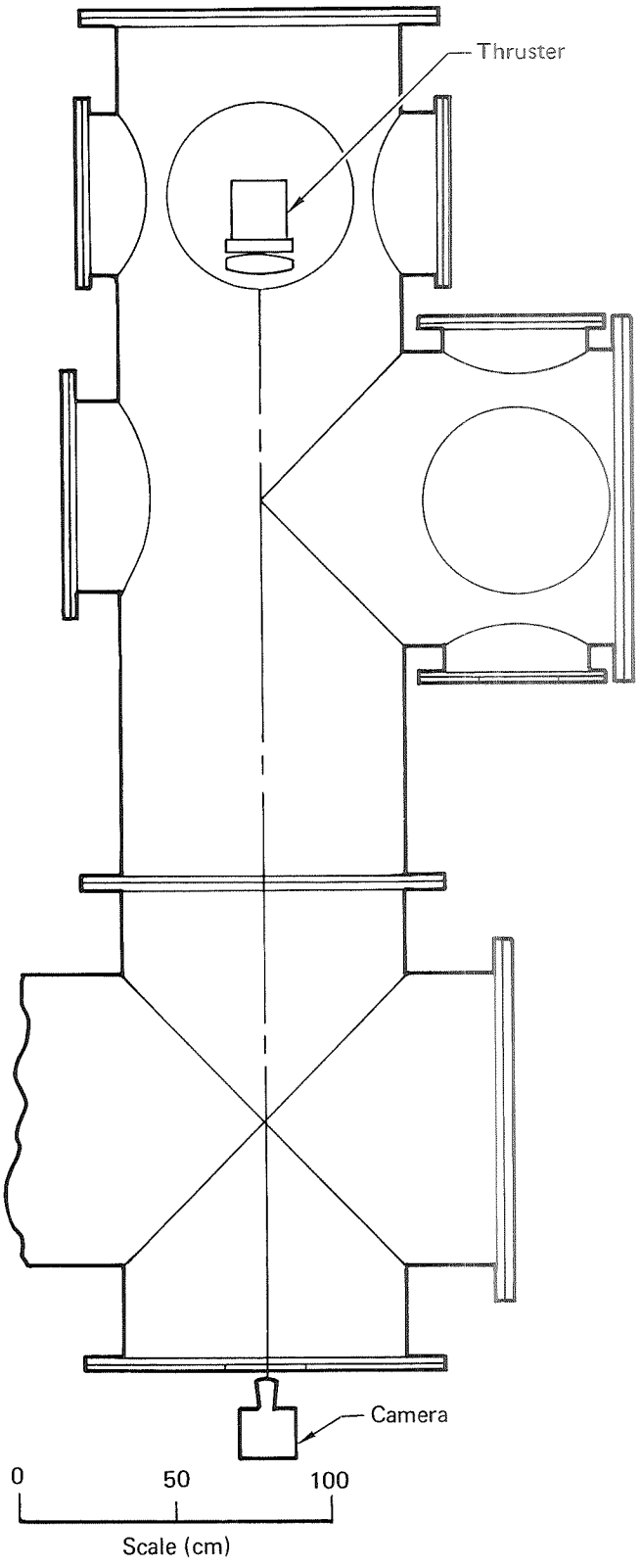

Fig. 2.3 Camera location for cathode-insulator study

3 Parametric test plan

The objective of this phase of the work was to determine the best method for controlling the arc attachment, and then, using this method, to determine the attachment pattern for optimum performance and thruster life. To accomplish this objective, the test plan was divided into three areas, i.e., cathode-insulator geometry, propellant feed arrangement, and propellants.

3.1 Cathode-insulator geometry

Systematic tests were devised to determine the optimum cathode configuration for the MDC X-7 radiation-cooled MPD arc thruster. The shape of the cathode was varied over a wide range to determine its effect on current attachment. The electrode insulator geometry was varied in an effort to eliminate the boron nitride insulator from the highest temperature region.

The following cathode geometries were investigated: solid conical (Fig. 3.1), hollow conical (with and without flow through the hollow section) (Fig. 3.2), buffered solid conical (Fig. 3.3) and the triple cathode (Fig. 3.4). The left column of Table 3.1 shows the original test plan. The right column shows the actual variations tested under the original test plan. The conical tips had an included angle of 90 deg, and are shown in Fig. 3.5a through 3.5c. The axial position of several cathodes was evaluated to determine its effect on the performance. The axial position or gap length (L_g) used throughout this report is the distance from the far downstream part of the cathode to the intersection of a 1.778 cm throat diameter with the diverging section of the anode. The gap length (L_g) is shown in Fig. 3.1. The hole diameters through the hollow cathode were varied.

Variation of the electrode insulator geometry was studied for two reasons: to control the arc attachment and to reduce or eliminate insulator erosion. Several of the electrode insulator geometries tested are shown in Fig. 3.6.

To remove the interelectrode insulator from the high temperature region of the discharge and thereby reduce insulator erosion, a second hollow cathode configuration was studied. This geometry is shown in Fig. 3.7. The anode throat diameter used with this cathode was increased to 2.54 cm.

A possible method of obtaining high arc voltages is the use of a buffer as shown in Fig. 3.3. The buffer ensures high gas pressures at the cathode tip, which results in high arc voltages. The buffer was located in a high heat flux region; thus provisions were required for radiation cooling to maintain the buffer below its melting temperature. A disadvantage of adding the buffer is a 2.5 kg increase of weight.

A possible method of increasing current levels was tested through the use of a triple cathode configuration shown in Fig. 3.4. Three individual cathodes, powered by separate power supplies, with common anode connections, were situated radially about the thruster centerline and enclosed by a single buffer. The buffer holes and cathode tips were arranged so that a virtual single cathode would be approximated at a distance of 1 cm downstream of the face of the assembly.

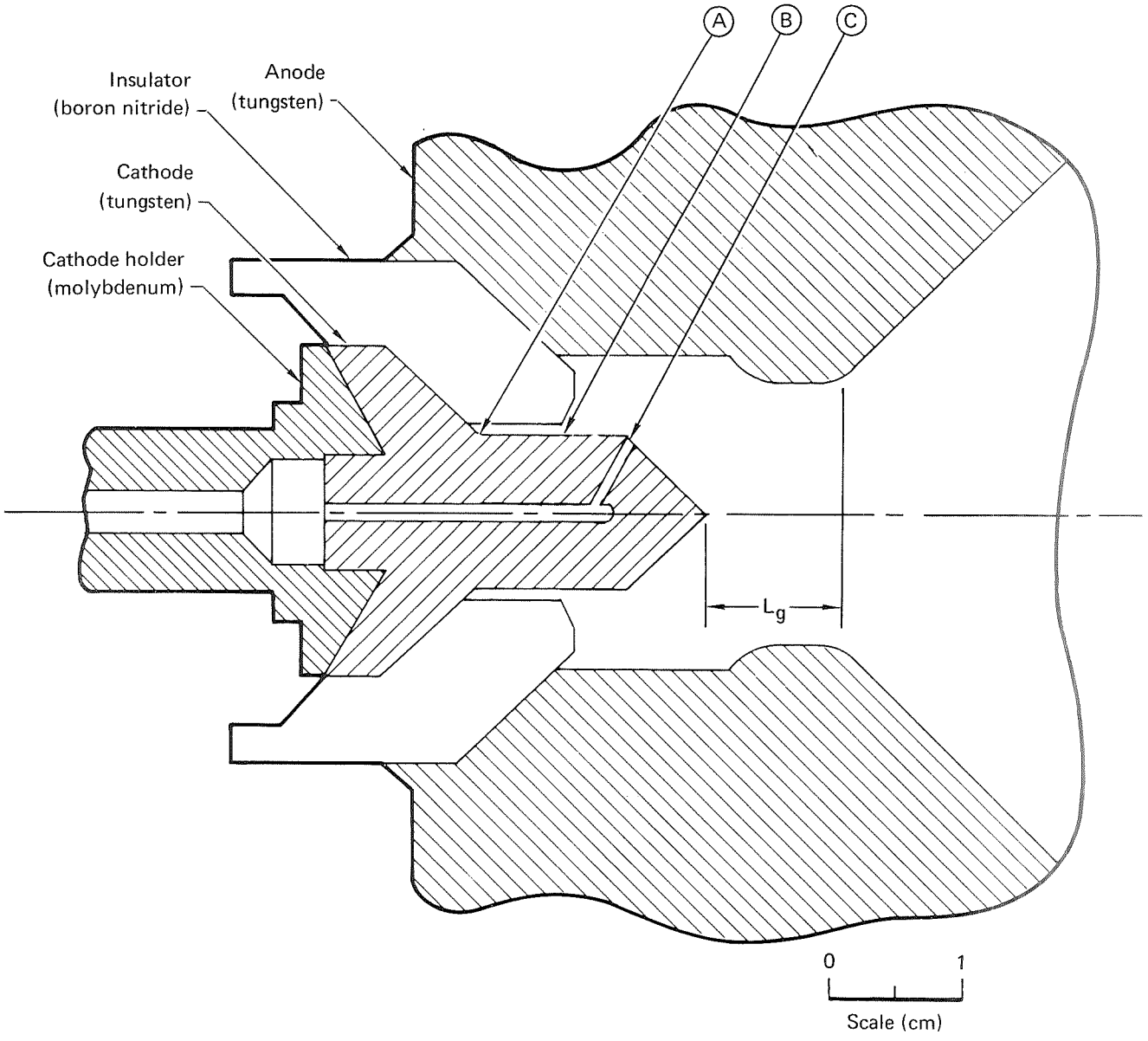

Fig. 3.1 MDC X-7 thruster cathode-insulator assembly (solid conical cathode)

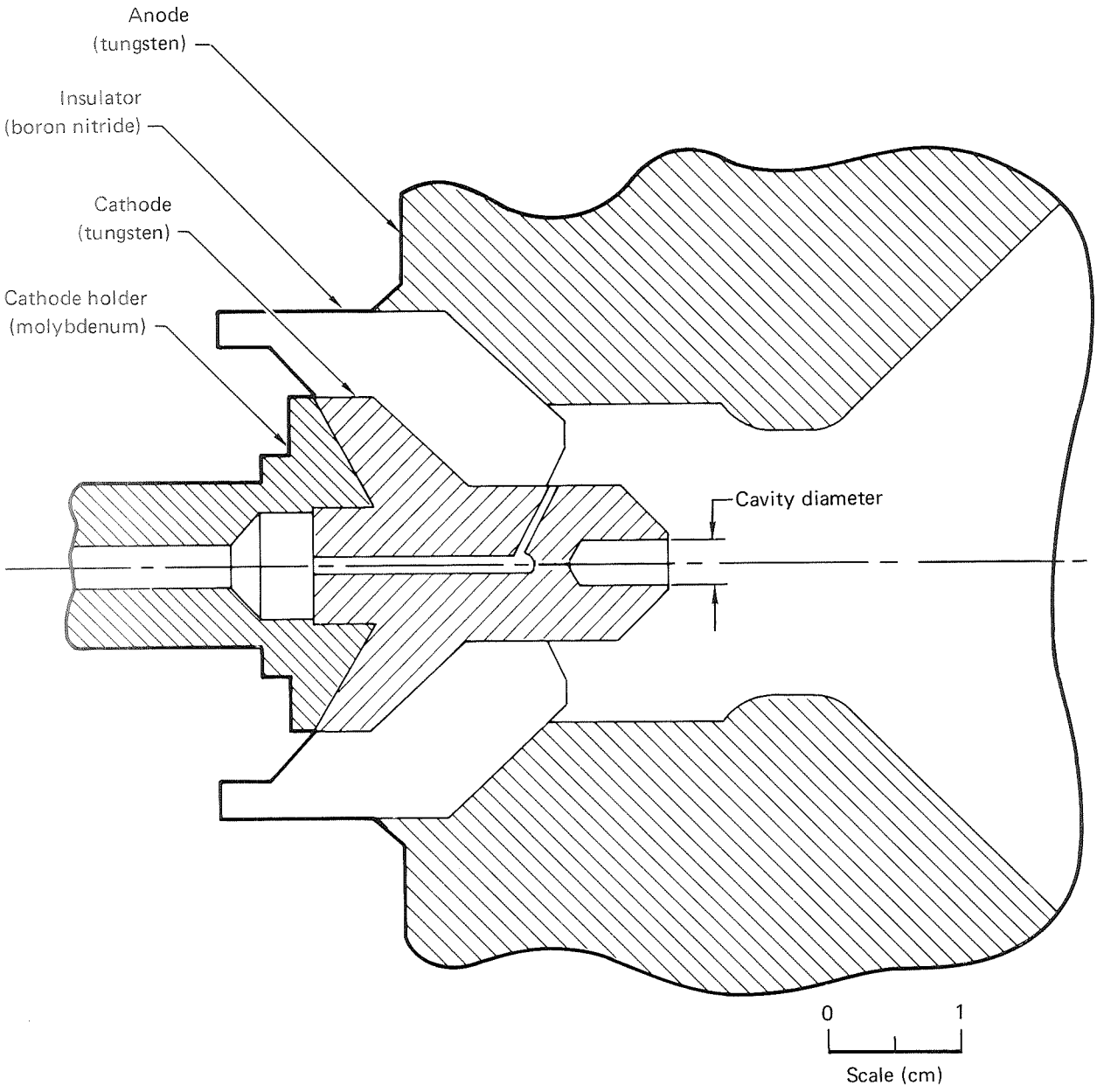

Fig. 3.2 MDC X-7 thruster cathode-insulator assembly (hollow conical cathode)

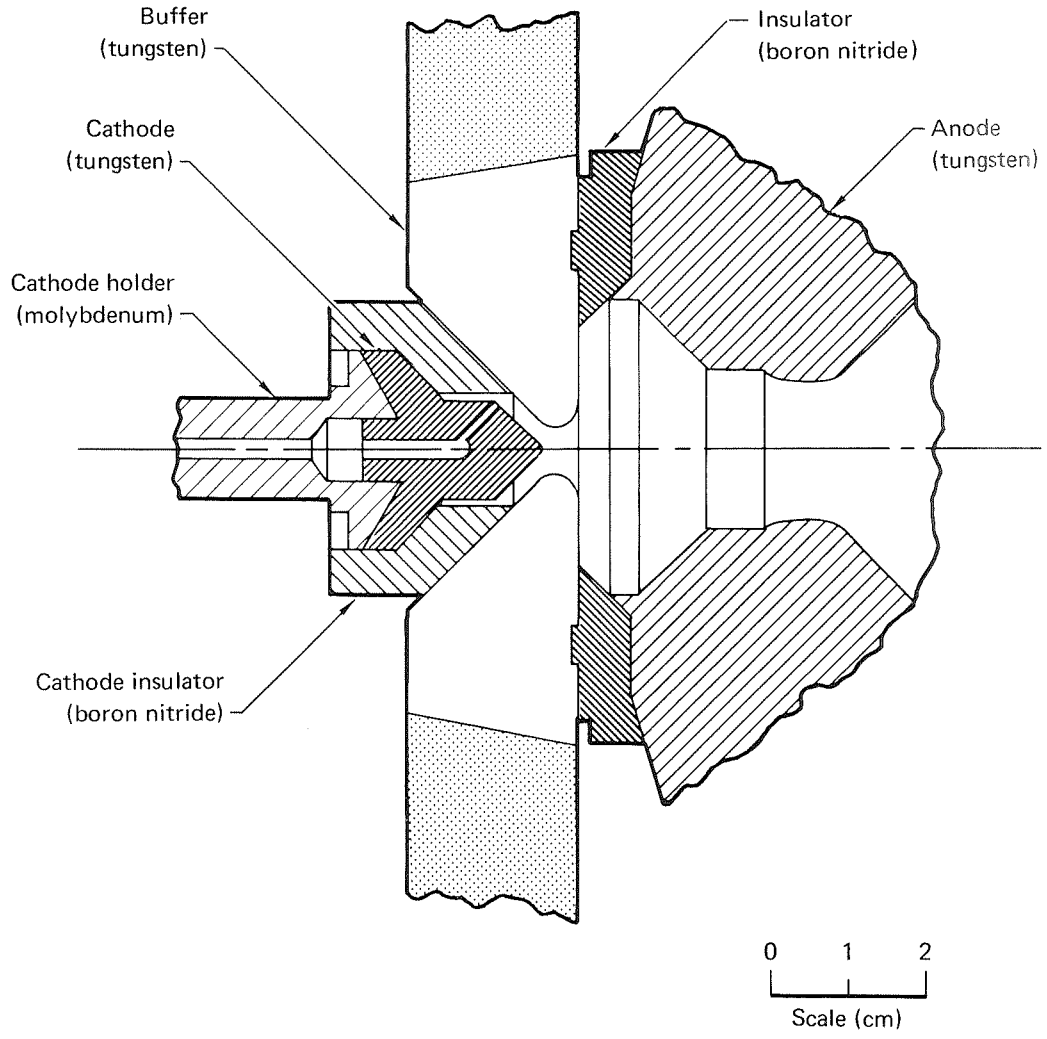

Fig. 3.3 MDC X-8 thruster cathode-insulator assembly (solid conical cathode and buffer)

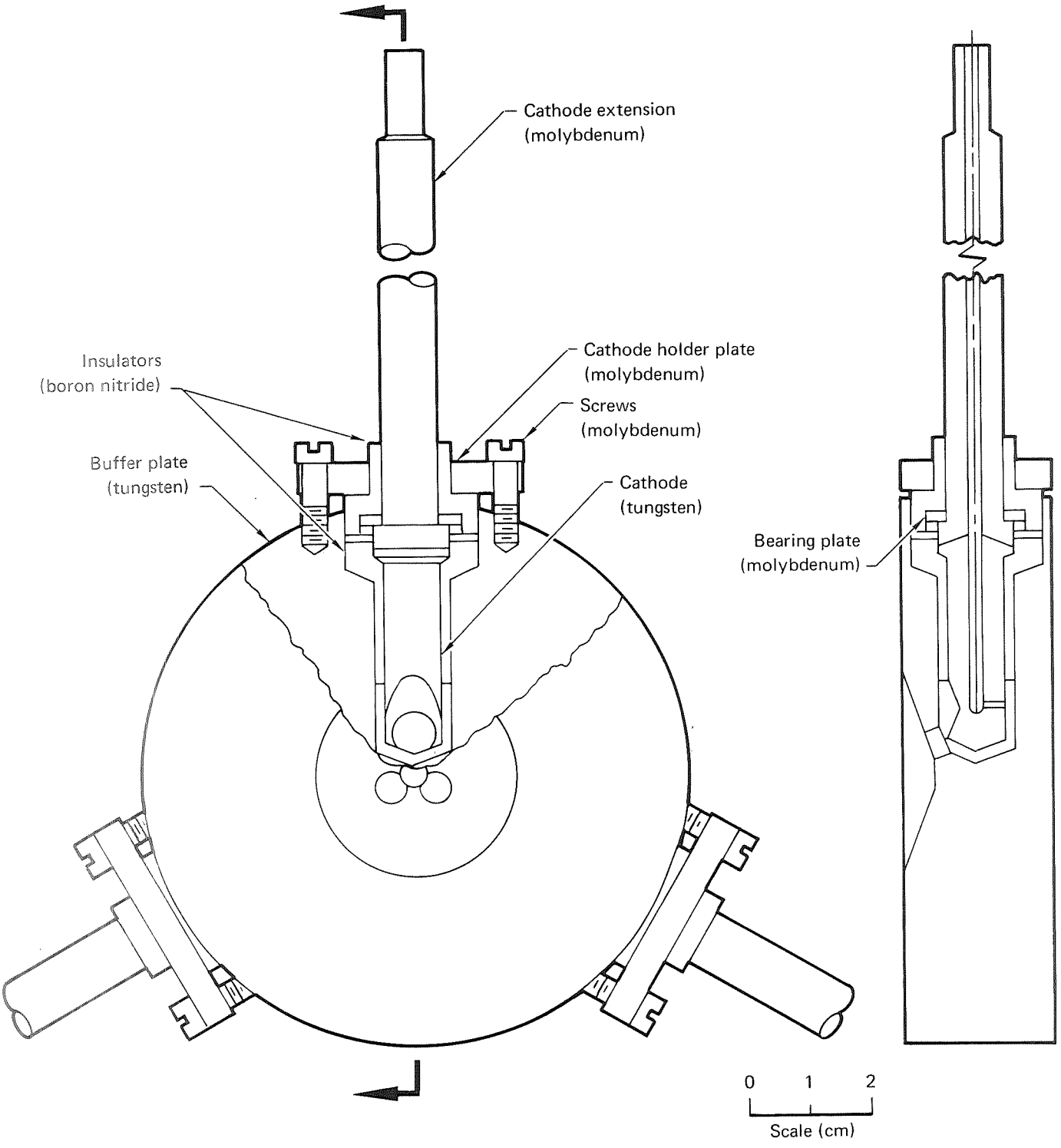

Fig. 3.4 Triple cathode assembly

Table 3.1 Parametric test scheme

Solid conical cathode (SC)		
(a)	Variation of axial position of cathode with respect to anode	L_g = 0.87, 0.95, 0.99, 1.07, 1.17 cm
(b)	Variation of injection ports	3 injection ports located at A or B or C or a combination of A and C for a total of 6 injection ports. See Figure 3.1.
Hollow cathode (HC2)		
(a)	Variation of axial position of cathode with respect to anode	L_g = 3.14, 3.05, 2.82, 1.70, 1.40 cm
(b)	Variation of anode throat diameter	Anode diameter = 1.778, 2.540 cm
(c)	Variation of cathode outside diameter	Outside diameter = 1.904, 1.585 cm
(d)	Variation of insulator geometry	
Hollow cathode (no flow) (HC1-FO)		
(a)	Variation of tip shape	SC cathode modified with cavity
(b)	Variation of cavity diameter	Cavity diameter =0.159, 0.318, 0.476 cm
(c)	Variation of axial position of cathode with respect to anode	L_g = 0.508, 0.660, 0.845, 0.991 cm
(d)	Variation of test chamber pressure	P = 0.003 to 0.68 Torr
Hollow cathode (with flow) (HC1-F1)		
(a)	Variation of internal hole	HC1-FO cathodes modified with 0.102 cm connection passage
(b)	Variation of injection ports	3 injection ports located at A or B or only the centerline passage port
(c)	Variation of cavity diameter	Cavity diameter = 0.159, 0.318, 0.476 cm
(d)	Variation of axial position of cathode with respect to anode	L_g = 0.711, 0.845, 0.991 cm
Hollow cathode (with flow) (HC1-F2)		
(a)	Variation of internal hole	HC1-F1 cathodes modified with 0.159 cm connection passage
(b)	Fixed location of injection ports	3 injection ports located at A plus the centerline cavity port
(c)	Variation of cavity diameter	Cavity diameter = 0.159, 0.318, 0.476 cm
(d)	Variation of axial position of cathode with respect to anode	L_g = 0.508, 0.685, 0.845, 0.871 cm
Hollow cathode (with flow) (HC1-F3)		
(a)	Variation of internal hole	HC1-F2 cathodes modified with 0.236 cm connection passage
(b)	Variation of cavity diameter	Cavity diameter = 0.159, 0.476 cm
(c)	Fixed axial position	L_g = 0.845 cm

Table 3.1 Parametric test scheme (continued)

Triple cathode geometry	
(a) Variation of buffer material	Tungsten and boron nitride were used to confine the arc
Buffered solid conical (BSC)	
(a) Variation of buffer internal hole diameter	Diameter = 0.636 through 1.524 cm
(b) Variation of cathode size	Cathode tip diameter = 2.54 and 1.27 cm. Three 0.102 cm diameter injection ports were at location B
Buffered hollow cathode (no flow) (BHC1-FO)	
(a) Variation of buffer internal hole diameter	Diameter = 0.636 through 1.524 cm
(b) Variation of cathode size	Cathode tip diameter = 2.54 and 1.27 cm. Three 0.102 cm diameter injection ports were at location B.
(c) Variation of tip geometry	BSC cathodes modified with 0.318 cm diameter cavity
Secondary propellant control	
(a) Variation of percentage flow through and around cathode	HC1-F1 with flow through centerline hole only, HC1-F1 with flow through centerline hole plus 3 external ports at location A, HC1-F2 with flow through centerline hole plus 3 ports at location A, HC4-F1, HC4-F2, HC4-F3, and HC5-F2

Tests of cathode-insulator modifications proposed under the original test plan were completed by the middle of the contract period. However, a serious problem associated with hollow cathode operation is the lack of long term stability of the arc attachment within the cavity (shown in Fig. 3.2). This conclusion was derived from unsuccessful attempts to duplicate the performance obtained earlier on a hollow cathode (HC1-F2), both at MDC and the NASA Lewis low pressure MPD facility.

To obtain reliable long term stability, several other cathode-insulator modifications were made. The tip or face of the cathode as well as the cavity shape were varied as shown in Fig. 3.5d through 3.5m. Table 3.2 shows the parametric test scheme used for these additional variations.

3.2 Propellant feed arrangement

Propellant injection arrangements with flow control around and through the cathode were investigated. Figure 3.5 depicts the various passages in the cathodes through which the propellant flows. Various

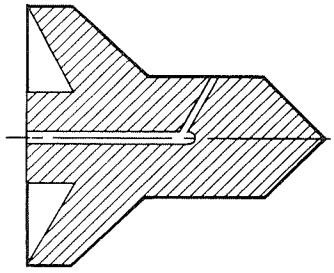

(a) SC (solid conical cathode)

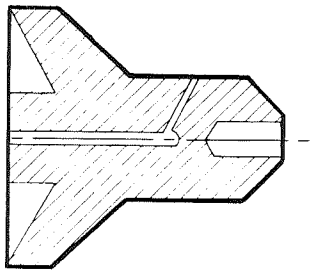

(b) HC1-F0

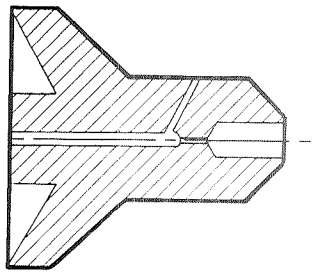

(c) HC1-FI

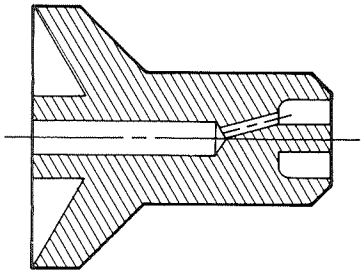

(d) HC600

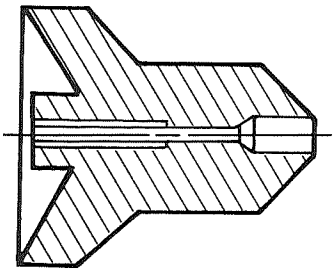

(e) HC6-F2

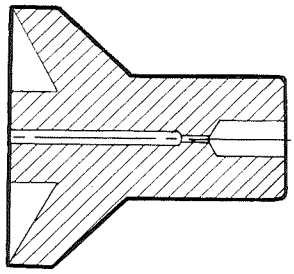

(f) HC9

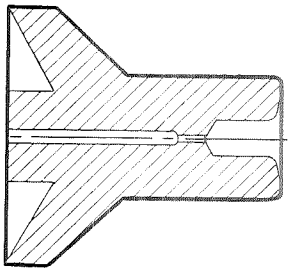

(g) HC9-A

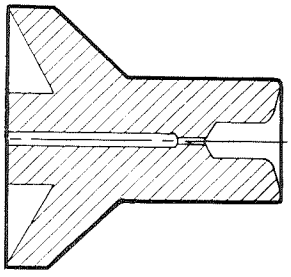

(h) HC9-B

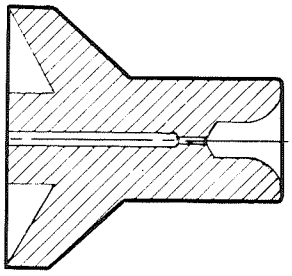

(i) HC9-C

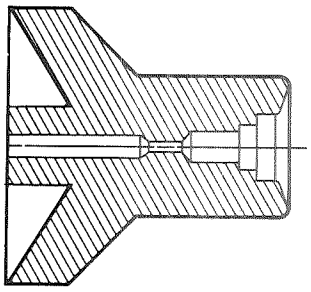

(j) HC9-E

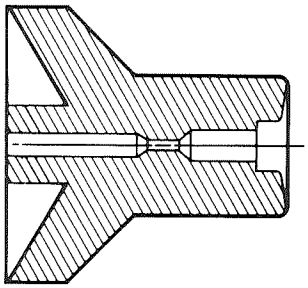

(k) HC9-D

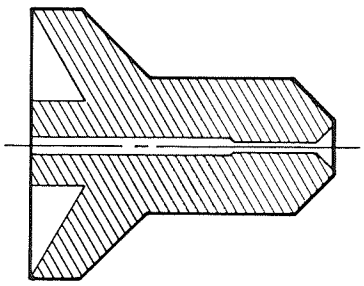

(l) HC4-F1

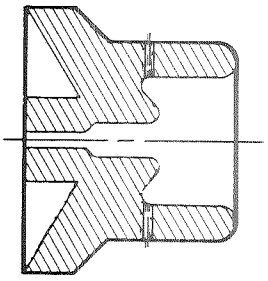

(m) HC5

Fig. 3.5 Cathode geometries

Table 3.2 Parametric test scheme

Hollow cathode (with flow) (HC4-F1)	
(a) Variation of cavity shape	HC1 cathodes modified with a 45^{o} half angle diverging cavity.
(b) Variation of connection passage diameter	—F1 diameter = 0.102 cm —F2 diameter = 0.159 cm —F3 diameter = 0.236 cm
(c) Fixed axial position	L_g = 0.845 cm
Hollow cathode (with flow) (HC5-F2)	
(a) Variation of cavity shape	HC2 cathode shape modified for secondary flow into the cavity
(b) Variation of axial position of cathode	L_g = 2.31, 2.54 cm
(c) Fixed connection passage diameter	Diameter = 0.159 cm
Hollow cathode (with flow) (HC600)	
(a) Variation of cavity shape	HC1 cathode modified with annular cavity
(b) Variation of injection ports	Three 0.102 cm injection ports into annular cavity
(c) Fixed axial position	L_g = 0.845 cm
Hollow cathode (with flow) (HC6-F2)	
(a) Variation of size	HC1-F2 cathode outside diameter enlarged to 1.908 cm
(b) Variation of cavity diameter	Cavity diameter = 0.318 and 0.476 cm
(c) Variation of axial position of cathode with respect to anode	L_g = 0.358, 0.406 cm
Hollow cathode (with flow) (HC9)	
(a) Variation of tip geometry	HC1-F2 cathode modified with flat face
(b) Fixed cavity diameter	Cavity diameter = 0.318 cm
(c) Variation of axial position of cathode with respect to anode	L_g = 0.864, 0.940 cm
Hollow cathode (with flow) (HC9-A)	
(a) Variation of tip geometry	HC9 cathode modified with 10^{o} half angle diverging tip
(b) Variation of axial position of cathode with respect to anode	L_g = 0.814, 0.952, 0.965, 0.990, 1.111 cm
Hollow cathode (with flow) (HC9-B)	
(a) Variation of tip geometry	HC9-A cathode modified with diverging 20^{o} half-angle tip
(b) Variation of cavity diameter	Cavity diameter = 0.318, 0.476 cm
(c) Variation of axial position of cathode with respect to anode	L_g = 0.724, 0.814 cm

Table 3.2 Parametric test scheme (continued)

Hollow cathode (with flow) (HC9-C)		
(a)	Variation of tip geometry	HC9-B cathode modified with 0.318 cm radius between cavity and diverging face of tip
(b)	Fixed cavity diameter	Cavity diameter = 0.318 cm
(c)	Variation of axial position of cathode with respect to anode	L_g = 0.838, 1.111 cm
Hollow cathode (with flow) (HC9-D)		
(a)	Variation of cavity shape	HC9-A cathode modified with a 0.476 cm diameter step in the cavity
(b)	Fixed axial position	L_g = 0.864 cm
Hollow cathode (with flow) (HC9-E)		
(a)	Variation of cavity shape	HC9-D cathode modified with the addition of a 0.636 cm diameter step in the cavity
(b)	Variation of axial position of cathode with respect to anode	L_g = 0.814, 0.838, 0.889, 1.092, 1.244 cm
(c)	Variation of electrode insulator geometry	Modified shape of electrode insulator near cathode
Propellants		
(a)	Variation of propellants	Ammonia, nitrogen, nitrogen-hydrogen, helium, neon, and xenon

ratios of flow rates supplied by two separate independently controlled feed systems were investigated in an effort to obtain fine control of the arc attachment. The flow through the cathode will be referred to as the primary flow whenever more than one flow is used. As a means of controlling the current attachment to the cathode, secondary propellant was admitted around the cathode in addition to the propellant supplied through the cathode (Fig. 3.8). Figure 3.6h and 3.6i show the insulators through which secondary propellant was admitted.

3.3 Propellants

The propellant used throughout most of this study was ammonia. During the investigation it became apparent that use of this propellant was at least partially the cause of the arc instability. Various ratios of nitrogen and hydrogen were then tested. Since the propellant was shown to affect both the arc stability and overall performance, additional tests, not originally planned, were conducted with neon, helium, and xenon.

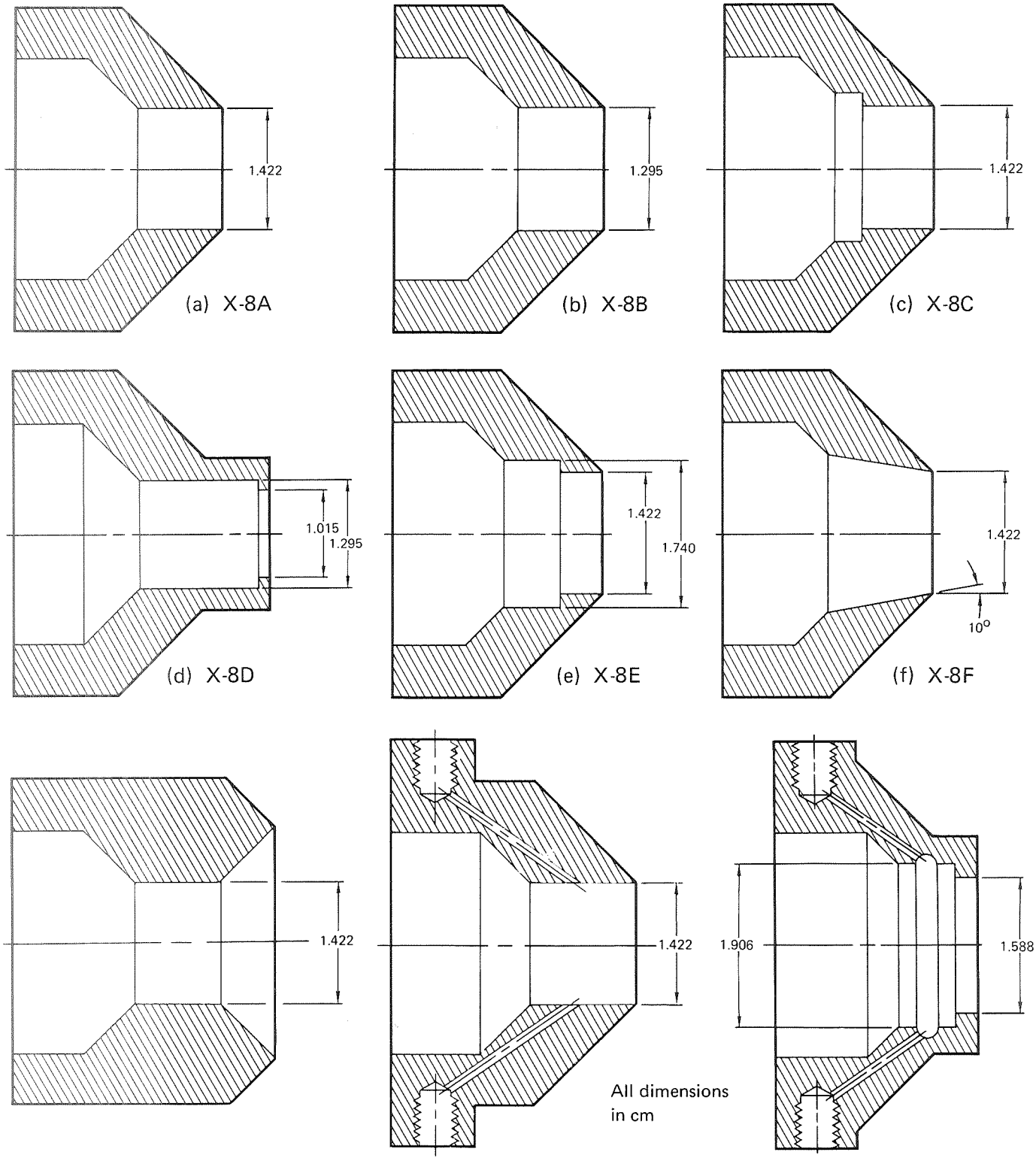

Fig. 3.6 Insulator geometries

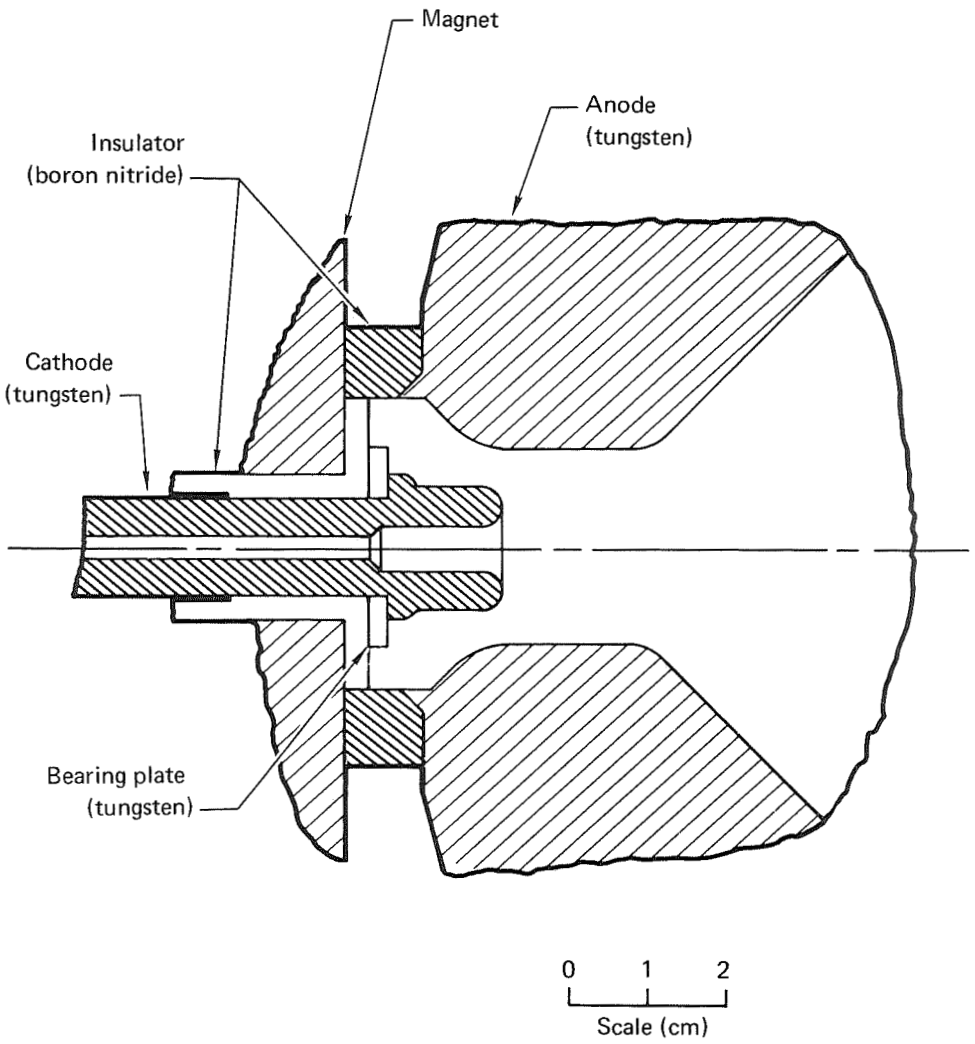

Fig. 3.7 HC2 - Hollow cathode geometry - with flow

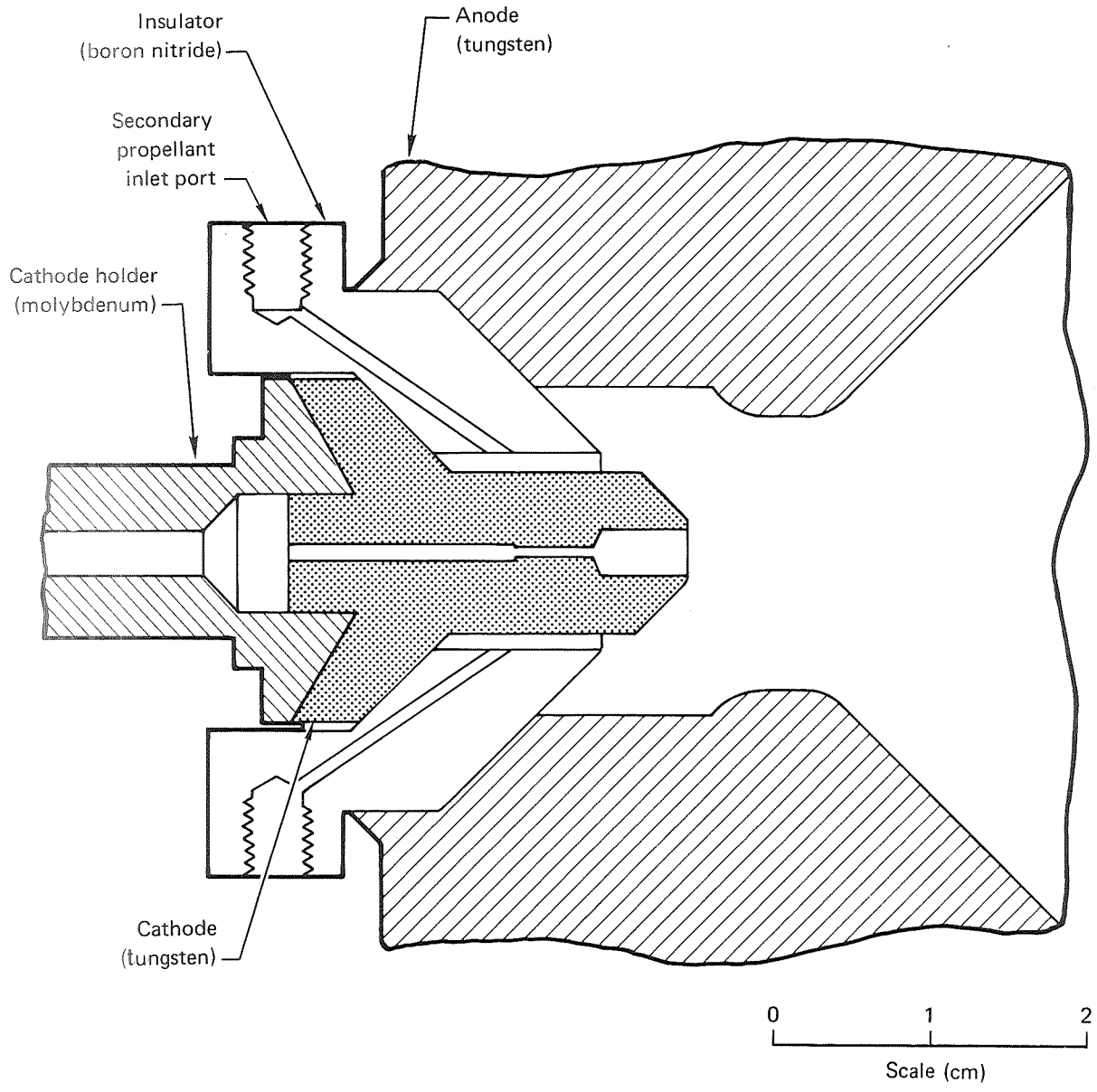

Fig. 3.8 Dual propellant flow geometry

4 Discussion of experimental results

This section presents the results of experiments on the X-7 cathode-insulator geometry modifications, propellant feed arrangements, and various propellants.

The various configurations were judged by their quantitatively measurable characteristics, mainly thrust performance, and on the basis of their ability to retain these characteristics for extended periods. In the qualitative description of the latter aspect, the term "stability" will be often used. Figure 4.1b shows a typical frame of the arc region during a stable mode of operation. The initially existing current distribution over the electrode surface (attachment) was repeatedly observed to change with time at some operating conditions. In many cases the arc initially attached to the tip portion of the cathode, but after varying times of operation the attachment moved upstream onto the outside cylindrical portion of the cathode surface. This process (shown in Fig. 4.1a) will be referred to as an "instability" and the corresponding current distribution will be called "unstable." Figure 4.1c shows the unstable operating condition. Attachment at the rear generally caused severe erosion. The characteristics thereafter were continuously changing because of the changes in geometry and surface properties of the eroding, melting cathode.

4.1 Cathode-insulator geometry modifications

There were 137 cathode-insulator assembly modifications of the X-7 thruster tested. These configurations may be classified into two general categories: solid conical and hollow. Most of the variations involved the hollow cathode.

4.1.1 Solid conical cathode

It was observed during the 500 hour lifetest of the X-7 thruster (Ref. 2) that the voltage increased with time. It was also observed that the cathode tip was moving forward or downstream because of erosion of the electrode insulator. It was hypothesized that the rise in arc voltage may have been due to the forward movement of the cathode. To test this hypothesis, the axial position or gap length (L_g) shown in Fig. 3.1 was varied as follows: L_g = 0.87, 0.95, 0.99, 1.07, and 1.17 cm. The highest voltage was measured with the cathode tip in the most forward position (L_g = 0.87 cm), suggesting that the rising voltage during the lifetest could have been caused by this effect. Figure 4.2 shows the electrical characteristics of the conical cathodes. Table B.1 lists the data obtained at the

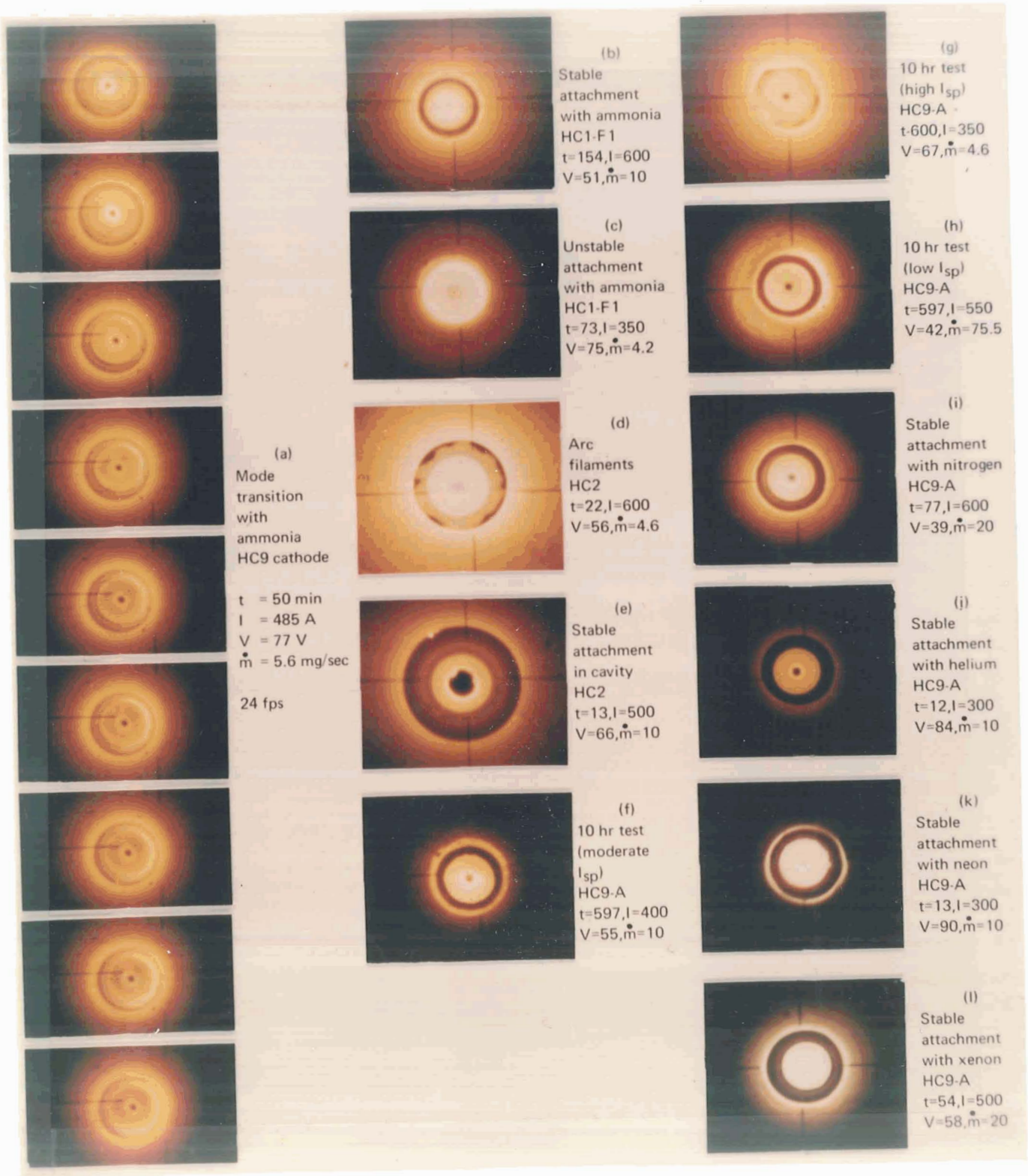

Fig. 4.1 Photographs of arc attachments

five axial positions. The three propellant injection ports in the above five cathodes were at position (C) as shown in Fig. 3.1. The injection ports in the 500 hour lifetest cathode were at location (B). On several of the cathodes, particularly on those with the short gap lengths, the arc discharge transferred behind the injection ports and caused local melting of the cathode. To circumvent this problem, three extra holes were added at location (A). These holes were located azimuthally between the downstream injection ports. This cathode was tested at an axial position (L_g) of 0.87 cm. Table B.2 lists the performance data obtained on this cathode. The electrical characteristics, shown in Fig. 4.2, indicate that this cathode had the highest voltage of the solid conical cathodes. The performance and stability of the six hole cathode was the highest of the solid conical cathodes.

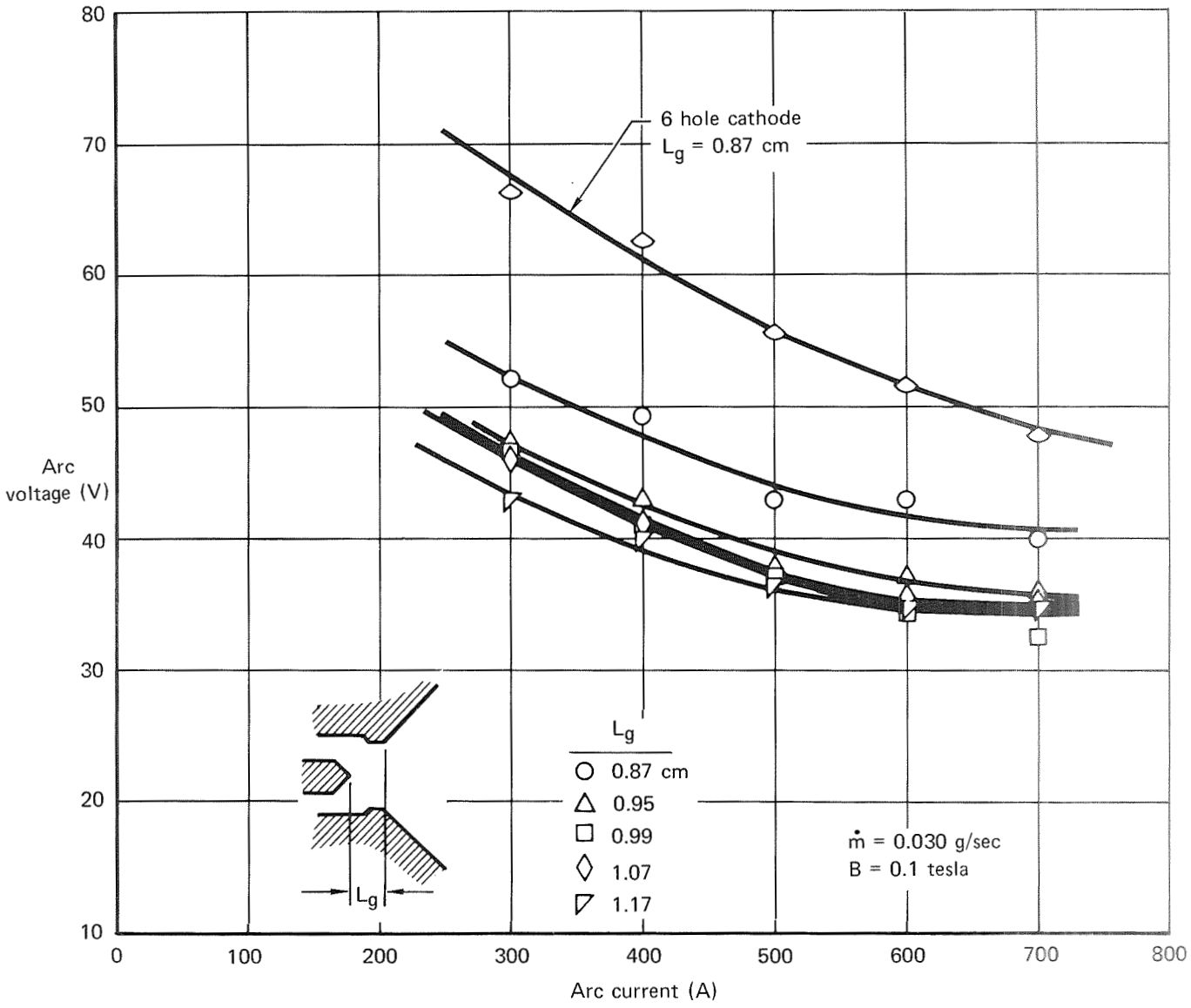

Fig. 4.2 Electrical characteristics of solid conical cathodes

Since placement of the injection ports at the rear of the cylindrical section resulted in some performance improvement, a cathode with only three holes placed at location (A) in Fig. 3.1 was tested at an axial position (L_g) of 0.95 cm. Table B.3 shows these performance data. The thrust performance was less than that of the six hole cathode.

The tests conducted on the solid conical cathodes showed that the overall performance was affected little by the axial position of the cathode. The arc voltage increased, and consequently higher input power could be achieved, with the smaller electrode gaps.

4.1.2 Hollow cathode (HC2)

In order to remove the electrode insulator from the high temperature region of the discharge and thereby reduce insulator erosion, a hollow cathode configuration was studied. This geometry, designated HC2, is shown in Fig. 3.7, and consists of a single piece tungsten electrode wherein all of the propellant was passed through the hollow section. An earlier X-7 anode was used in this design. The initial tests of the HC2 geometry were conducted with an anode throat diameter of 2.54 cm. The axial position (L_g) variation consisted of the following: 3.14, 3.05, 2.82, 1.70, and 1.40 cm.

Unstable arc operation was encountered during all but one of the 11 different tests. At flow rates of 53 and 40 mg/sec stable operation was achieved at several current levels. These data are shown in Table B.4. Visual observations of the cathode indicated that the cathode was uniformly heated, and emission appeared to be uniform from the outer diameter and from the forward rounded edge. At higher currents, distinct arc filaments could be seen between the rounded edge and the upstream corner of the anode throat section (Fig. 4.1d). These filaments were formed sporadically and caused local melting of the anode at the upstream corner.

Stable operation was achieved after some initial instability during one test by lowering the propellant flow rate to 4.6 mg/sec. The arc attachment was observed to move from the outside diameter into the hollow section of the cathode. When this arc movement occurred, the exhaust narrowed into a tight beam approximately 3-4 cm in diameter for a length of roughly 20 cm downstream of the thruster. Performance measurements obtained during this period are presented in Table B.5. There is a possibility that entrainment of ambient gas into the acceleration region was occurring during the test. The background pressure was 4.6×10^{-3} Torr. Three noteworthy observations were made: (a) the measured specific impulse levels of the radiation cooled thruster were above 4000 sec for ammonia; (b) the thrust efficiencies at 500 and 600 A conditions were the highest achieved for ammonia in a radiation cooled thruster; and (c) the thrust-to-power ratios decreased with decreasing flow rate as would be expected from mass flow rate trends found at higher flow rates. The significant fact here is the high voltage obtained at a corresponding low flow rate. The X-7 thruster operation at 30 kW input power with 5.0 mg/sec was prohibited since currents above 900 A would be required. Thus in effect, the measured high performance was consistent with past MPD performance; the difference was that the HC2 cathode allows operation in a region which could not be reached with the solid conical cathodes.

Attempts to duplicate the above performance for long periods of time were unsuccessful. Arc attachment within the hollow section was attained for approximately 5 min and recorded on film (Fig. 4.1e); however, filament formation between the outside diameter and the upstream throat area prevented thrust measurement.

The anode throat diameter was rebored to 3.18 cm in an effort to increase the separation distance in the region where the arc filaments were formed. Several attempts were made to obtain thruster performance on the HC2 cathode with only slight success. Stable arc operation could be

obtained for periods up to 30 min with current emission on the internal diameter of cathode; subsequently the discharge would transfer abruptly to the outside diameter of the cathode necessitating termination of the test. A modification to the cathode insulator to shield the outside diameter of the cathode allowed stable operation for periods sufficiently long to obtain thrust data; however, insertion of the thrust killer caused the attachment to shift to the outside diameter. Successive restarts enabled the data shown on Table B.6 to be recorded.

No significant increases in efficiency or in arc voltage were recorded with this cathode configuration. In view of the difficulties encountered no further tests were made on this geometry.

4.1.3 Hollow cathode (HC1-FO)

To increase the cathode arc attachment spot area while maintaining a relatively sharp edge, the HC1-FO (Fig. 3.5b) geometry was conceived. This cathode series is simply the solid conical cathode with a blind hole located on the axis to a depth of 0.953 cm. No propellant flows through this blind hole or cavity. The cavity diameter shown in Fig. 3.2 was varied as 0.159, 0.318, and 0.476 cm.

Table B.7 shows performance data for a HC1-FO cathode with a cavity diameter of 0.159 cm. The arc voltages recorded are generally higher than observed on solid conical cathodes at comparable operating conditions; however, the thrust-to-power ratios are slightly lower. In addition, the arc discharge became unstable at currents above 500 A. Table B.8 shows the data obtained on the HC1-FO cathode with a cavity diameter of 0.318 cm. The data of Tables B.7 and B.8 were taken with an axial distance (L_g) of 0.845 cm. The performance is slightly reduced from the smaller cavity data and the arc voltages are also lower by several volts. Mode changes were encountered at currents around 600 A with a voltage difference of ~ 20-25V between modes.

The thrust performance obtained on the HC1-FO cathode with a cavity diameter of 0.476 cm is presented in Table B.9. These data were obtained with a L_g setting of 0.845 cm. Figures 4.3 through 4.5 show the electrical characteristics of the three HC1-FO cathodes at a common L_g distance of 0.845 cm. Several features of these data contrast with the electrical characteristics of solid conical cathodes: (a) the range of stable arc operation was somewhat narrower than achieved with solid cathodes (data acquisition was attempted for currents between 300 and 600 A), (b) at the higher currents a positive characteristic was obtained, and (c) the voltage at higher currents generally increased with decreasing mass flow.

The effect of a variation of L_g on the HC1-FO cathode with a 0.476 cm cavity was next investigated. Values of L_g tested were 0.998, 0.845, 0.660, and 0.508 cm and the performance data obtained are presented in Tables B.9, B.10, B.11, and B.12, respectively. Operation was somewhat erratic at the two shortest gaps with thrust performance comparable to the solid conical cathodes. Figures 4.6 and 4.7 show the effect of L_g variation on arc voltage. The highest voltage was almost always recorded on the cathode with L_g = 0.845 cm.

The high specific impulses recorded on the hollow cathode geometry with mass flow rates near 5 mg/sec are subject to possible error because of entrainment of ambient gas into the acceleration region. To explore this possibility a test of the HC1-FO (0.476 cm cavity) cathode was conducted during which the thruster arc current, mass flow rate, and magnetic field were held constant and the background pressure was varied by introducing cold ammonia downstream of the thruster but upstream of the vacuum pumps. The data obtained during this test are shown in Table B.13. The voltage, thrust and power decreased as the background pressure increased resulting in a lower thrust-to-power ratio. The test conducted here was not sufficient to determine the effects of entrainment. It is worthwhile to note, however, that the trend observed has been reported by Connolly and Sovie[4] for ammonia propellants at roughly two orders of magnitude lower background pressure.

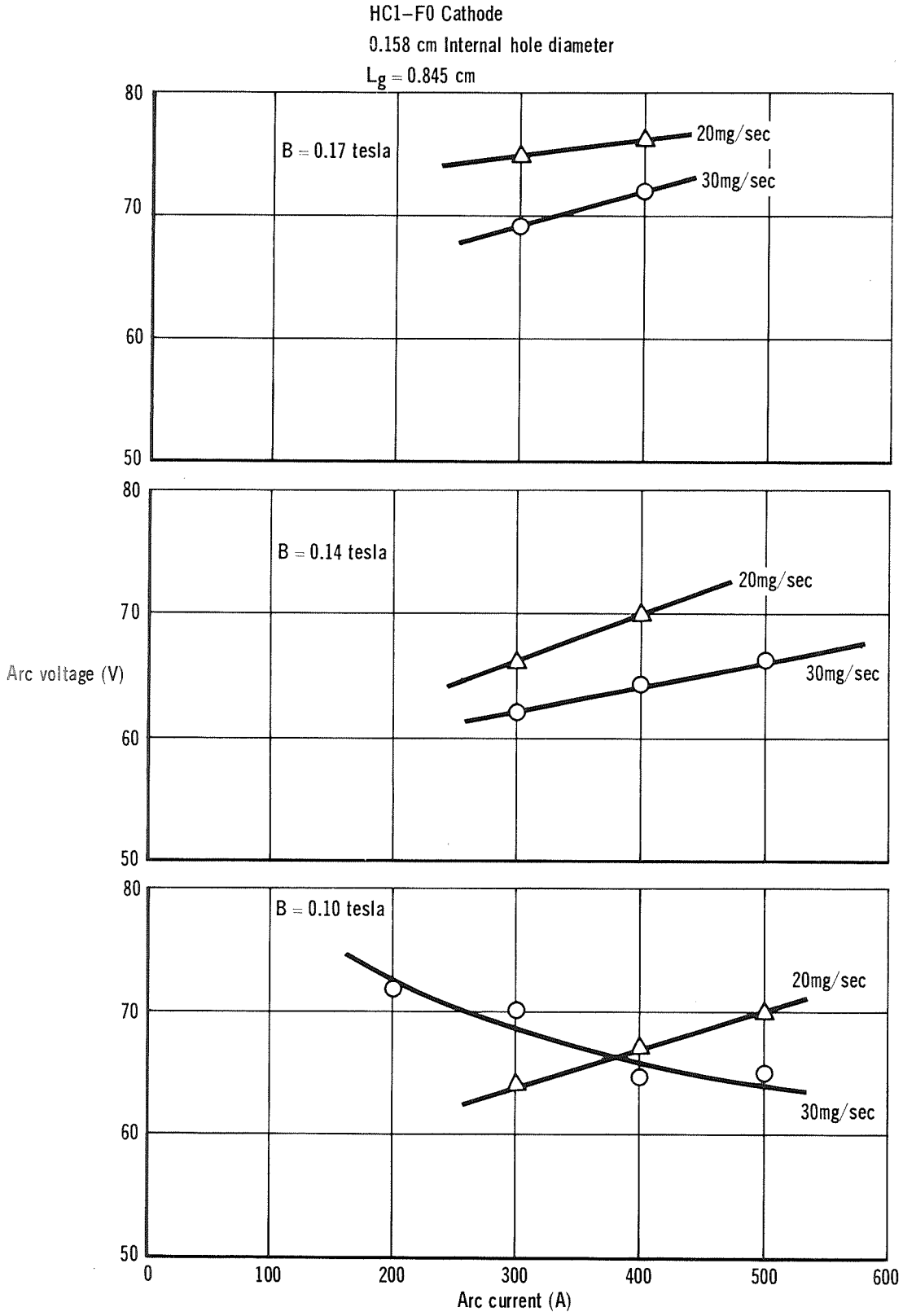

Fig. 4.3 Electrical characteristics, HC1-FO cathode (0.158cm i.d.)

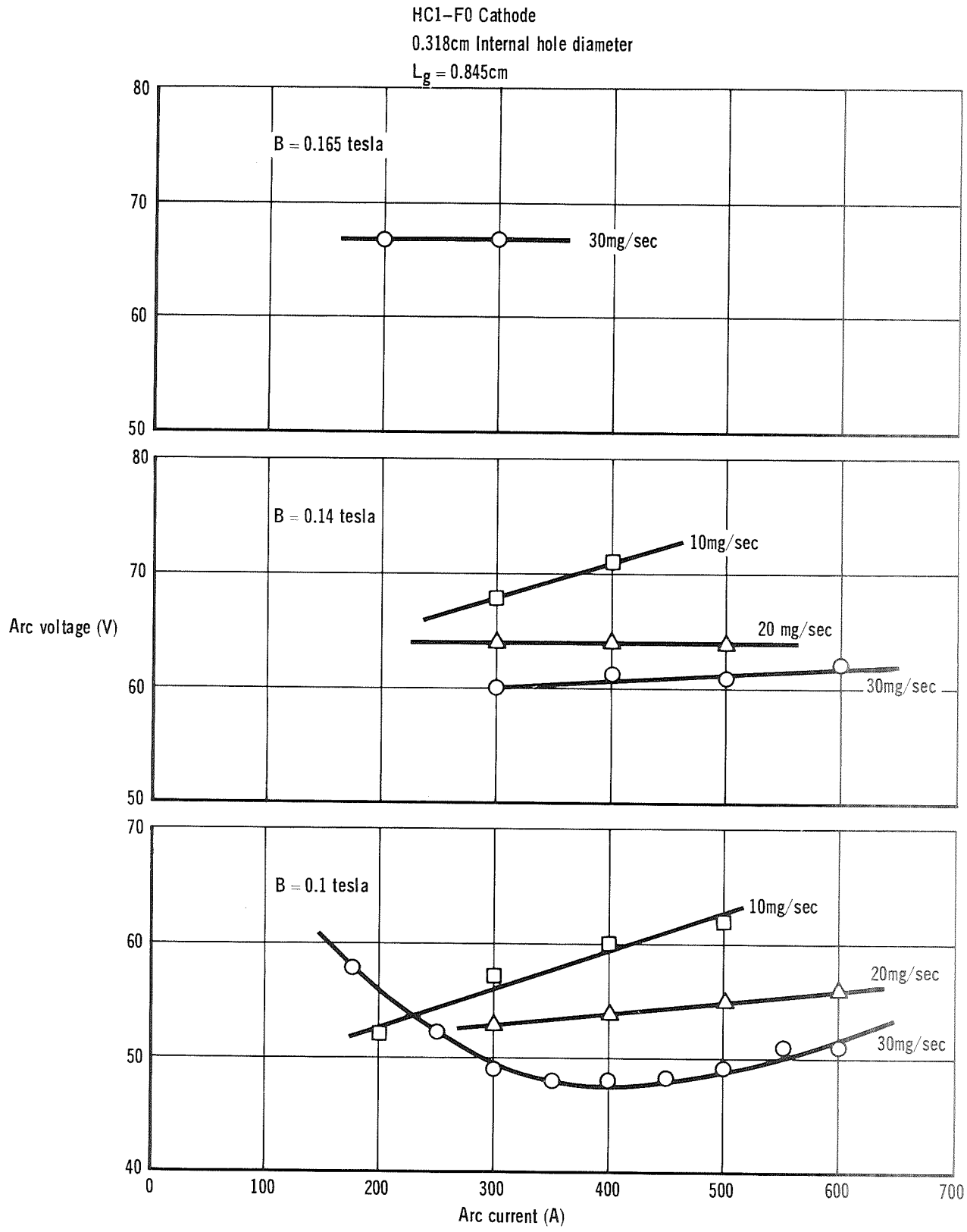

Fig. 4.4 Electrical characteristics, HC1-FO cathode (0.316cm i.d.)

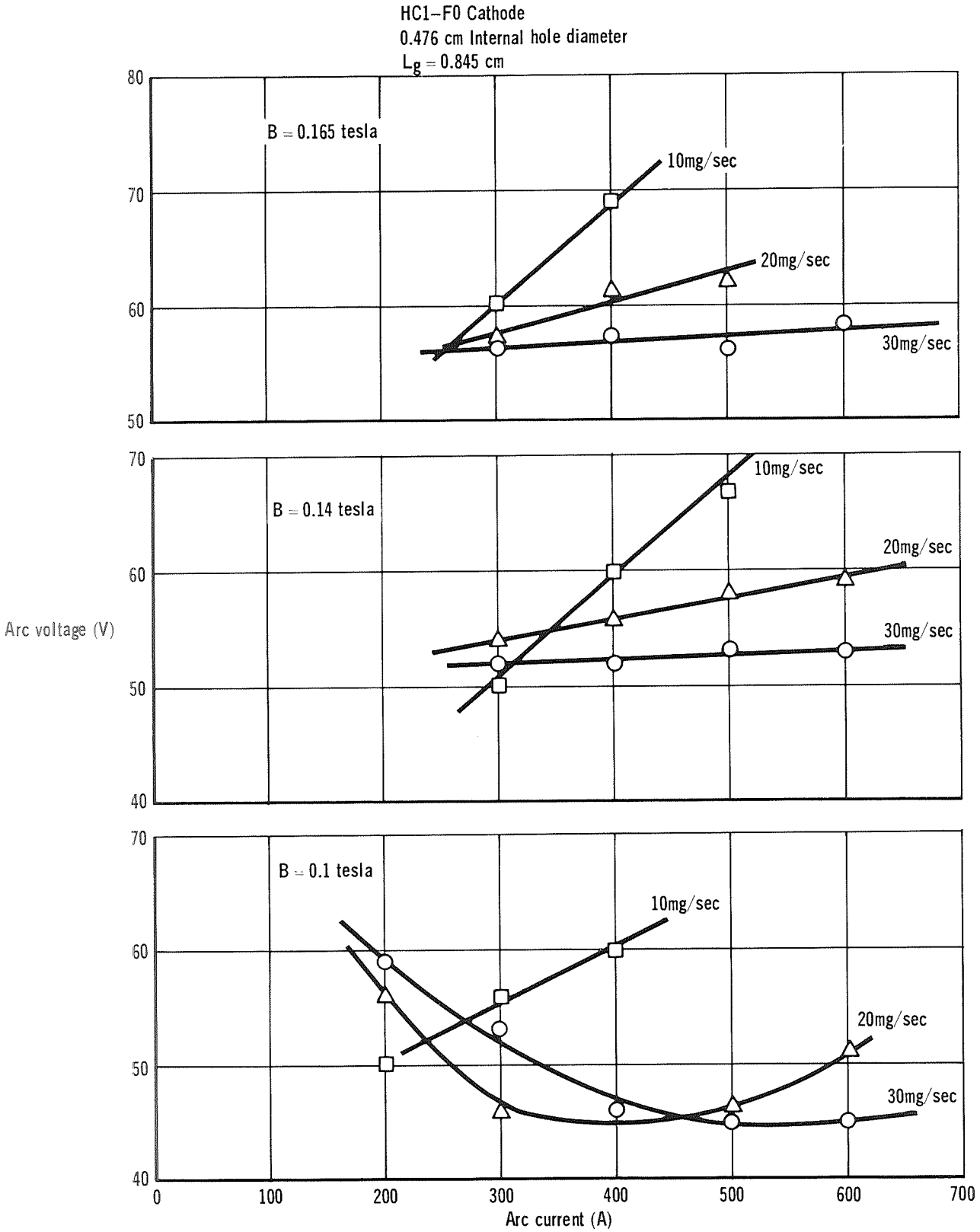

Fig. 4.5 Electrical characteristics, HC1-FO cathode (0.476cm i.d.)

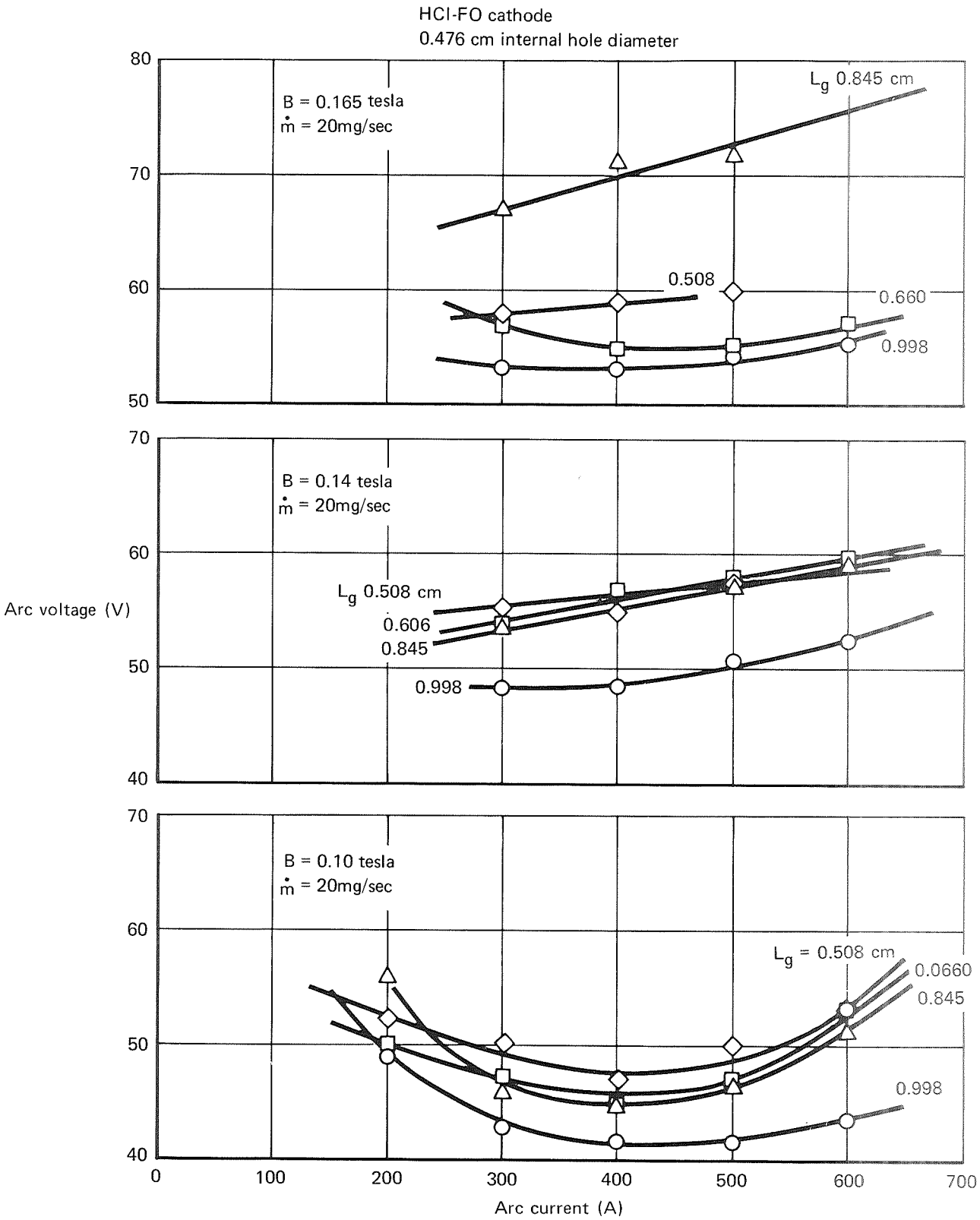

Fig. 4.6 The effects of (L_g) on arc voltage, HC1-FO cathode (0.476 cm i.d.)

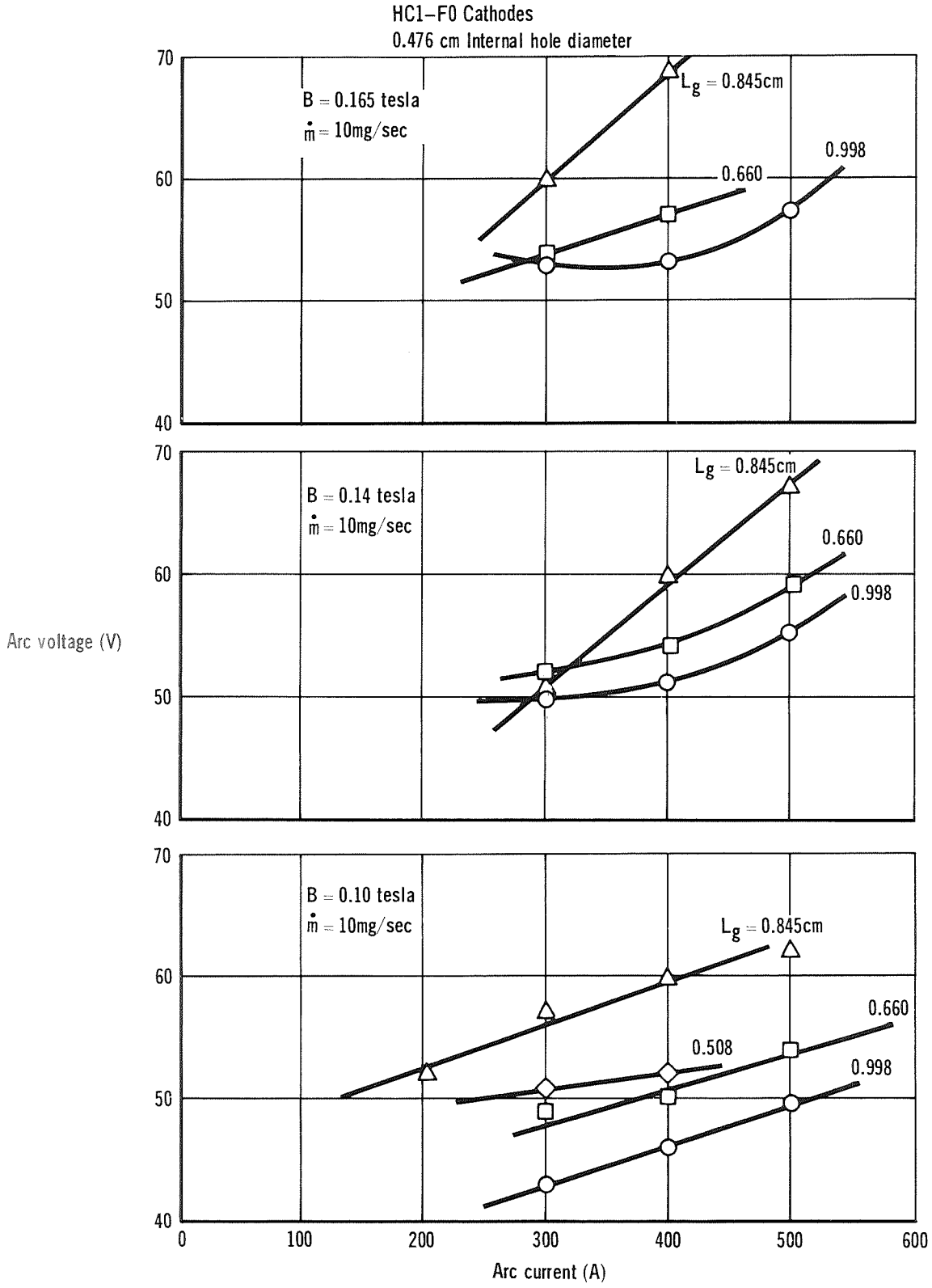

Fig. 4.7 The effects of (L_g) on arc voltage, HC1-FO cathode (0.476cm i.d.)

4.1.4 Hollow cathode (HC1- F1)

To increase the propellant flow rate into the cathode arc attachment region, the HC1-F1 cathode was modified by drilling a 0.102 cm connection hole between the cavity and the propellant passage, thereby admitting a portion of the propellant flow through the cavity. Tables B.14 through B.16 show the performance data for HC1-F1 cathodes (Fig. 3.5c) with 0.159, 1.318, and 0.476 cm cavity diameters situated at an L_g distance of 0.845 cm. Stable arc operation was generally achieved only at the lower mass flow rates. Voltages as high as 80 V were recorded on the cathodes with the 0.159 cm diameter cavity. Specific impulse values approaching 10,000 sec were measured with this cathode configuration at the rather modest current level of 450 A.

Further tests were made with the HC1-F1 cathode in the dual propellant feed configurations. Discussion of these will be presented in Section 4.3.

4.1.5 Hollow cathode (HC1-F2)

The HC1-F2 cathode is similar to the HC1-F1 except that the connection passage diameter was 0.159 cm, and the cavity diameters were 0.159, 0.318 and 0.476 cm.

Table B.17 shows three data points obtained with a cathode having a 0.159 cm cavity. The stability range of this configuration was limited to these three points because of intermittent changes in attachment from the cathode tip to the base of the cathode. Performance values were almost identical with the smaller connection hole cathode (HC1-F1), although the voltage was reduced somewhat by the increased flow through the hollow section.

Table B.18 shows the performance on the HC1-F2 cathode with a cavity diameter of 0.318 cm. This cathode possessed a wider range of stability than the previous hollow cathodes tested. The thrust-to-power ratios for mass flows of 4, 10, and 20 mg/sec are higher by approximately 0.002 N/kW than those obtained on the other hollow cathodes at comparable conditions. The 30 and 40 mg/sec thrust-to-power data are approximately equal to those obtained with the other hollow cathodes.

The HC1-F2 cathode with a 0.476 cm diameter cavity yielded the performance shown in Table B.19. The thrust-to-power ratios are again somewhat higher at flow rates of 4 and 10 mg/sec; however, the 20, 30, and 40 mg/sec data are nearly equal to the bulk of the hollow cathode data.

The decrease in arc voltage with increasing cavity diameter reported on the HC1-FO and HC1-F1 cathodes was also obtained on the HC1-F2 cathode. The tests described above were made at an electrode gap L_g value of 0.845 cm. A test of the 0.476 cm cavity HC1-F2 cathode was also made at L_g values of 0.685 and 0.516 cm. Tables B.20 and B.21 show the data obtained which have a narrow specific impulse range because of stability problems at L_g values smaller than 0.845 cm. The voltages recorded indicate again that a broad maximum exists near a L_g value of 0.845 cm.

The HC1-F2 cathode was used also in the dual propellant feed tests, the results of which are presented in Section 4.3.

4.1.6 Hollow cathode (HC1-F3)

The HC1-F2 cathode was modified by enlarging the connection passage diameter to 0.236 cm. Operation of the HC1-F3 cathode was very erratic. Only the largest cavity diameter (0.476 cm) cathode was sufficiently stable to obtain performance data. The axial position had an L_g of 0.845 cm. The data obtained for this cathode are listed in Table B.22 and show thrust-to-power ratios comparable to the other cathodes tested. The arc voltage was reduced somewhat to 40-45 V.

4.1.7 Hollow cathode (HC600)

In a further attempt to increase the propellant mass flow in the cathode arc attachment region, the HC600 cathode (Fig. 3.5d) has an annular cavity with three connection passages supplying the propellant. The injection ports in the cylindrical section were omitted.

Table B.23 shows the performance obtained with the HC600 cathode during the initial test which operated for 51 min. The exhaust of this cathode had a particularly tight cathode jet as compared to the previous cathodes; however, the performance at m = 20 mg/sec was significantly below previously tested cathodes. Inspection of the cathode after this test showed that the center plug had eroded leaving the plug rounded and recessed approximately 1 mm.

After the initial test a second test was made on the same HC600 cathode without any modification or repair. This test was started at a mass flow of 4.6 mg/sec and then increased to 40 mg/sec. After 70 min of operation the center plug of the cathode was ejected from the cathode and the test was terminated. The results of this test are presented in Table B.24. The performance at 4.6 mg/sec appears to be the best obtained thus far; however, the data at higher flows were well below those obtained on previous cathodes. The high erosion characteristics of the HC600 cathode indicate that this cathode is unsuitable for operation in the 2000 to 3500 sec specific impulse range.

4.1.8 Hollow cathode (HC6-F2)

Efforts to increase arc voltage by changing the methods of gas injection proved to be unsuccessful. An alternative means of increasing the voltage was to increase the anode throat diameter. An X-7 anode was modified to increase the throat diameter to 2.54 cm. The cathode was enlarged to a 1.908 cm outside diameter. This cathode, designated HC6-F2 (Fig. 3.5e), was an enlarged HC1-F2 type cathode. The outer injection ports were omitted, so the propellant was injected only through the axial cavity. The cavity diameter was varied as 0.318 and 0.476 cm.

A total of six tests were made on this cathode-anode configuration. Tables B.25 through B.27 list the performance data obtained on the HC6-F2 cathode at various axial positions and cavity diameters. Several anomalies were noted. First, the cathode surface was found to be extremely roughened and eroded compared with previous cathodes, and second, the arc voltage did not show the positive characteristics with arc current at 4.6 mg/sec as recorded on other hollow cathodes. The increased erosion and low arc voltage (40-60 V) observed on this cathode were recorded at only moderate arc current levels (200-600 A) and led to the suspicion that some impurities were present in the tungsten cathode, or were introduced into the propellant flow system. A second cathode was fabricated from a new tungsten billet and when tested for a short period resulted in erosion similar to the first cathode.

A thorough leak check of the ammonia propellant inlet flow system was carried out next. A small air leak was detected at one of the solenoid valves in the flow system. This small leak permitted air entry in the flow inlet whenever the propellant mass flow was less than 15 mg/sec. The solenoid valve was replaced and the 2.54 cm throat engine was operated with the HC6-F2 cathode. At a mass flow of 5 mg/sec and an arc current of 300 A, the arc voltage was about 113-117 V. At this arc voltage, various corona or plasma glows appeared about the engine and thrust stand, and after a period of several minutes breakdown occurred across the bus bar terminals at the top of the thrust stand, and the test was terminated.

4.1.9 Hollow cathode (HC9)

Since little progress was made in attaining long term stability with the HC1 type cathodes, a new cathode design, designated HC9 (Fig. 3.5f), was tested. The conical tip or the HC1-F2 was replaced with a flat face and the outer injection ports were eliminated. This cathode had a cavity diameter of 0.318 cm and a connection passage diameter of 0.159 cm.

The thrust readout of the HC9 was noisy compared with the solid conical cathodes. Visual observation of the cathode showed the arc attachment to move sporadically on the downstream face. The stability range of this cathode was somewhat greater than that of the HC1 cathodes. At the high arc currents the arc attachment tended to shift to the outside diameter. The introduction of the thrust

killer into the exhaust occasionally caused the same type of arc shift. A reduction of the arc current usually allowed reattachment of the discharge in the cathode cavity.

Because of the arc attachment shifts, the accuracy of the thrust data is subject to question. Table B.28 presents the performance data obtained during a test with a L_g of 0.940 cm; the performance as recorded is somewhat lower than the HC1-F2 results. The arc voltage characteristic of the HC9 cathode was extremely sensitive to mass flow rate in the range of 10 to 4 mg/sec as is shown in Fig. 4.8.

In several instances the arc attachment could not be returned to the cavity, so the thruster was shut down, allowed to cool and subsequently restarted. Table B.29 presents data obtained on the HC9 cathode taken over several start and stop cycles. The poor reproducibility of the thruster performance may have been due at least partially to the irregular shape which the cavity assumed after approximately 10 hours of testing. Nevertheless, the HC9 cathode produced some improvement in stability over previous hollow cathodes.

4.1.10 Hollow cathode (HC9-A)

Encouraged by the stability improvement observed with the HC9 cathode, a similar geometry, the HC9-A (Fig. 3.5g) was tested. The HC9-A cathode had a 10 deg inverted conical face rather than the flat one of the HC9 cathode. This change in the cathode geometry improved the cathode attachment stability significantly and resulted in operation over a wider range of mass flow rates than the HC9 cathode. Table B.30 shows the performance data obtained in the first run of the HC-9A cathode. These data were encouraging; However, performance data (Table B.31) obtained the next day at the same conditions showed a degradation in overall efficiency of ~ 10%. To determine

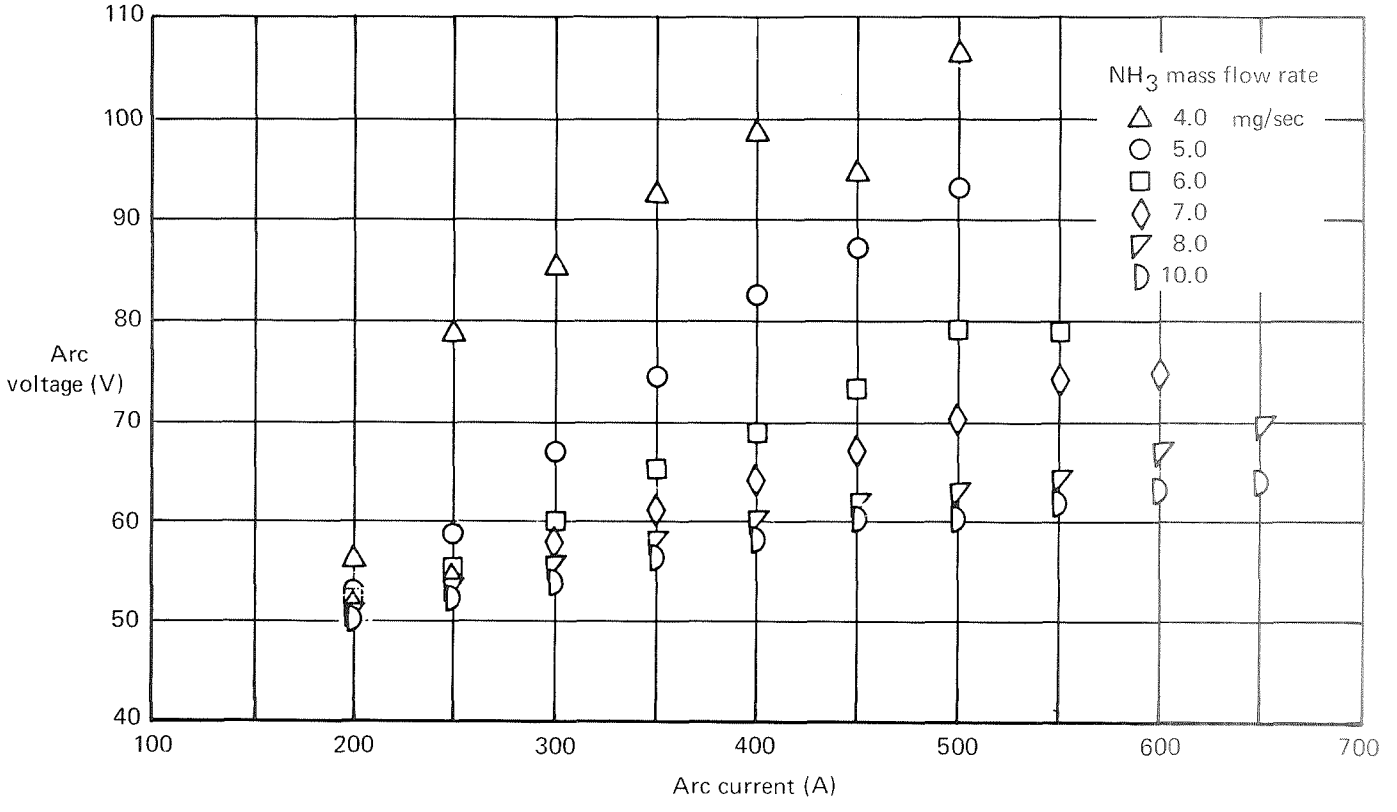

Fig. 4.8 Electrical characteristics of HC9 cathode

the extent of the degradation as a function of test duration, a 10 hour test of this cathode was conducted at a nominal specific impulse level of 3400 sec. The performance results of that test, shown in Table B.32, are in fair agreement with results obtained during the second run of this cathode. The results suggest that the performance degradation leveled off after the first run of the cathode. Figure 4.1f is a frame showing the arc region during operation. Figure 4.9 is a photograph of this cathode taken after the 10 hour test.

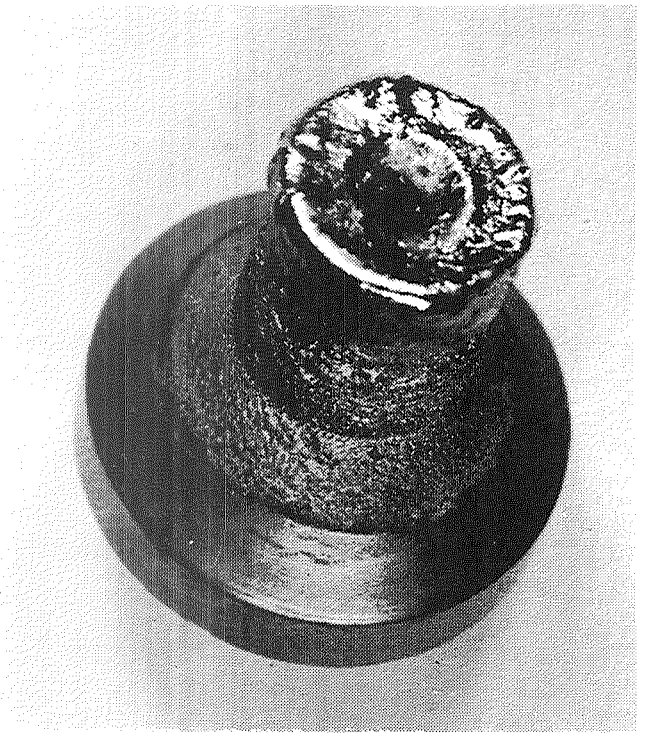

Fig. 4.9 HC9-A Cathode after 10 hour duration test

The effects of the cathode length on the HC9-A cathode performance were investigated. The interelectrode gap (L_g) was increased to a value of 1.11 cm for the test data shown in Table B.33. Comparison of these data with the performance obtained earlier with a gap setting of 0.87 cm shows little difference in performance. However, the increased gap did allow operation at a mass flow of 30 mg/sec which was not possible with the smaller interelectrode gap. Stable operation at 30 mg/sec could not be obtained during the last test of this cathode.

Although several variations of the HC9 series cathode were tested and are discussed below, the HC9-A cathode was the best configuration found. For this reason, this geometry was selected for two additional 10 hour tests of the X-7 thruster. The tests were made on ammonia to document the long term performance of this cathode at high and low specific impulse values.

The goal of the first test was to operate at a specific impulse value of 6500 to 7000 sec at a mass flow rate of 4.6 mg/sec. Stable operation was achieved up to a current level near 400 A; however, the discharge moved out of the cavity section sporadically upon further increase in current. The mass flow was increased to 7 mg/sec and the magnetic field was reduced to 0.08 tesla to stabilize the cathode attachment within the hollow section, at the expense of a reduced specific impulse. After 6 hours of operation, the mass flow was reduced to 4.6 mg/sec with some visual indications that a portion of the discharge was attaching to the outside diameter of the cathode. Figure 4.1g shows a typical frame of the arc region during operation. Attempts to further reduce the mass flow below 4.6 mg/sec resulted in some melting on the outside diameter of the cathode and consequently the mass flow was held at 4.6 mg/sec for the remainder of the test. Table B.34 shows the performance data taken during the above test. Figure 4.10 is a photograph of the HC9-A cathode after the 10 hour test, and indicates the extent of melting and erosion caused by the attachment to the outside diameter.

The results of the test indicate that the high specific impulse values reported earlier on this cathode over short duration tests cannot be maintained for periods on the order of several hours.

The second 10 hour test was made with a goal of operating the HC9-A cathode at high ammonia mass flow and low specific impulse. The test was conducted at a mass flow of 75.5 mg/sec and an arc current level of 550 A. Table B.35 presents the

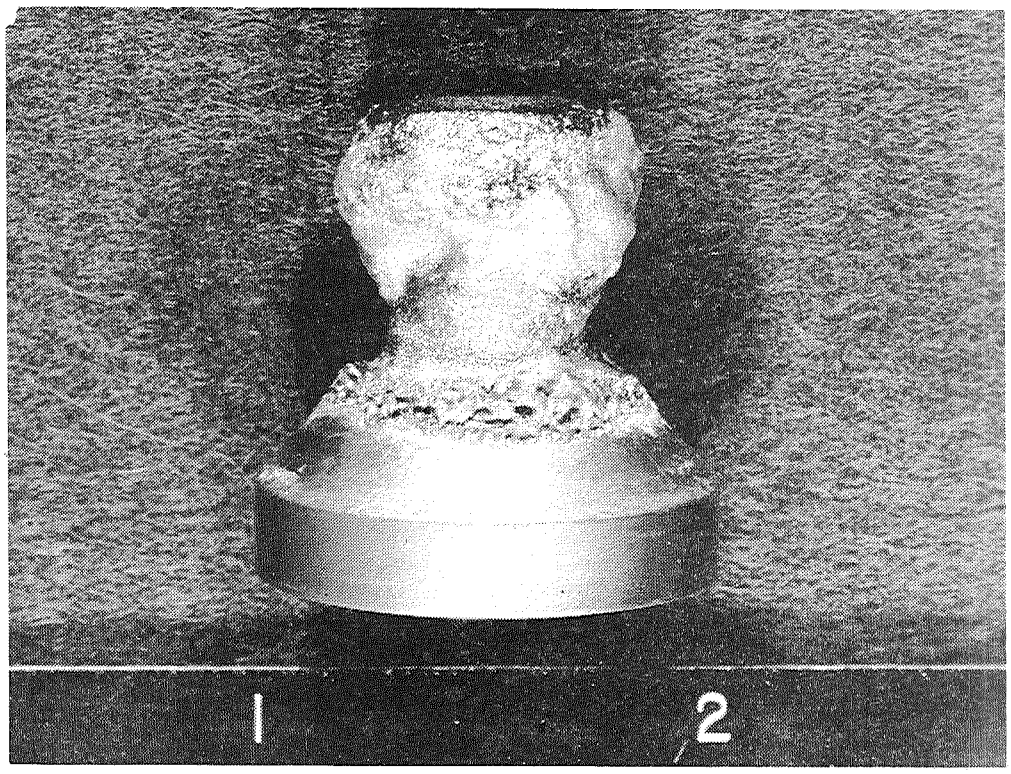

Fig. 4.10 HC9-A Cathode after 10 hour test at high specific impulse

performance data obtained during this test. As indicated on Table B.35, the applied magnetic field was increased to 0.14 tesla after 3 hours of operation to increase the voltage and power levels. The arc voltage readout throughout the test was erratic with slow fluctuation occurring between 35 and 45 V. Visual observation and motion pictures (Fig. 4.1h) of the cathode indicated that the cathode attachment was taking place on both the downstream face and the outside diameter. A photograph (Fig. 4.11) of the HC9-A cathode after this 10 hour test shows that some slight erosion occurred on the outside diameter.

The results of the three 10 hour duration tests conducted on the HC9-A cathode are summarized below:

- **High specific impulse tests** – High specific impulse could not be maintained for periods greater than several hours. Cathode instability resulted in arc attachment to the outside diameter with attendant melting and erosion. Operation at this condition for long duration is definitely not possible.

- **Moderate specific impulse test** – Operation at 3400 sec specific impulse with an overall efficiency of 24% is feasible. Cathode erosion was negligible although some melting of the cathode face was indicated. The possibility of long duration use is considered good.

- **Low specific impulse tests** – Operation at a 600 sec specific impulse range for 10 hours was achieved; however, the arc stability appears marginal for a long duration. In addition, the overall efficiency level is too low to be of much interest.

The HC9-A cathode was also tested with various insulator geometries and various propellants. The results of these tests are reported in Sections 4.1.15 and 4.4.

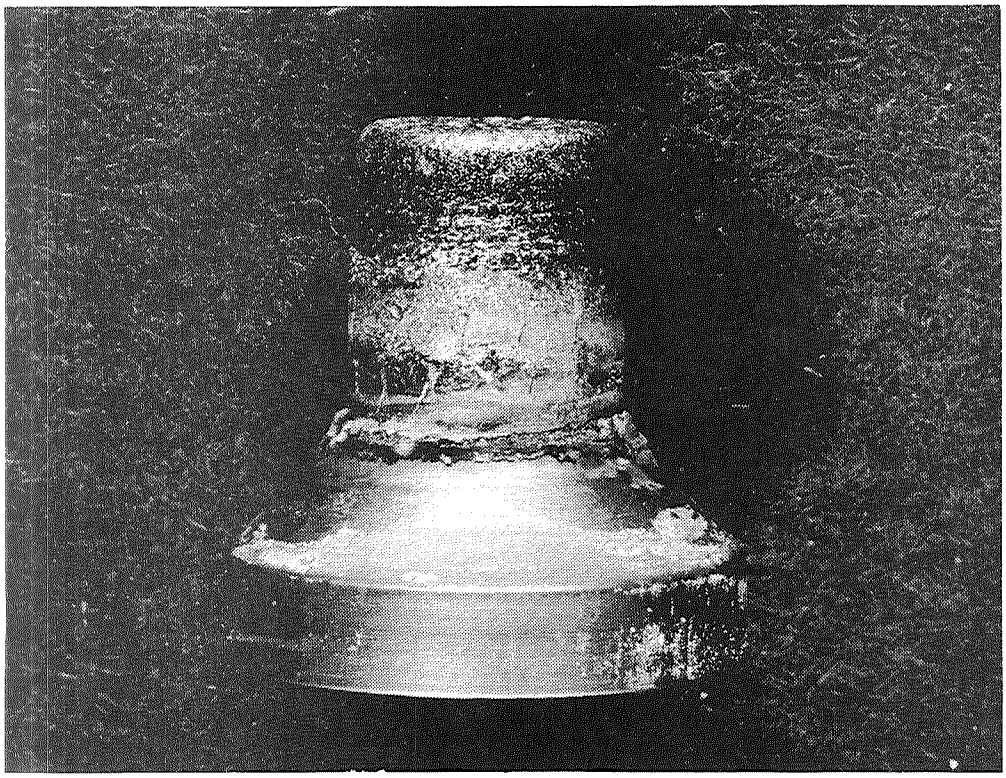

Fig. 4.11 HC9-A Cathode after 10 hour test at low specific impulse

4.1.11 Hollow cathode (HC9-B)

The increase in thrust efficiency gained by inverting the cathode face 10 deg prompted a test of a 20 deg inverted cone cathode (HC9-B) shown in Fig. 3.5h. Unfortunately, this modification merely decreased the stability range of this cathode as compared to the HC9-A cathode. Table B.36 presents the limited performance data obtained on this configuration. The results of the tests of the HC9 type cathode suggest that the range of geometry where stable operation is achieved is quite narrow and is located near a geometry which has a 10 deg inverted conical surface.

Temperatures of the HC9-B cathode front surface were measured during the last four conditions shown in Table B.36. Temperatures were obtained by means of a pyrometer, at the juncture or corner formed by the cavity and inverted conical face surface and also on the inverted conical face close to the outside diameter of the cathode. The temperatures for an emissivity of one, uncorrected for window losses (estimated to be approximately 100 K), are given below:

Arc current (A)	Arc voltage (V)	NH_3 flow rate (mg/sec)	Temperature (internal corner) (K)	Temperature (outside diameter) (K)
400	51	10	3140	–
300	65	4	3130	–
300	56	7	3090	2590
400	60	7	3110	2650

4.1.12 Hollow cathode (HC9-C)

An additional cathode geometry, the HC9-C shown in Fig. 3.5i, was tested. This cathode consisted of a bell mouth shaped cavity. The operating stability of this cathode was quite poor and no performance data were obtained.

4.1.13 Hollow cathode (HC9-D)

Observation of the HC9-A cathode showed that the arc attachment on the cathode under stable conditions occurred at the corner formed by the 10 deg inverted face and the cavity. Since the arc attachment on a corner appeared to be a preferred mode, the HC9-A cavity was modified with a step thus providing an additional corner. This modification, designated HC9-D, is shown in Fig. 3.5k. The HC9-D cathode was difficult to start and stability was achieved only over a narrow range of arc currents. The discharge moved to the outside diameter of the cathode after insertion of the thrust killer and necessitated shut down of the thruster. Several starts were made at various flow rates with little success. During stable operation the arc was attached to both steps. No performance data were taken on this cathode.

4.1.14 Hollow cathode (HC9-E)

The HC9-D cathode was modified with an additional step or corner in the cavity. This three cornered cavity cathode is the HC9-E (Fig. 3.5j). The stability range of this cathode was much wider than that of the HC9-D cathode. Table B.37 shows the performance data obtained on the HC9-E cathode. The efficiency recorded on this cathode is slightly less than that obtained on the HC9-A cathode configuration and as such does not represent an improvement. Visual observation of the cathode indicated that the arc attachment was predominantly on the downstream corner rather than on the internal steps. During initiation of the HC9-E cathode test, when argon comprised the majority of the gas flow, the arc attachment was seen to be evenly distributed on each of the three cavity corners of the cathode. After switching to ammonia flow, the arc localized on the downstream corner.

4.1.15 Insulators

The insulator located between the electrodes (Fig. 3.1) must form a gas seal at the electrode to insulator interfaces, and it also positions the cathode relative to the anode. All of the electrode insulators used in this investigation were made of HBR grade boron nitride.

The geometrical changes of the insulator were made with three purposes: first, to change the position of the cathode, second, to reduce or eliminate insulator erosion, and third, to control arc attachment. The only way to satisfy the second purpose completely seems to be elimination of the insulator from the arc region. Such an approach was taken with the HC2 hollow cathode geometry (Fig. 3.7). The arc was observed to be attached to the bearing plate and also at the interface of the cathode and bearing plate. A closely fitted insulator covering the bearing plate and cathode collar was necessary to eliminate arc attachment in that region. The insulator life was prolonged with this arrangement; however, the cathode attachment could not be easily stabilized.

Using an insulator to serve the third purpose, i.e., to control the arc attachment, was less fruitful. Figure 3.6a shows the insulator used throughout most of the tests. When operating in the unstable mode, the arc seemed to prefer to attach to the cathode outer surface just under the insulator. Several geometries were tried which represent minor modifications of the X-8A insulator (Fig. 3.6b through Fig. 3.6f). The X-8D insulator was designed to constrict the area of arc attachment. It did accomplish the constriction, but only for a short time because the lip eroded away. From observation of these and other insulators it appears that shielding the cathode with an insulator is not the proper approach.

Figure 3.6g shows an insulator used with the large throat anode. Figures 3.6h and 3.6i show insulators with secondary propellant passages. This approach was another scheme used to control the arc attachment and will be discussed further in Section 4.3.

In conclusion, no significant improvement in insulator geometry was achieved.

4.2 Buffered cathode

Several tests of a solid conical buffered cathode were made in a thruster configuration designated X-8, as shown in Fig. 3.3. Generally the buffer serves to ensure higher gas pressures at the cathode tip and consequently higher arc voltages.

Both hollow and solid conical cathodes with tip diameters of 1.27 and 2.54 cm were tested with buffers. The tungsten buffers were 0.635 and 2.223 cm long. The buffer throat diameter was varied from 0.636 to 1.524 cm.

Slightly higher thrust-to-power ratios were obtained on this configuration as compared to the X-7 thruster. However, the buffer throat erosion was intolerable at any current above 200 A.

4.3 Dual propellant feed

The arrangement for supplying dual flow is shown in Fig. 3.8. It consists of two additional inlet ports located in the boron nitride electrode insulator. Separate flow control and metering were provided through the primary (through cathode) and through the secondary (around cathode) flow systems.

The performance data obtained with primary flow only are shown in Table B.38. The arc voltage during this test was the highest thus far recorded on the X-7 thruster. Upon increasing the arc current, the voltage would increase abruptly then drop back about 7%. The drop in voltage appeared to correlate with the time required for the cathode temperature to adjust to the increased current which was the order of a few minutes. The voltage initially recorded at the 500 A condition and listed in Table B.38 was 101 V.

The thruster was started with primary flow through the cathode and then secondary flow was introduced around the cathode. A stable discharge was obtained with the primary flow over a range of flow rates; however, the cathode attachment would move from the cavity to the outside diameter when the secondary flow was introduced. Upon shutting the secondary flow off, the discharge could be made to move back inside the cavity by reducing the primary flow. Table B.39 shows the performance data obtained with only the primary flow.

Comparison of the data of Table B.39 with data obtained on the HC1-F1 0.158 cm cavity cathode (Table B.14) indicates that improved performance is obtained when all of the propellant is introduced through the hollow section. An increase of approximately 10% in the thrust-to-power ratio is obtained when the three injection ports are omitted from the cathode.

The stability problems encountered with secondary injection on the above cathode were circumvented by using the previously tested HC1 cathodes. Introduction of secondary propellant was accomplished, however, at the expense of complete control over the primary flow caused by the three injection ports. It appears that the secondary flow must be injected at the juncture of the cylindrical section and the ramp angle to prevent arc filaments behind the injection location. Table B.40 presents the performance data obtained with a HC1-F1 cathode possessing a cavity diameter of 0.476 cm, over a variety of primary and secondary flow rates. Several features of the data are evident. First, the voltage levels for all mass flows are relatively low, and second, the best performance is achieved when the majority of the flow is introduced through the primary flow circuit. Thrust-to-power ratios are approximately 10-15% lower when the total flow rate is injected through the secondary as compared with the primary system. The low voltage levels were disappointing since it was hoped that higher voltage associated with low primary flow rates could be maintained with high secondary flows: this was not the case with the cathode tested.

Table B.41 shows the performance data obtained with a HC1-F2 cathode having a 0.476 cm diam-

eter cavity. The performance is similar to that obtained with the previous cathode.

A second attempt to operate without the three injection holes at the base of the HC1-F1 (0.476 cm cavity diameter) cathode was made. The electrode gap was reduced to L_g = 0.813 cm. Stability was obtained with mass flow rates to 20 mg/sec through both primary and secondary flow systems. Transfer of the arc attachment from the cavity to the outside diameter of the cathode occurred when the primary mass flow rate was increased above 30 mg/sec. Table B.42 shows the performance data obtained with this cathode. The data points with only primary flow compare well with the data for the HC1-F2 cathodes with the base injection holes. The secondary propellant introduction caused a degradation of the thrust performance.

The next configuration tested was the HC4-F1 cathode shown in Fig. 3.5ℓ. The shape of the cathode tip conforms to the geometry which the HC1-F1 cathodes assumed after several hours of operation. The connection hole identification is the same as for the HC1 cathode (i.e., F1 = 0.158 cm). Table B.43 shows the data obtained with this cathode. Primary mass flows up to 50 mg/sec could be operated with good arc stability; however, the arc voltages were low, falling in the range of 45 to 50 V. Increasing mass flow increases the thrust-to-power ratio to a saturation value of 0.02 N/kW, at a flow rate of 30 mg/sec.

Tables B.44 and B.45 show the performance recorded on the HC4-F2 and HC4-F3 respectively. The thrust-to-power ratios are slightly below the HC4-F1; however, the difference lies within the probable error in the data.

The HC4 cathodes acted similarly to the HC1-F2 which has provided good performance. Thus it is concluded that the shape of the entrance to the cavity section does not significantly affect the overall performance level.

The dual flow cathode data obtained thus far indicates that introducing the total flow into the hollow section provides the best performance. Improved overall efficiency in the I_{sp} range of 2000 to 3500 sec appears to require mass flows above 20 mg/sec coupled with increased power inputs to levels near 40 kW. Only the HC4 cathodes have allowed operation at primary mass flow rate above 20 mg/sec with good stability; however, this operation was accompanied by low arc voltages and hence low efficiencies.

The HC5 cathode shown in Fig. 3.5m was designed to introduce the secondary flow into the arc attachment region. Several attempts have been made to operate this cathode stably. The first attempt was made with the standard X-7 anode with a 1.7 cm anode throat diameter. Arc filaments between the forward edge of the cathode and the upstream corner of the anode throat prevented stable arc operation. The forward edge was then reduced by 0.254 cm and retested; however, the same problem prevented stable operation. The next attempt was made with an additional 0.254 cm removed from the forward edge and with an anode having a 2.54 cm throat diameter. This configuration stabilized operation for a short period with arc attachment on the center portion of the cathode; however, after several minutes the arc transferred to the forward edge and became unstable.

A test of the HC5 cathode was made with the insulator shown in Fig. 3.6i which moved the cathode forward to an interelectrode distance L_g of 0.75 cm. Stable operation was achieved with primary flow through the center of the cathode; however, introduction of the secondary flow caused the arc discharge to attach again to the forward edge and outside diameter resulting in severe erosion. No further testing of this cathode was conducted since the design goal was to increase the mass flow into the cathode attachment region, and this increase by the secondary flow method resulted only in producing gross instabilities in the arc discharge.

4.4 Propellants

The principal test propellant was ammonia. However, if a particular cathode-insulator configuration would not start on ammonia, argon was admitted into the propellant line to initiate the discharge, and then after arc initiation ammonia propellant flow was started. During the initiation of the HC9-E cathode test when argon comprised the majority of the gas flow, the arc attachment was seen to be evenly distributed on each of the three internal corners of the cathode cavity. After the ammonia flow was introduced, the arc attachment localized on the downstream corner.

Subsequently, a number of tests were conducted with an argon-ammonia mixture as the propellant in an attempt to find the proper ratio which would give improved arc attachment stability. Only pure argon gave long term arc stability, but the performance was low. The thrust readout with a 75% volume concentration of argon in the propellant became noticeably smoother than the noisy readout with 100% ammonia.

These observations suggest that the propellant plays a role in establishing cathode attachment stability. With ammonia as the propellant the arc in a hollow cathode configuration is difficult to stabilize whereas operation with argon and lithium produces stable discharges.[5,6]

A series of tests was carried out with the HC9-A cathode with nitrogen as a propellant. Table B.46 presents the performance data obtained during the first run of a new HC9-A cathode. The thrust-to-power ratios measured on this run are all higher than those recorded on the same cathode using ammonia as the propellant. The arc attachment stability on nitrogen was much improved over ammonia and operation over a wider range of mass flow rate was possible. Figure 4.1i is a representative motion picture frame of the arc region with nitrogen. Figure 4-12 shows the thrust performance of the HC9-A cathode with ammonia.

Table B.47 presents performance data obtained on the following day, with the same HC9-A cathode. A slight drop in performance is seen; however, the decrease occurs on the experimental series associated with the thrust measurement. Figure 4.13 shows the thrust performance of the HC9-A cathode with nitrogen.

Since arc attachment stability was improved by operating with nitrogen, the next test sought to determine the effect of hydrogen on arc stability. This test was accomplished by operating the thruster at a constant nitrogen mass flow and varying the amount of hydrogen in the propellant. The results of this test are shown in Table B.48. Except for the first three data points, the nitrogen flow rate was held constant at 24.7 mg/sec throughout the test. With 100% nitrogen, currents up to 700 A were run without difficulty at an average thrust-to-power ratio of 0.0105 N/kW. As hydrogen was introduced, the arc voltage became noticeably more noisy and the arc attachment on the cathode began to fluctuate with excursions of the attachment out of the hollow section on to the front face of the cathode. When the hydrogen mass flow was such as to have approximately equal mole flow rates (i.e., N_2 = 24.7 mg/sec, H_2 = 1.7 mg/sec) or greater, the thrust-to-power ratio decreased to an average value of 0.0141 N/kW. This test indicates that hydrogen plays a detrimental role in terms of hollow cathode arc stability and thrust performance.

Several additional tests of the HC9-A cathode with nitrogen were conducted to further document its performance. Table B.49 presents the performance data taken over a two day period on a new HC9-A cathode. In general, the overall efficiency at a given specific impulse is slightly higher for nitrogen than ammonia with good improvement in arc stability with nitrogen compared with ammonia.

A test was next conducted on a HC1-F2 hollow cathode with nitrogen propellant for purposes of comparison with previous ammonia performance data. Table B.50 shows data obtained for two consecutive runs on nitrogen. Arc attachment to the

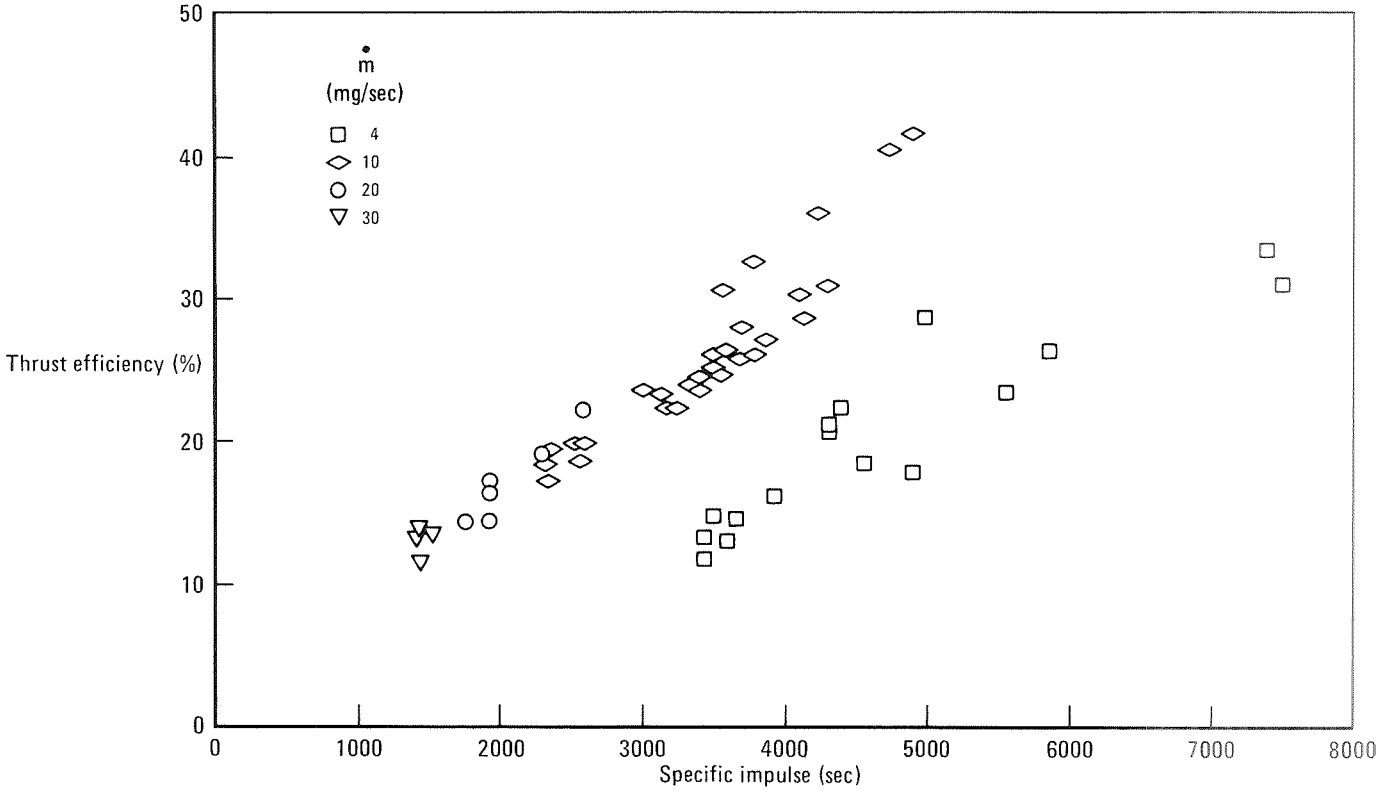

Fig 4.12 Thrust performance of HC9-A cathode with ammonia

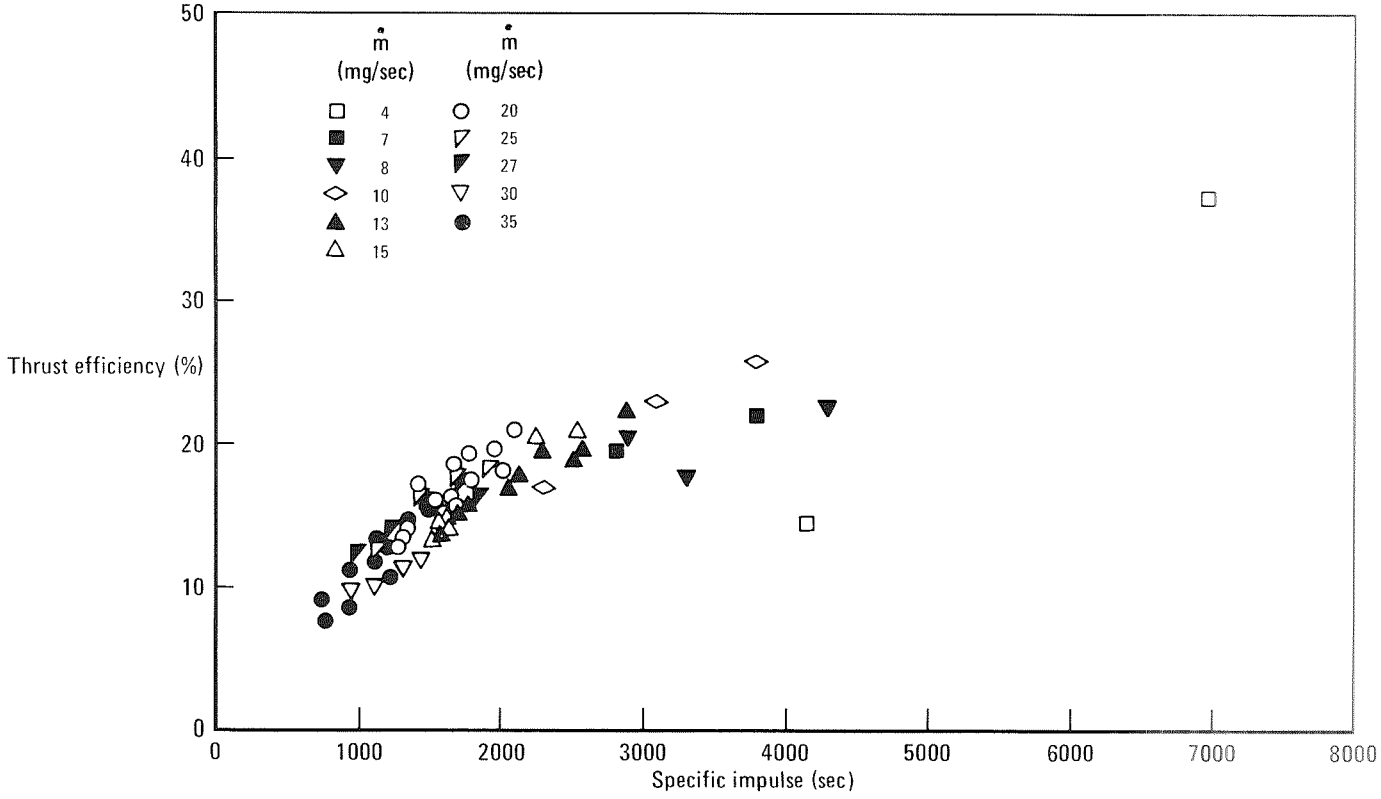

Fig. 4.13 Thrust performance of HC9-A cathode with nitrogen

cathode was not as stable on the HC1-F2 cathode when compared with the HC9-A cathode. The nitrogen performance data for the HC1-F2 cathode are well below those obtained previously on ammonia. Thus, propellant type is shown to affect both arc stability and overall performance with the HC9-A cathode.

Several tests were made of the X-7 thruster with HC9-A hollow cathodes using helium, neon, and xenon as propellants. Table B.51 presents part of the performance data with helium. Some of the first data are questionable because the thrust stand was not moving freely. The thruster operation was very stable. The latter part of Table B.51 shows relatively lower performance which is probably attributable to the condition of the cathode that was damaged when the arc attachment was forced to the outside diameter of the cathode while the killer was in the exhaust plume.

Table B.52 presents the results of additional tests at lower helium mass flow rates. In general, the performance with helium was higher than with ammonia. Figure 4.14 shows the thrust efficiency of the HC9-A cathode with helium. Operation on helium is shown in Fig. 4.1j.

The higher voltages were between 60 and 80 V at helium mass flow rates of 15 and 10 mg/sec, respectively. Insertion of the killer into the stream at voltages above 60 V often caused the arc attachment to shift to the outside of the cathode. The damage caused by the arc attachment on the outside of the cathode was more severe with helium. Melting occurred on the cathode as well as on the anode throat.

Table B.53 presents the data obtained with neon used as the propellant. The performance was comparable to that with ammonia. Figure 4.15 shows

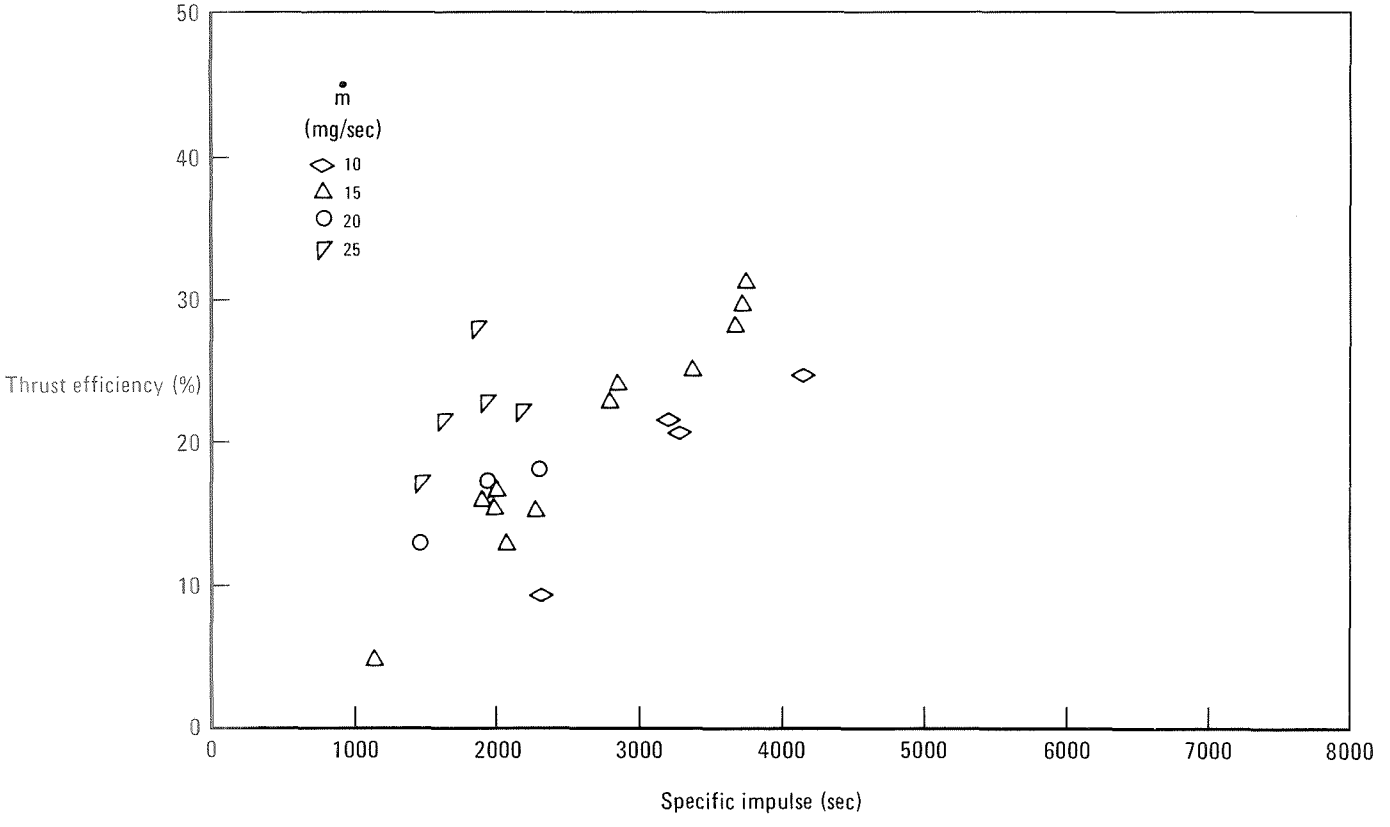

Fig 4.14 Thrust performance of HC9-A cathode with helium

the thrust performance of the HC9-A cathode with neon. Figure 4.1k shows the arc region with neon propellant; however, thruster operation was not stable. Starts were made with argon and after about 10 min of warm-up, the propellant was switched to neon. On two occasions the cathode arc attachment shifted to the outside of the cathode when the propellant was switched from argon to neon. The arc attachment could be returned to the cathode tip cavity by adding argon.

The voltage was high, about 90 V, at a neon flow rate of 10 mg/sec. Cathode tip attachment was almost impossible to maintain at 5 mg/sec. Operation at currents above 300 A was not accomplished. However, the input power was high because of the high voltages. Only one data point was obtained at a flow rate of 15 mg/sec because of exhaustion of the propellant supply.

Table B.54 presents the performance data with xenon propellant. At the low flow rates (5 and 10 mg/sec) the xenon performance was comparable to that with ammonia. Performance was insensitive to flow rate variation as compared with ammonia. Figure 4.16 shows the thrust performance of the HC9-A cathode with xenon. Thruster operation was very stable. Although the arc attachment generally was forced away from the cathode tip by the killer at the higher currents, it could be returned simply by reducing the current. Figure 4.1ℓ is a representative motion picture frame of the arc region with xenon.

Start and warm-up were made on argon, which gave an initial voltage less than 45 V. A few seconds after switching to xenon, the voltage increased to around 80 V. About a minute-and-a-half later, the voltage dropped to about 50 V. The cathode attachment appeared to be the same during both conditions. The exhaust plume was brighter and more

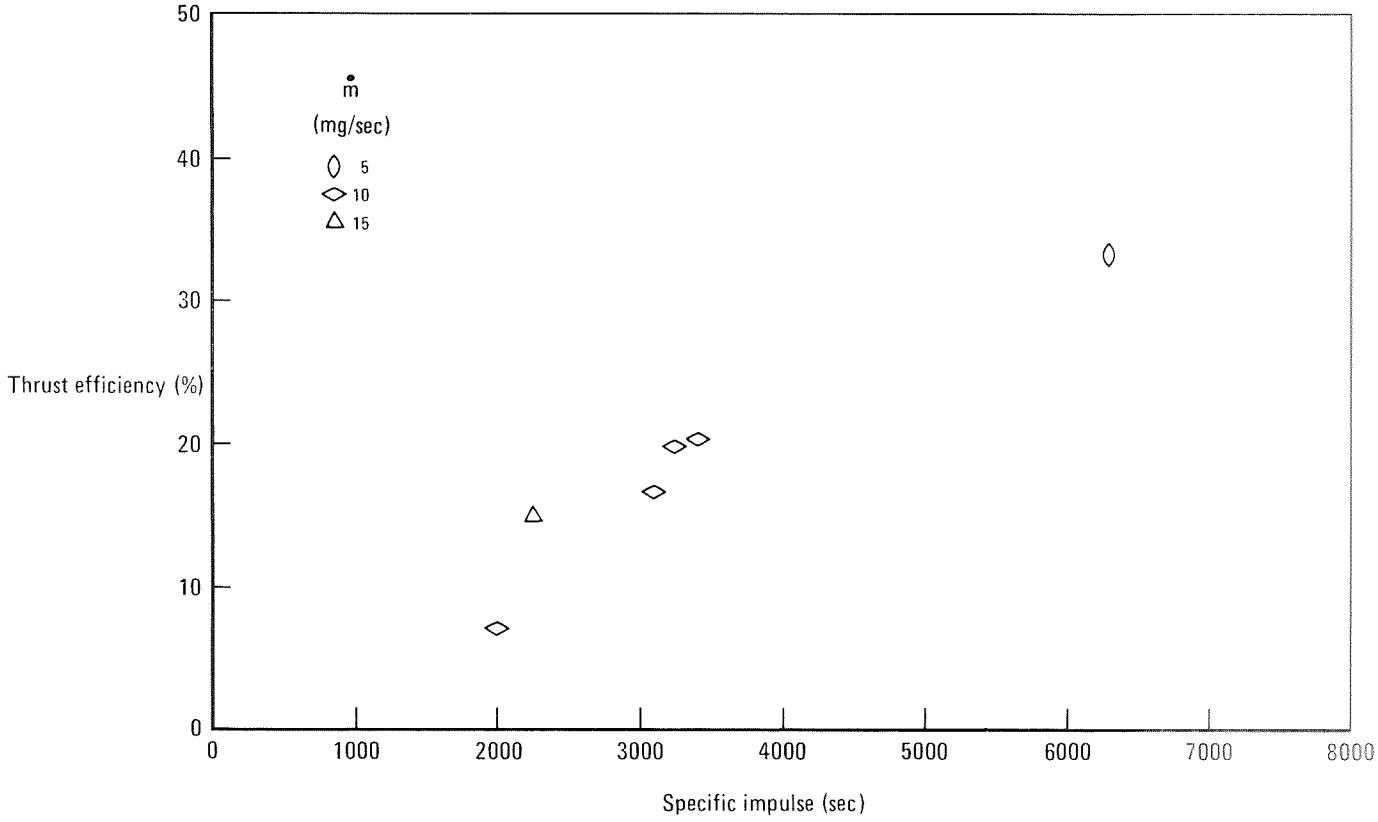

Fig 4.15 Thrust performance of HC9-A cathode with neon

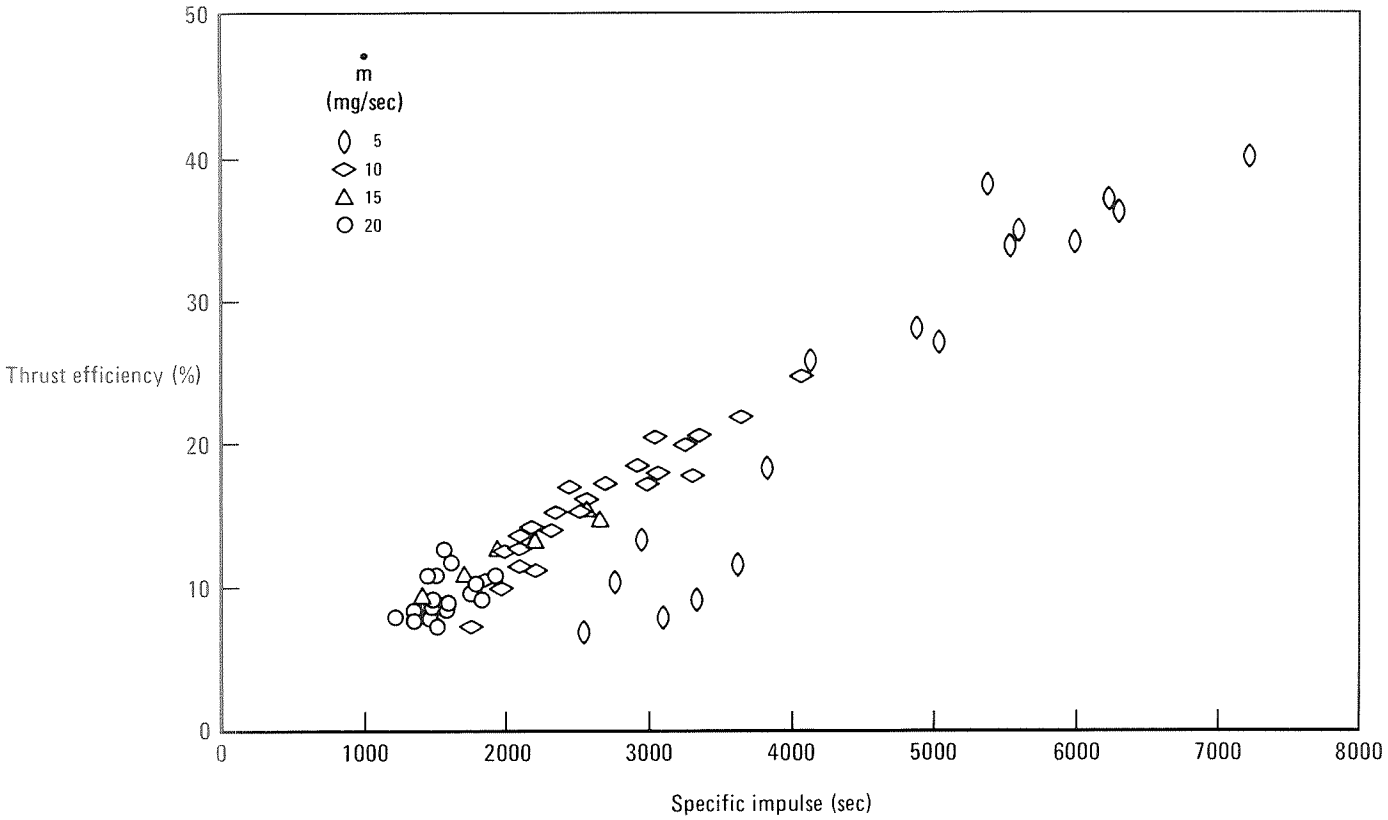

Fig 4.16 Thrust performance of HC9-A cathode with xenon

diffuse during the higher voltage, which is characteristic of a higher energy plume. To test the idea that the higher voltage was caused by an argon-xenon mix, a small burst of argon was added to the xenon flow. The voltage increased to 62 V, supporting the hypothesis.

Summarizing the results of the various propellants tested, the following comparisons may be made relative to ammonia:

(1) Helium performance was somewhat higher although the cathode tip attachment was unstable. Electrode melting was severe.

(2) Neon performance was comparable. Cathode tip attachment was very unstable. The voltages were the highest among all five gases tested.

(3) Xenon performance was comparable at flow rates of 5 to 10 mg/sec. Performance spread caused by flow rate variation was narrow. Thruster operation was very stable. Cathode erosion was low.

(4) Nitrogen performs better than ammonia at specific impulses below 2300 sec. Operation was more stable over a wider range of propellant flow rates. Addition of hydrogen was detrimental to arc stability and thrust performance.

Although the type of propellant does affect the arc stability, the overall performance of the HC9-A cathode varies very little considering the fact that ionization potentials and molecular (atomic) weights of the tested propellants are quite different.

5 Conclusions

Cathode-insulator modification

- The use of hollow cathodes in the X-7 MPD thruster configuration greatly increases the specific impulse capability of this device over short operation time. Maximum specific impulse near 10,000 sec was obtained with hollow cathodes whereas a maximum of only 3200 sec was recorded with solid conical cathodes.
- Cathode attachment instabilities with ammonia prevent operation at high specific impulse values for long periods.
- The range of propellant flow rate operation is lower with the hollow cathodes as compared with the solid conical cathodes. The propellant flow rate with hollow cathodes varied from 4 to 30 mg/sec, compared with 20 to 40 mg/sec with solid conical cathodes.
- The overall performance of the solid conical cathodes was affected very little by the axial position of the cathode.
- The arc voltage increased with smaller axial gaps; consequently, higher input power can be achieved with the smaller gaps.
- Long term arc attachment control by shielding the cathode with an insulator is not feasible because of severe insulator erosion.
- The hollow cathodes possess a positive current-voltage character at low mass flow rates in contrast to a decreasing slope for the solid conical cathodes. The voltage increases with decreasing mass flow rates.
- The cavity shape does not significantly affect the overall performance.

Buffered cathode

- Slightly higher thrust-to-power ratios were obtained on this configuration as compared with the X-7 thruster.
- The buffer throat erosion rate was intolerable at current levels above 200 A.

Dual propellant feed

- The best performance was obtained when the majority of the propellant flow was introduced through the primary flow system.
- The effect of introducing a secondary propellant was a degradation of thrust performance which generally caused a loss of stable arc operation.

- Thrust-to-power ratios were approximately 10-15% lower when the total flow was injected through the secondary instead of the primary flow system.
- The higher voltage associated with low primary flow rates could not be maintained with high secondary flows.

Propellants

- With ammonia as a propellant, the arc is difficult to stabilize in a hollow cathode configuration. Tests of argon-ammonia mixtures showed that the propellant plays an important role in establishing cathode attachment stability.
- Nitrogen performs better than ammonia at specific impulses below 2300 sec. Operation was more stable over a wider range of propellant flow rates.
- Addition of hydrogen to nitrogen was detrimental to arc stability and thrust performance.
- Helium performance was somewhat higher than ammonia although cathode tip arc attachment was unstable. Electrode melting was severe.
- Neon performance was comparable with ammonia. Cathode tip attachment was very unstable. The voltages were the highest among all gases tested.
- Xenon performance was comparable with ammonia at flow rates of 5 to 10 mg/sec. Performance spread caused by flow variation was narrow. Thruster operation was very stable. Cathode erosion was low.
- Although the propellant does affect the arc stability, the overall performance of the HC9-A cathode varies very little considering the fact that ionization potentials and molecular (atomic) weights of tested propellants were quite different.

6 Recommendations for future work

Modification of the X-7 MPD arc thruster have brought about increased specific impulse and thrust efficiency. While power levels up to 46 kW have been tested for short periods, operation for long periods would not be possible at this power. The ways to increase thruster lifetime are not clear. On the other hand, efficiency improvements could be achieved through the development of a high current MPD thruster.

To accomplish this task, the following future work is recommended:

- Scale up the X-7 MPD thruster to increase the power capability. Scaling up would provide room in which one could vary the cathode geometry more freely. Heating and cooling of the cathode could be implemented, and other measures, aimed at increasing lifetime, would also become possible.
- A large rotating cathode could be investigated as a means of increasing the current capability.

Other aspects of thruster technology could be improved by doing work on the following problem areas:

- The variation of propellants, including blends, should be investigated further.
- A lifetest should be conducted with a radiation-cooled minimum weight permanent magnet.
- The effect of pressure on entrainment should be investigated further.

7 Appendix A - triple cathode

A possible method of increasing the current capability of a thruster would be through the use of a multiple cathode. A triple cathode (Fig. 3.4) configuration was devised. The cathodes were situated radially about the thruster centerline and enclosed by a single buffer. The buffer holes and cathode tips were arranged such that a virtual single cathode would be approximated at a distance of 1 cm downstream of the assembly face. The triple cathode assembly (Fig. A-1) was sandwiched between the anode and the magnet.

Three attempts were made to obtain stable arc operation on the triple cathode assembly. In the first start-up, arc-over occurred from the cathodes to the buffer and from the buffer to the anode several minutes after starting. The discharges appeared to be stabilized when the exhaust radiation completely disappeared with an accompanied decrease in arc voltage.

From the arc "tracks" observed it appeared that the cathode to buffer current path took place just behind the gas injection port. The tungsten buffer could not sustain the localized thermal stresses and two radial cracks occurred.

In the next attempt, the tungsten buffer was replaced by boron nitride and 0.41 cm thick tungsten plate 4.0 cm in diameter. The plate was inserted into the boron nitride and had three holes, one in front of each cathode. This configuration was tested for a period of 24 min with the following currents and voltages on the three cathodes: 105, 55, 30 A at 50, 20 and 30 V, respectively. The currents and voltages indicated a non-symmetric arc operation and the test was terminated when some local melting of the plate was observed.

The final test of the triple cathode was made without the tungsten plate. The arc currents were increased in this test up to several hundred amperes, resulting in severe erosion of the boron nitride.

In view of the difficulties encountered with this cathode configuration, no further tests were made.

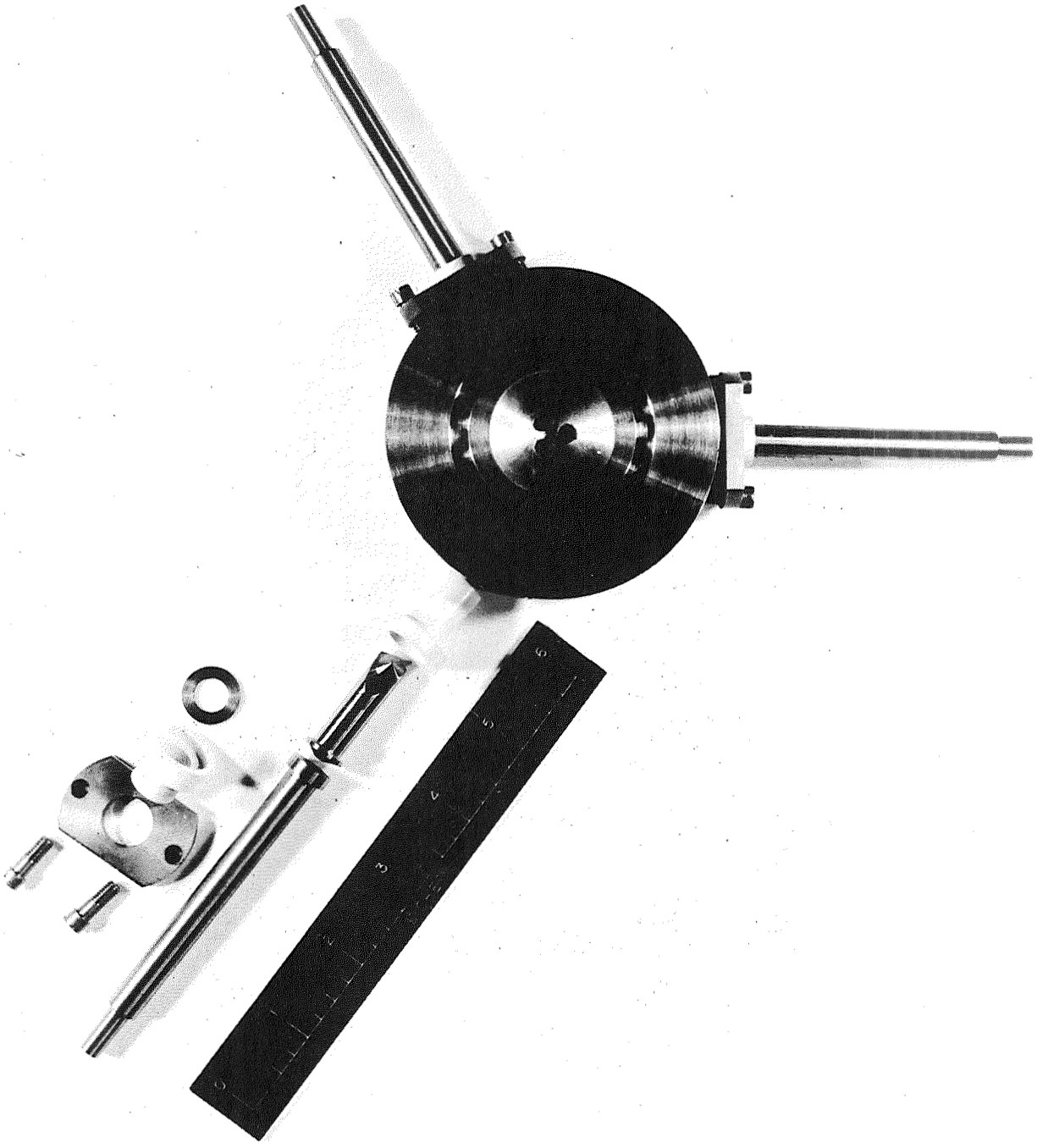

Fig. A-1 Triple cathode geometry

8 Appendix B - X-7 thruster performance data

Table B.1 X-7 thruster performance data

Solid conical cathode, L_g = 1.17 cm

Arc current (A)	Arc voltage (V)	NH_3 flow rate (mg/sec)	Thrust (N)	Power (kW)	Specific impulse (sec)	Thrust power (N/kW)	Thrust efficiency (%)	Magnetic field (tesla)
300	50.0	30	0.262	15.0	894	0.0175	7.62	0.1
300	53.0	40	0.309	15.9	791	0.0194	7.50	
400	41.0	40	0.302	16.4	773	0.0183	6.95	
500	39.0	40	0.355	19.5	909	0.0181	8.08	
600	38.0	40	0.438	22.9	1123	0.0192	10.54	
700	37.0	40	0.481	26.0	1231	0.0185	11.15	
300	43.0	30	0.223	12.9	760	0.0172	6.40	
400	40.0	30	0.268	16.0	910	0.0167	7.37	
500	36.0	30	0.288	18.0	984	0.0160	7.70	
600	34.0	30	0.338	20.5	1155	0.0166	9.35	
700	35.0	30	0.397	24.6	1356	0.0162	10.73	
300	42.0	20	0.169	12.6	864	0.0133	5.64	
400	39.0	20	0.226	15.6	1155	0.0144	8.15	
500	34.0	20	0.242	17.0	1241	0.0142	8.63	
600	32.0	20	0.259	19.2	1326	0.0134	8.73	
300	40.0	10	0.159	12.0	1628	0.0132	10.52	
400	32.0	10	0.151	12.8	1547	0.0118	8.91	
500	30.0	10	0.163	15.0	1668	0.0108	8.84	
600	30.0	10	0.194	18.0	1989	0.0108	10.48	0.1
300	55.0	40	0.283	16.5	723	0.0171	6.04	0.14
400	49.0	40	0.357	19.6	914	0.0181	8.13	
500	43.0	40	0.407	21.6	1042	0.0189	9.63	
600	42.0	40	0.485	25.3	1241	0.0192	11.65	
700	41.0	40	0.540	28.8	1384	0.0187	12.72	
300	51.0	30	0.263	15.3	897	0.0172	7.53	
400	46.0	30	0.317	18.4	1082	0.0172	9.09	
500	41.0	30	0.352	20.6	1202	0.0172	10.08	0.14

Table B.1 X-7 thruster performance data (cont'd)

Solid conical cathode

Arc current (A)	Arc voltage (V)	NH_3 flow rate (mg/sec)	Thrust (N)	Power (kW)	Specific impulse (sec)	Thrust power (N/kW)	Thrust efficiency (%)	Magnetic field (tesla)
				L_g = 1.17 cm				
600	39.0	30	0.375	23.5	1279	0.0160	10.00	0.14
700	38.0	30	0.456	26.7	1557	0.0171	13.03	
300	50.0	20	0.234	15.0	1195	0.0155	9.08	
400	43.0	20	0.245	17.2	1256	0.0142	8.74	
500	40.0	20	0.301	20.0	1542	0.0150	11.33	
600	35.0	20	0.278	21.1	1422	0.0131	9.17	
300	51.0	10	0.222	15.3	2271	0.0144	16.06	
400	51.0	10	0.271	20.5	2773	0.0132	17.97	
500	35.0	10	0.188	17.5	1929	0.0107	10.13	
600	35.0	10	0.236	21.1	2422	0.0112	13.30	0.14
300	57.0	40	0.275	17.1	703	0.0160	5.51	0.165
400	51.0	40	0.360	20.5	922	0.0172	7.94	0.165
500	46.0	40	0.435	23.1	1115	0.0189	10.31	0.165
600	44.0	40	0.500	26.5	1281	0.0189	11.85	0.165
300	54.0	30	0.251	16.2	857	0.0155	6.48	0.170
400	48.0	30	0.305	19.2	1041	0.0158	8.08	0.165
500	43.0	30	0.380	21.6	1296	0.0177	11.17	
600	41.0	30	0.438	24.7	14.97	0.0178	13.02	
700	40.0	30	0.525	28.1	1792	0.0187	16.39	
700	44.0	40	0.633	30.9	1620	0.0205	16.25	
300	49.0	20	0.223	14.7	1140	0.0151	8.43	
400	44.0	20	0.281	17.6	1437	0.0159	11.18	
500	41.0	20	0.332	20.6	1698	0.0161	13.40	
600	39.0	20	0.368	23.5	1884	0.0157	14.46	
300	46.0	10	0.198	13.8	2030	0.0143	14.22	
400	43.0	10	0.261	17.2	2673	0.0151	19.79	
500	41.0	10	0.277	20.6	2834	0.0134	18.66	
600	35.0	10	0.240	21.1	2462	0.0113	13.75	0.165
				L_g = 1.07 cm				
300	61.0	102	0.510	18.3	512	0.0279	6.97	0.10
400	57.0	102	0.636	22.9	638	0.0279	8.68	
500	54.0	102	0.730	27.1	733	0.0270	9.67	
600	52.0	102	0.842	31.3	846	0.0270	11.15	
300	48.0	40	0.298	14.4	763	0.0207	7.72	
400	43.0	40	0.335	17.2	859	0.0194	8.18	0.10

Table B.1 X-7 thruster performance data (cont'd)

Solid conical cathode

Arc current (A)	Arc voltage (V)	NH_3 flow rate (mg/sec)	Thrust (N)	Power (kW)	Specific impulse (sec)	Thrust power (N/kW)	Thrust efficiency (%)	Magnetic field (tesla)
			L_g = 1.07 cm					
500	40.0	40	0.396	20.0	1017	0.0198	9.86	0.10
300	47.0	40	0.243	14.1	623	0.0172	5.24	
400	43.0	30	0.292	17.2	748	0.0170	6.21	
500	40.0	40	0.363	20.0	929	0.0181	8.23	
600	38.0	40	0.421	22.9	1077	0.0184	9.71	
700	36.0	40	0.437	25.3	1120	0.0173	9.49	
300	46.0	30	0.215	13.8	733	0.0155	5.57	
400	40.0	30	0.257	16.0	877	0.0160	6.88	
500	37.0	30	0.291	18.5	994	0.0157	7.64	
600	36.0	30	0.341	21.7	1165	0.0158	8.99	
700	36.0	30	0.410	25.3	1400	0.0162	11.12	
300	40.0	20	0.159	12.0	814	0.0132	5.26	
400	36.0	20	0.190	14.4	974	0.0131	6.28	
500	34.0	20	0.227	17.0	1160	0.0132	7.55	0.10
300	55.0	40	0.273	16.5	698	0.0165	5.63	0.17
			L_g = 0.99 cm					
300	60.0	40	0.378	18.0	967	0.0209	9.90	0.10
400	47.0	40	0.376	18.8	962	0.0199	9.38	
500	40.0	40	0.478	20.0	1223	0.0238	14.26	
600	37.0	40	0.423	22.3	1082	0.0190	10.06	
700	37.0	40	0.483	26.0	1236	0.0185	11.24	
300	47.0	30	0.244	14.1	834	0.0173	7.05	
400	41.0	30	0.270	16.4	921	0.0164	7.39	
500	38.0	30	0.322	19.0	1098	0.0169	9.08	
600	34.0	30	0.347	20.5	1185	0.0170	9.85	
700	32.0	30	0.368	22.5	1256	0.0164	10.07	
300	39.0	20	0.157	11.7	803	0.0133	5.26	
400	33.0	20	0.149	13.2	763	0.0113	4.21	
500	31.0	20	0.192	15.5	984	0.0124	5.96	
600	30.0	20	0.240	18.0	1231	0.0133	8.02	
300	40.0	10	0.177	12.0	1808	0.0147	12.99	
400	40.0	10	0.228	16.0	2331	0.0142	16.18	
500	37.0	10	0.229	18.5	2341	0.0123	14.12	
600	28.0	10	0.189	16.8	1939	0.0112	10.67	0.10

Table B.1 X-7 thruster performance data (cont'd)

Solid conical cathode, L_g = 0.95 cm

Arc current (A)	Arc voltage (V)	NH_3 flow rate (mg/sec)	Thrust (N)	Power (kW)	Specific impulse (sec)	Thrust power (N/kW)	Thrust efficiency (%)	Magnetic field (tesla)
300	50.0	40	0.270	15.0	690	0.0179	6.06	0.10
400	46.0	40	0.348	18.4	891	0.0188	8.24	
500	41.0	40	0.392	20.6	1004	0.0191	9.39	
600	39.0	40	0.475	23.5	1216	0.0202	12.04	
700	38.0	40	0.517	26.7	1324	0.0194	12.56	
300	46.0	30	0.216	13.8	736	0.0156	5.62	
400	43.0	30	0.304	17.2	1038	0.0177	8.96	
400	40.0	30	0.252	16.0	860	0.0157	6.62	
500	37.0	30	0.313	18.5	1068	0.0169	8.82	
500	37.0	30	0.282	18.5	961	0.0152	7.14	
600	37.0	30	0.364	22.3	1242	0.0164	9.94	
700	36.0	30	0.406	25.3	1386	0.0161	10.91	
300	46.0	20	0.199	13.8	1020	0.0144	7.18	
400	36.0	20	0.149	14.4	763	0.0103	3.86	
500	34.0	20	0.214	17.0	1095	0.0126	6.72	
600	31.0	20	0.235	18.6	1205	0.0127	7.45	
700	31.0	20	0.311	21.8	1592	0.0143	11.14	
300	40.0	10	0.162	12.0	1658	0.0134	10.91	
400	39.0	10	0.201	15.6	2060	0.0128	12.96	
500	32.0	10	0.145	16.0	1487	0.0090	6.58	
600	27.0	10	0.165	16.2	1688	0.0101	8.38	0.10
300	48.0	40	0.243	14.4	620	0.0168	5.09	0.14
400	48.0	40	0.330	19.2	844	0.0172	7.07	
500	46.0	40	0.430	23.1	1100	0.0186	10.03	
600	48.0	40	0.439	28.9	1125	0.0152	8.38	
700	40.0	40	0.438	28.1	1123	0.0156	8.58	
300	45.0	30	0.184	13.5	629	0.0136	4.19	
400	43.0	30	0.244	17.2	830	0.0141	5.73	
500	41.0	30	0.312	20.6	1065	0.0152	7.91	
600	40.0	30	0.397	24.1	1356	0.0165	10.96	
700	39.0	30	0.427	27.4	1457	0.0156	11.11	
700	39.0	30	0.382	27.4	1306	0.0139	8.93	0.14

Table B.1 X-7 thruster performance data (cont'd)

Solid conical cathode, L_g = 0.95 cm

Arc current (A)	Arc voltage (V)	NH_3 flow rate (mg/sec)	Thrust (N)	Power (kW)	Specific impulse (sec)	Thrust power (N/kW)	Thrust efficiency (%)	Magnetic field (tesla)
300	50.0	20	0.197	15.0	1010	0.0131	6.48	0.14
400	43.0	20	0.234	17.2	1195	0.0135	7.92	
500	39.0	20	0.279	19.5	1427	0.0142	9.95	
600	36.0	20	0.318	21.7	1628	0.0147	11.69	
700	32.0	20	0.339	22.5	1738	0.0151	12.85	
700	32.0	20	0.283	22.5	1447	0.0126	8.90	
300	40.0	10	0.155	12.0	1587	0.0128	10.01	
400	42.0	10	0.201	16.8	2060	0.0120	12.03	0.14
300	53.0	40	0.264	15.9	675	0.0167	5.47	0.17
400	54.0	40	0.333	21.7	854	0.0154	6.43	0.17
400	46.0	40	0.333	18.4	854	0.0180	7.55	0.17
500	50.0	40	0.375	25.1	959	0.0149	7.02	0.165
600	41.0	40	0.405	24.7	1037	0.0164	8.34	
600	41.0	40	0.368	24.7	942	0.0149	6.87	
700	45.0	40	0.463	31.6	1185	0.0146	8.50	
700	40.0	40	0.414	28.1	1060	0.0147	7.65	
300	50.0	30	0.198	15.0	676	0.0131	4.36	
300	44.0	30	0.198	13.2	676	0.0150	4.95	
400	52.0	30	0.340	20.9	1162	0.0163	9.28	
400	44.0	30	0.242	17.6	827	0.0137	5.56	
500	50.0	30	0.376	25.1	1283	0.0150	9.41	
500	44.0	30	0.376	22.1	1283	0.0171	10.69	
600	46.0	30	0.412	27.7	1406	0.0149	10.25	
600	40.0	30	0.412	24.1	1406	0.0172	11.79	
700	43.0	30	0.407	30.2	1390	0.0134	9.17	
700	38.0	30	0.407	26.7	1390	0.0153	10.38	
300	48.0	20	0.150	14.4	768	0.0104	3.91	
300	43.0	20	0.150	12.9	768	0.0116	4.36	0.165

Table B.1 X-7 thruster performance data (cont'd)

Solid conical cathode, L_g = 0.87 cm

Arc current (A)	Arc voltage (V)	NH_3 flow rate (mg/sec)	Thrust (N)	Power (kW)	Specific impulse (sec)	Thrust power (N/kW)	Thrust efficiency (%)	Magnetic field (tesla)
300	52.0	40	0.302	15.6	773	0.0193	7.31	0.10
400	49.0	40	0.366	19.6	937	0.0186	8.54	
500	45.0	40	0.424	22.6	1085	0.0188	9.97	
600	41.0	40	0.499	24.7	1278	0.0202	12.67	
700	41.0	40	0.562	28.8	1439	0.0195	13.76	
800	38.0	40	0.613	30.5	1570	0.0201	15.45	
300	52.0	30	0.290	15.6	991	0.0185	9.00	
400	49.0	30	0.382	19.6	1306	0.0194	12.44	
500	43.0	30	0.375	21.6	1283	0.0175	10.94	
500	37.0	30	0.261	18.5	891	0.0140	6.13	
600	43.0	30	0.446	25.9	1524	0.0173	12.87	
600	35.0	30	0.312	21.1	1065	0.0148	7.72	
700	40.0	30	0.470	28.1	1604	0.0168	13.14	
700	35.0	30	0.401	24.6	1370	0.0163	10.95	
300	41.0	20	0.138	12.3	708	0.0112	3.88	
300	41.0	20	0.181	12.3	924	0.0146	6.62	
400	37.0	20	0.155	14.8	793	0.0104	4.05	
500	35.0	20	0.193	17.5	989	0.0110	5.33	
600	34.0	20	0.233	20.5	1195	0.0114	6.68	
700	33.0	20	0.266	23.2	1361	0.0115	7.64	
300	50.0	30	0.265	15.0	904	0.0177	7.79	
300	45.0	10	0.188	13.5	1929	0.0139	13.14	
300	56.0	10	0.188	16.8	1929	0.0112	10.55	
400	47.0	10	0.215	18.8	2200	0.0114	12.27	
500	31.0	10	0.148	15.5	1517	0.0095	7.07	
600	26.0	10	0.162	15.6	1658	0.0103	8.39	
700	27.0	10	0.180	18.9	1839	0.0094	8.52	0.10
300	56.0	40	0.277	16.8	708	0.0164	5.69	0.14
400	54.0	40	0.390	21.7	999	0.0180	8.82	
500	51.0	40	0.463	25.6	1185	0.0181	10.51	
600	48.0	40	0.545	28.9	1396	0.0189	12.91	
700	47.0	40	0.649	33.0	1663	0.0197	16.02	
800	45.0	40	0.734	36.1	1879	0.0203	18.69	
300	56.0	30	0.273	16.8	931	0.0162	7.37	0.14

Table B.1 X-7 thruster performance data (cont'd)

Solid conical cathode, L_g = 0.87 cm

Arc current (A)	Arc voltage (V)	NH_3 flow rate (mg/sec)	Thrust (N)	Power (kW)	Specific impulse (sec)	Thrust power (N/kW)	Thrust efficiency (%)	Magnetic field (tesla)
400	54.0	30	0.356	21.7	1216	0.0165	9.78	0.14
500	50.0	30	0.410	25.1	1400	0.0164	11.21	
600	48.0	30	0.490	28.9	1671	0.0170	13.86	
700	45.0	30	0.530	31.6	1808	0.0168	14.84	
700	37.0	30	0.530	26.0	1808	0.0204	18.06	
300	38.0	20	0.112	11.4	572	0.0098	2.74	
400	51.0	20	0.280	20.5	1432	0.0136	9.58	
400	41.0	20	0.207	16.4	1050	0.0126	6.53	
500	46.0	20	0.330	23.1	1693	0.0143	11.88	
500	40.0	20	0.283	20.0	1447	0.0141	9.97	
600	44.0	20	0.377	26.5	1929	0.0142	13.43	
600	38.0	20	0.377	22.9	1929	0.0165	15.56	
700	44.0	20	0.420	30.9	2150	0.0135	14.31	
700	37.0	20	0.337	26.0	1728	0.0129	10.99	
300	46.0	10	0.160	13.8	1638	0.0116	9.26	
400	39.0	10	0.203	15.6	2080	0.0129	13.21	
500	44.0	10	0.250	22.1	2562	0.0112	14.22	
500	40.0	10	0.250	20.0	2562	0.0125	15.64	
600	40.0	10	0.280	24.1	2874	0.0117	16.40	0.14
300	47.0	40	0.244	14.1	625	0.0173	5.29	0.165
400	48.0	40	0.322	19.2	824	0.0167	6.74	
500	48.0	40	0.441	24.1	1130	0.0183	10.15	
600	48.0	40	0.559	28.9	1432	0.0193	13.57	
700	47.0	40	0.698	33.0	1788	0.0212	18.53	
800	46.0	40	0.714	36.9	1932	0.0204	19.33	
300	50.0	30	0.223	15.0	760	0.0148	5.51	
400	50.0	30	0.293	20.0	1001	0.0146	7.17	
500	50.0	30	0.399	25.1	1363	0.0159	10.62	
600	46.0	30	0.454	27.7	1551	0.0164	12.45	
700	43.0	30	0.502	30.2	1715	0.0167	13.97	
300	52.0	20	0.225	15.6	1150	0.0143	8.08	
400	49.0	20	0.275	19.6	1406	0.0139	9.62	
500	46.0	20	0.309	23.1	1582	0.0133	10.38	
600	40.0	20	0.328	24.1	1678	0.0136	11.18	
700	38.0	20	0.359	26.7	1839	0.0134	12.11	
300	44.0	10	0.133	13.2	1366	0.0101	6.74	
400	41.0	10	0.146	16.4	1497	0.0088	6.51	
500	38.0	10	0.169	19.0	1728	0.0088	7.49	0.165

Table B.2 X-7 thruster performance data

Solid conical cathode, 6 hole, L_g = 0.87 cm

Arc current (A)	Arc voltage (V)	NH_3 flow rate (mg/sec)	Thrust (N)	Power (kW)	Specific impulse (sec)	Thrust power (N/kW)	Thrust efficiency (%)	Magnetic field (tesla)
300	70.0	40	0.408	21.1	1045	0.0194	9.91	0.10
400	60.0	40	0.464	24.1	1188	0.0193	11.21	
500	55.0	40	0.542	27.6	1389	0.0197	13.37	
600	51.0	40	0.629	30.7	1610	0.0205	16.15	
700	47.9	40	0.701	33.6	1796	0.0209	18.34	
800	45.2	40	0.746	36.3	1912	0.0206	19.26	
300	66.4	30	0.394	20.0	1346	0.0197	13.01	
400	62.5	30	0.454	25.1	1551	0.0181	13.75	
500	55.8	30	0.533	28.0	1819	0.0190	16.95	
600	51.6	30	0.598	31.1	2043	0.0193	19.27	
700	47.8	30	0.639	33.6	2184	0.0190	20.38	
800	44.9	30	0.669	36.0	2284	0.0185	20.77	0.10
300	69.8	40	0.439	21.0	1125	0.0209	11.53	0.14
400	60.4	40	0.525	24.2	1344	0.0217	14.25	
500	58.5	40	0.642	29.3	1645	0.0219	17.64	
600	56.0	40	0.726	33.7	1859	0.0216	19.60	
700	55.1	40	0.769	38.7	1969	0.0199	19.17	
700	44.0	40	0.619	30.9	1585	0.0200	15.55	
800	53.0	40	0.833	42.6	2133	0.0196	20.45	
300	57.3	30	0.364	17.2	1242	0.0211	12.84	
400	58.9	30	0.452	23.6	1544	0.0191	14.46	
500	59.3	30	0.552	29.7	1886	0.0185	17.14	
600	55.9	30	0.616	33.7	2103	0.0183	18.86	
700	42.0	30	0.549	29.5	1875	0.0186	17.11	
300	57.0	30	0.353	17.1	1205	0.0206	12.15	
300	61.5	20	0.289	18.5	1482	0.0156	11.34	
400	62.3	20	0.372	25.0	1909	0.0149	13.94	
500	61.1	20	0.470	30.7	2406	0.0153	18.07	
600	60.8	20	0.581	36.6	2974	0.0159	23.11	
700	35.2	20	0.367	24.7	1884	0.0149	13.73	0.14
300	62.2	40	0.379	18.7	972	0.0204	9.65	0.165
400	63.0	40	0.487	25.3	1248	0.0193	11.79	
500	62.5	40	0.610	31.4	1562	0.0195	14.89	
600	61.6	40	0.722	37.1	1849	0.0195	17.63	0.165
700	59.0	40	0.835	41.5	2138	0.0202	21.09	0.160
300	64.2	30	0.382	19.3	1306	0.0198	12.66	0.165

Table B.2 X-7 thruster performance data (continued)

Solid conical cathode, 6 hole, L_g = 0.87 cm

Arc current (A)	Arc voltage (V)	NH_3 flow rate (mg/sec)	Thrust (N)	Power (kW)	Specific impulse (sec)	Thrust power (N/kW)	Thrust efficiency (%)	Magnetic field (tesla)
400	64.0	30	0.482	25.7	1644	0.0187	15.10	0.165
500	63.2	30	0.589	31.7	2013	0.0186	18.33	0.165
300	66.5	20	0.306	20.0	1567	0.0153	11.74	0.160
400	65.5	20	0.412	26.3	2110	0.0157	16.20	0.160
500	64.8	20	0.507	32.5	2597	0.0156	19.85	0.160
600	64.0	20	0.633	38.5	3241	0.0164	26.06	0.160
700	40.0	20	0.466	28.1	2386	0.0166	19.38	0.160
300	47.5	10	0.179	14.3	1829	0.0125	11.18	0.160

Table B.3 X-7 thruster performance data

Solid conical cathode, 3 hole at location (A), L_g = 0.95 cm

Arc current (A)	Arc voltage (V)	NH_3 flow rate (mg/sec)	Thrust (N)	Power (kW)	Specific impulse (sec)	Thrust power (N/kW)	Thrust efficiency (%)	Magnetic field (tesla)
300	54.0	40	0.295	16.2	756	0.0181	6.72	0.10
400	50.0	40	0.378	20.0	967	0.0188	8.91	
500	53.0	40	0.525	26.6	1344	0.0197	12.99	
600	54.0	40	0.635	32.5	1628	0.0196	15.59	
700	51.0	40	0.616	35.8	1577	0.0172	13.29	
800	53.0	40	0.771	42.6	1974	0.0181	17.52	
300	69.0	30	0.322	20.8	1098	0.0155	8.33	
400	67.0	30	0.454	26.9	1551	0.0169	12.83	
600	55.0	30	0.557	33.1	1902	0.0169	15.68	
700	40.0	30	0.490	28.1	1674	0.0175	14.32	0.10
300	71.0	20	0.338	21.4	1733	0.0158	13.44	0.14
400	70.0	20	0.432	28.1	2216	0.0154	16.71	
500	47.0	20	0.363	23.6	1859	0.0154	14.01	
600	47.0	20	0.398	28.3	2009	0.0138	13.65	
700	46.0	20	0.425	32.3	2175	0.0131	14.01	
300	65.0	30	0.373	19.5	1272	0.0190	11.87	
400	64.0	30	0.456	25.7	1557	0.0177	13.54	
500	66.0	30	0.556	33.1	1899	0.0168	15.62	
600	48.0	30	0.496	28.9	1695	0.0172	14.26	
700	46.0	30	0.535	32.3	1825	0.0166	14.79	
800	48.0	30	0.589	38.5	2013	0.0153	15.08	
300	66.0	40	0.404	19.8	1035	0.0204	10.31	
400	63.0	40	0.478	25.3	1223	0.0189	11.32	
500	64.0	40	0.588	32.1	1507	0.0183	13.53	
600	65.0	40	0.702	39.1	1798	0.0179	15.81	
700	46.0	40	0.618	32.3	1582	0.0191	14.82	
800	47.0	40	0.712	37.7	1824	0.0189	16.86	0.14
300	69.0	40	0.392	20.8	1004	0.0189	9.29	0.165
400	71.0	40	0.486	28.5	1246	0.0171	10.42	0.165
500	71.0	40	0.615	35.6	1575	0.0173	13.32	0.165
600	70.0	40	0.708	42.2	1814	0.0168	14.93	0.165
700	48.0	40	0.659	33.7	1688	0.0196	16.16	0.160
700	66.0	40	0.784	46.4	2007	0.0169	16.62	0.160
800	46.0	40	0.703	36.9	1801	0.0190	16.80	0.160
300	71.0	30	0.358	21.4	1222	0.0168	10.03	0.165
400	71.0	30	0.451	28.5	1540	0.0158	11.95	0.160

Table B.3 X-7 thruster performance data (continued)

Solid conical cathode, 3 hole at location (A), L_g = 0.95 cm

Arc current (A)	Arc voltage (V)	NH_3 flow rate (mg/sec)	Thrust (N)	Power (kW)	Specific impulse (sec)	Thrust power (N/kW)	Thrust efficiency (%)	Magnetic field (tesla)
500	72.0	30	0.551	36.1	1882	0.0153	14.07	0.160
600	52.0	30	0.527	31.3	1798	0.0169	14.82	0.160
300	76.0	20	0.308	22.9	1577	0.0134	10.40	0.165
400	75.0	20	0.405	30.1	2075	0.0134	13.68	0.165
500	73.0	20	0.502	36.6	2572	0.0137	17.28	0.165
600	52.0	20	0.404	31.3	2070	0.0129	13.09	0.165

Table B.4 X-7 thruster performance data

Hollow cathode - with flow HC2 cathode

Arc current (A)	Arc voltage (V)	NH_3 flow rate (mg/sec)	Thrust (N)	Power (kW)	Specific impulse (sec)	Thrust power (N/kW)	Thrust efficiency (%)	Magnetic field (tesla)
300	46.0	40	0.185	13.8	472	0.0133	3.08	0.17
400	39.0	40	0.197	15.6	505	0.0126	3.11	0.17
500	35.0	40	0.210	17.5	537	0.0120	3.14	0.17
300	60.0	53	0.335	18.0	648	0.0186	5.90	0.1
400	52.0	53	0.370	20.9	714	0.0178	6.20	0.1
400	59.0	53	0.427	23.7	824	0.0180	7.28	0.14

Table B.5 X-7 thruster performance data

Hollow cathode - with flow HC2 cathode

Arc current (A)	Arc voltage (V)	NH_3 flow rate (mg/sec)	Thrust (N)	Power (kW)	Specific impulse (sec)	Thrust power (N/kW)	Thrust efficiency (%)	Magnetic field (tesla)
300	57.0	4.6	0.186	17.1	4151	0.0109	22.08	0.1
400	53.0	4.6	0.227	21.3	5046	0.0106	26.33	0.1
500	52.0	4.6	0.349	26.1	7777	0.0133	50.99	0.1
600	50.0	4.6	0.429	30.1	9569	0.0143	66.90	0.1

Table B.6 X-7 thruster performance data

Hollow cathode - with flow HC2

Arc current (A)	Arc voltage (V)	NH_3 flow rate (mg/sec)	Thrust (N)	Power (kW)	Specific impulse (sec)	Thrust power (N/kW)	Thrust efficiency (%)	Magnetic field (tesla)
400	65.0	10	0.343	26.1	3517	0.0131	22.67	0.10
500	66.0	10	0.394	33.1	4040	0.0119	23.56	0.10
450	60.0	20	0.367	27.1	1879	0.0135	12.46	0.10
400	64.0	20	0.323	25.7	1653	0.0126	10.17	0.10

Table B.7 X-7 thruster performance data

Hollow cathode - no flow HC1-F2, 0.159 cm cavity

Arc current (A)	Arc voltage (V)	NH_3 flow rate (mg/sec)	Thrust (N)	Power (kW)	Specific impulse (sec)	Thrust power (N/kW)	Thrust efficiency (%)	Magnetic field (tesla)
200	62.0	30	0.222	12.4	757	0.0178	6.60	0.10
300	60.0	30	0.315	18.0	1075	0.0174	9.18	↓
400	55.0	30	0.430	22.1	1467	0.0195	13.98	
500	55.0	30	0.526	27.6	1795	0.0190	16.75	
300	54.0	20	0.280	16.2	1437	0.0173	12.14	
400	57.0	20	0.367	22.9	1879	0.0161	14.76	↓
500	60.0	20	0.477	30.1	2442	0.0159	18.94	0.10
300	62.0	30	0.370	18.6	1262	0.0198	12.25	0.14
400	64.0	30	0.447	25.7	1527	0.0174	13.02	↓
500	66.0	30	0.565	33.1	1929	0.0171	16.12	
300	66.0	20	0.317	19.8	1623	0.0160	12.67	↓
400	70.0	20	0.426	28.1	2180	0.0152	16.18	0.14
300	69.0	30	0.358	20.8	1222	0.0173	10.32	0.17
400	72.0	30	0.456	28.9	1557	0.0158	12.04	↓
300	75.0	20	0.329	22.6	1683	0.0145	12.00	↓
400	76.0	20	0.436	30.5	2236	0.0143	15.67	0.17

Table B.8 X-7 thruster performance data

Hollow cathode - no flow HC1-FO, 0.318 cm cavity

Arc current (A)	Arc voltage (V)	NH_3 flow rate (mg/sec)	Thrust (N)	Power (kW)	Specific impulse (sec)	Thrust power (N/kW)	Thrust efficiency (%)	Magnetic field (tesla)
200	52.0	10	0.136	10.4	1396	0.0130	8.94	0.10
300	57.0	10	0.211	17.1	2160	0.0123	13.00	↓
400	60.0	10	0.310	24.1	3175	0.0128	20.02	
500	62.0	10	0.426	31.1	4361	0.0137	29.24	
600	30.0	10	0.275	18.0	2813	0.0152	20.96	0.10
600	36.0	10	0.275	21.7	2813	0.0127	17.46	0.14
300	60.0	30	0.318	18.0	1085	0.0177	9.35	
400	61.0	30	0.416	24.5	1420	0.0170	11.81	
500	61.0	30	0.420	30.6	1433	0.0137	9.63	
600	62.0	30	0.416	37.3	1420	0.0111	7.75	
300	64.0	20	0.282	19.2	1447	0.0147	10.39	
400	64.0	20	0.372	25.7	1904	0.0145	13.50	
500	64.0	20	0.369	32.1	1889	0.0115	10.63	
600	40.0	20	0.298	24.1	1527	0.0124	9.26	
600	46.0	20	0.334	27.7	1713	0.0121	10.13	
300	68.0	10	0.270	20.5	2763	0.0131	17.84	↓
400	71.0	10	0.375	28.5	3839	0.0131	24.72	0.14
300	67.0	30	0.324	20.2	1105	0.0161	8.69	0.167
400	67.0	30	0.326	26.9	1112	0.0121	6.59	0.165
400	67.0	30	0.358	26.9	1222	0.0133	7.97	0.165
500	50.0	30	0.329	25.1	1122	0.0131	7.20	0.165
500	60.0	30	0.329	30.1	1122	0.0109	6.00	0.165
300	57.0	10	0.237	17.1	2432	0.0137	16.48	0.10
400	60.0	10	0.311	24.1	3185	0.0129	20.14	↓
500	63.0	10	0.402	31.6	4120	0.0127	25.68	
175	58.0	30	0.164	10.2	559	0.0161	4.40	
250	52.0	30	0.229	13.0	781	0.0176	6.71	
300	49.0	30	0.268	14.7	914	0.0181	8.13	
350	48.0	30	0.307	16.8	1048	0.0182	9.35	
400	48.0	30	0.351	19.2	1199	0.0182	10.70	
450	48.0	30	0.391	21.7	1336	0.0180	11.82	
500	49.0	30	0.429	24.6	1463	0.0175	12.50	
550	51.0	30	0.419	28.1	1430	0.0149	10.42	
600	51.0	30	0.400	30.7	1366	0.0130	8.72	
300	53.0	20	0.243	15.9	1246	0.0152	9.30	
400	54.0	20	0.314	21.7	1607	0.0145	11.40	
500	55.0	20	0.395	27.6	2025	0.0143	14.21	
600	56.0	20	0.535	33.7	2738	0.0159	21.27	0.10

Table B.9 X-7 thruster performance data

Hollow cathode - no flow, HC1-FO
0.476 cm cavity, L_g = 0.845 cm)

Arc current (A)	Arc voltage (V)	NH_3 flow rate (mg/sec)	Thrust (N)	Power (kW)	Specific impulse (sec)	Thrust power (N/kW)	Thrust efficiency (%)	Magnetic field (tesla)
200	56.0	20	0.186	11.2	949	0.0165	7.67	0.10
300	46.0	20	0.248	13.8	1271	0.0180	11.16	
400	45.0	20	0.319	18.0	1633	0.0176	14.11	
500	46.0	20	0.382	23.1	1954	0.0166	15.83	
600	51.0	20	0.495	30.7	2537	0.0162	20.05	0.10
300	54.0	20	0.268	16.2	1371	0.0165	11.06	0.14
400	56.0	20	0.361	22.5	1849	0.0161	14.54	
500	58.0	20	0.458	29.1	2346	0.0158	18.09	
600	59.0	20	0.550	35.5	2819	0.0155	21.39	0.14
300	57.0	20	0.286	17.1	1467	0.0167	11.99	0.17
400	61.0	20	0.396	24.5	2030	0.0162	16.09	0.17
500	62.0	20	0.488	31.1	2497	0.0157	19.17	0.165
600	49.0	20	0.464	29.5	2376	0.0157	18.31	0.165
300	45.0	20	0.255	13.5	1356	0.0196	12.99	0.10
300	50.0	10	0.235	15.0	2411	0.0157	18.47	
400	56.0	10	0.306	22.5	3120	0.0136	20.83	
500	60.0	10	0.396	30.1	4040	0.0131	25.92	0.10
300	50.0	10	0.242	15.0	2482	0.0161	19.57	0.14
400	60.0	10	0.340	24.1	3487	0.0141	24.14	
500	67.0	10	0.460	33.6	4713	0.0137	31.59	0.14
300	60.0	10	0.282	18.0	2884	0.0156	22.02	0.17
400	69.0	10	0.398	27.7	4080	0.0144	28.74	0.17
200	59.0	30	0.204	11.8	696	0.0173	5.88	0.10
300	53.0	30	0.280	15.9	954	0.0176	8.19	
400	46.0	30	0.354	18.4	1209	0.0192	11.36	
500	45.0	30	0.420	22.6	1433	0.0186	13.06	
600	45.0	30	0.493	27.1	1685	0.0182	15.03	0.10
300	52.0	30	0.304	15.6	1038	0.0194	9.88	0.14
400	52.0	30	0.385	20.9	1316	0.0184	11.91	
500	53.0	30	0.477	26.6	1628	0.0179	14.29	
600	53.0	30	0.532	31.9	1815	0.0167	14.81	0.14
300	56.0	30	0.311	16.8	1061	0.0184	9.59	0.17
400	57.0	30	0.413	22.9	1410	0.0180	12.47	0.17
500	56.0	30	0.505	28.1	1725	0.0179	15.19	0.165
600	58.0	30	0.482	34.9	1644	0.0138	11.11	0.165

Table B.10 X-7 thruster performance data

Hollow cathode - no flow, HC1-FO
0.476 cm cavity, L_g = 0.845 cm)

Arc current (A)	Arc voltage (V)	NH_3 flow rate (mg/sec)	Thrust (N)	Power (kW)	Specific impulse (sec)	Thrust power (N/kW)	Thrust efficiency (%)	Magnetic field (tesla)
200	49.0	20	0.135	9.8	693	0.0137	4.67	0.10
300	43.0	20	0.193	12.9	989	0.0149	7.23	↓
400	42.0	20	0.266	16.8	1361	0.0158	10.51	
500	42.0	20	0.344	21.1	1763	0.0164	14.11	
600	44.0	20	0.436	26.5	2236	0.0165	18.04	0.10
300	49.0	20	0.238	14.7	1221	0.0162	9.66	0.14
400	49.0	20	0.325	19.6	1663	0.0165	13.45	↓
500	51.0	20	0.412	25.6	2160	0.0165	17.44	
600	53.0	20	0.533	31.9	2728	0.0167	22.31	0.14
300	53.0	20	0.247	15.9	1266	0.0155	9.61	0.165
400	53.0	20	0.364	21.3	1864	0.0172	15.62	0.165
500	55.0	20	0.451	27.6	2311	0.0164	18.51	0.16
600	55.0	20	0.500	33.1	2562	0.0151	18.96	0.16
300	43.0	10	0.202	12.9	2070	0.0156	15.83	0.10
400	47.0	10	0.259	18.8	2653	0.0137	17.84	0.10
500	49.0	10	0.329	24.6	3366	0.0133	22.04	0.10
300	50.0	10	0.210	15.0	2150	0.0139	14.69	0.14
400	51.0	10	0.281	20.5	2874	0.0137	19.29	0.14
500	55.0	10	0.386	27.6	3959	0.0140	27.16	0.14
300	53.0	10	0.233	15.9	2381	0.0146	17.00	0.165
400	53.0	10	0.295	21.3	3025	0.0138	20.56	0.165
500	57.0	10	0.402	28.6	4120	0.0140	28.38	0.16

Table B.11 X-7 thruster performance data

(Hollow cathode - no flow, HC1-FO
0.476 cm cavity, L_g = 0.660)

Arc current (A)	Arc voltage (V)	NH_3 flow rate (mg/sec)	Thrust (N)	Power (kW)	Specific impulse (sec)	Thrust power (N/kW)	Thrust efficiency (%)	Magnetic field (tesla)
200	50.0	20	0.153	10.0	783	0.0153	5.85	0.10
300	47.0	20	0.217	14.1	1110	0.0153	8.33	↓
400	45.0	20	0.290	18.0	1482	0.0160	11.63	↓
500	47.0	20	0.392	23.6	2009	0.0167	16.38	↓
600	48.0	20	0.458	28.9	2346	0.0159	18.22	0.10
300	54.0	20	0.258	16.2	1321	0.0159	10.27	0.14
400	52.0	20	0.341	20.9	1748	0.0164	14.00	↓
500	53.0	20	0.424	26.6	2170	0.0160	16.94	↓
600	54.0	20	0.515	32.5	2638	0.0159	20.46	0.14
300	57.0	20	0.272	17.1	1391	0.0158	10.79	0.17
400	55.0	20	0.361	22.1	1849	0.0164	14.81	0.165
500	55.0	20	0.443	27.6	2271	0.0161	17.87	0.165
600	57.0	20	0.459	34.3	2351	0.0163	15.40	0.165
300	49.0	10	0.192	14.7	1969	0.0130	12.57	0.10
400	50.0	10	0.268	20.0	2743	0.0133	17.93	0.10
500	54.0	10	0.349	27.1	3577	0.0128	22.58	0.10
300	52.0	10	0.225	15.6	2301	0.0143	16.17	0.14
400	54.0	10	0.312	21.7	3195	0.0144	22.53	0.14
500	59.0	10	0.379	29.6	3879	0.0127	24.30	0.14
300	54.0	10	0.228	16.2	2331	0.0140	15.98	0.17
400	57.0	10	0.309	22.9	3165	0.0135	20.94	0.165

Table B.12 X-7 thruster performance data

(Hollow cathode - no flow, HC1-FO
0.476 cm cavity, L_g = 0.845 cm)

Arc current (A)	Arc voltage (V)	NH_3 flow rate (mg/sec)	Thrust (N)	Power (kW)	Specific impulse (sec)	Thrust power (N/kW)	Thrust efficiency (%)	Magnetic field (tesla)
200	52.0	20	0.139	10.4	713	0.0133	4.66	0.10
300	50.0	20	0.211	15.0	1080	0.0140	7.41	↓
400	47.0	20	0.288	18.8	1477	0.0153	11.06	
500	50.0	20	0.390	25.1	1999	0.0156	15.24	
600	53.0	20	0.496	31.9	2542	0.0156	19.37	0.10
300	55.0	20	0.250	16.5	1281	0.0151	9.48	0.14
400	55.0	20	0.343	22.1	1758	0.0156	13.39	0.14
500	58.0	20	0.454	29.1	2326	0.0156	17.78	0.14
300	58.0	20	0.269	17.4	1376	0.0154	10.38	0.17
400	59.0	20	0.363	23.7	1859	0.0153	13.95	0.165
500	60.0	20	0.487	30.1	2492	0.0162	19.73	0.165
300	51.0	10	0.213	15.3	2180	0.0138	14.81	0.10
400	52.0	10	0.281	20.9	2884	0.0134	19.05	0.10

Table B.13 X-7 thruster performance data

Hollow cathode - no flow, HC1-FO, 0.476 cm cavity hole

Arc current (A)	Arc voltage (V)	NH_3 flow rate (mg/sec)	Thrust (N)	Power (kW)	Thrust power (N/kW)	Magnetic field (tesla)	Background pressure (10^{-3} Torr)
400	57.0	6.0	0.291	22.9	0.0127	0.10	10
↓	56.0	↓	0.298	22.5	0.0132	↓	15
	55.0		0.301	22.1	0.0136		18
	55.0		0.305	22.1	0.0138		20
	53.0		0.284	21.3	0.0133		22
	54.0		0.275	21.7	0.0127		26
	52.0		0.269	20.9	0.0128		32
	52.0		0.266	20.9	0.0127		36
	52.0		0.248	20.9	0.0119		41
	52.0		0.250	20.9	0.0120		45
	51.0		0.251	20.5	0.0123		50
400	50.0	6.0	0.222	20.0	0.0111	0.10	68

Table B.14 X-7 thruster performance data

Hollow cathode - with flow, HC1-F1
0.159 cm cavity, L_g = 0.845 cm

Arc current (A)	Arc voltage (V)	NH_3 flow rate (mg/sec)	Thrust (N)	Power (kW)	Specific impulse (sec)	Thrust power (N/kW)	Thrust efficiency (%)	Magnetic field (tesla)
200	52.0	10	0.141	10.4	1447	0.0135	9.59	0.10
200	65.0	4	0.155	13.0	3780	0.0119	22.00	
250	69.0	4	0.200	17.3	4881	0.0116	27.64	
300	72.0	4	0.254	21.7	6197	0.0117	35.58	
350	75.0	4	0.303	26.3	7393	0.0115	41.67	
400	77.0	4	0.359	30.9	8757	0.0116	49.83	
450	80.0	4	0.409	36.1	9978	0.0113	55.34	
200	51.0	10	0.172	10.2	1757	0.0168	14.44	
300	53.0	10	0.251	15.9	2572	0.0158	19.83	
400	58.0	10	0.320	23.3	3276	0.0137	22.04	
500	62.0	10	0.434	31.1	4442	0.0139	30.32	
600	52.0	10	0.437	31.3	4472	0.0139	30.54	
600	47.0	20	0.472	28.3	2417	0.0167	19.74	0.10

Table B.15 X-7 thruster performance data

Hollow cathode - with flow, HC1-F1
0.318 cm cavity, L_g = 0.845 cm

Arc current (A)	Arc voltage (V)	NH_3 flow rate (mg/sec)	Thrust (N)	Power (kW)	Specific impulse (sec)	Thrust power (N/kW)	Thrust efficiency (%)	Magnetic field (tesla)
200	57.0	4	0.121	11.4	2709	0.0106	14.11	0.10
300	63.0	4	0.223	18.9	4930	0.0118	28.50	
400	67.0	4	0.315	26.9	7013	0.0117	40.22	
300	44.0	20	0.279	13.2	1427	0.0211	14.70	
400	45.0	20	0.360	18.0	1844	0.0199	18.00	
500	46.0	20	0.495	23.1	2537	0.0215	26.68	
600	47.0	20	0.509	28.3	2607	0.0180	22.98	0.10
300	57.0	20	0.292	17.1	1497	0.0191	12.49	0.14
400	55.0	20	0.379	22.1	1939	0.0172	16.29	0.14

Table B.16 X-7 thruster performance data

Hollow cathode - with flow, HC1-F1
0.476 cm cavity, L_g = 0.845 cm

Arc current (A)	Arc voltage (V)	NH_3 flow rate (mg/sec)	Thrust (N)	Power (kW)	Specific impulse (sec)	Thrust power (N/kW)	Thrust efficiency (%)	Magnetic field (tesla)
200	52.0	4	0.099	10.4	2206	0.0095	10.26	0.10
300	47.0	4	0.147	14.1	3277	0.0104	16.69	
350	47.0	4	0.180	16.5	3998	0.0109	21.29	
400	46.0	4	0.209	18.4	4653	0.0113	25.79	
450	47.0	4	0.241	21.2	5374	0.0114	29.93	
500	48.0	4	0.272	24.1	6051	0.0113	33.44	
400	41.0	10	0.251	16.4	2572	0.0153	19.23	
450	40.0	10	0.292	18.0	2994	0.0162	23.74	
500	41.0	10	0.328	20.6	3356	0.0159	26.18	
550	41.0	10	0.356	22.6	3648	0.0157	28.12	
600	41.0	10	0.356	24.7	3648	0.0144	25.77	0.10

Table B.17 X-7 thruster performance data

Hollow cathode - with flow, HC1-F2
0.159 cm cavity, L_g = 0.845 cm

Arc current (A)	Arc voltage (V)	NH_3 flow rate (mg/sec)	Thrust (N)	Power (kW)	Specific impulse (sec)	Thrust power (N/kW)	Thrust efficiency (%)	Magnetic field (tesla)
200	59.0	4	0.138	11.8	3080	0.0117	17.62	0.10
300	61.0	4	0.234	18.3	5199	0.0127	32.38	0.10
400	70.0	4	0.328	28.1.	7297	0.0117	41.68	0.10

Table B.18 X-7 thruster performance data

Hollow cathode - with flow, HC1-F2
0.318 cm cavity, $L_g = 0.845$

Arc current (A)	Arc voltage (V)	NH_3 flow rate (mg/sec)	Thrust (N)	Power (kW)	Specific impulse (sec)	Thrust power (N/kW)	Thrust efficiency (%)	Magnetic field (tesla)
200	50.0	4	0.126	10.0	2818	0.0127	17.40	0.10
300	56.0	4	0.204	16.8	45.44	0.0121	26.94	
400	60.0	4	0.301	24.1	6707	0.0125	41.08	
500	43.0	20	0.459	21.6	2351	0.0213	24.51	
600	42.0	20	0.530	25.3	2713	0.0210	27.84	
400	44.0	20	0.364	17.6	1864	0.0206	18.81	
300	47.0	20	0.281	14.1	1437	0.0198	13.95	
300	45.0	10	0.233	13.5	2381	0.0172	20.02	
400	46.0	10	0.296	18.4	3035	0.0161	23.85	
500	45.0	10	0.355	22.6	3638	0.0157	28.02	
600	48.0	10	0.424	28.9	4341	0.0147	31.18	
400	47.0	30	0.390	18.8	1333	0.0207	13.51	
500	47.0	30	0.491	23.6	1678	0.0209	17.13	
600	46.0	30	0.535	27.7	1825	0.0193	17.26	
300	55.0	40	0.349	16.5	894	0.0211	9.24	
400	51.0	40	0.438	20.5	1123	0.0215	11.78	
500	49.0	40	0.531	24.6	1359	0.0216	14.37	
600	47.0	40	0.544	28.3	1394	0.0192	13.14	0.10
300	58.0	40	0.363	17.4	929	0.0208	9.46	0.14
400	57.0	40	0.451	22.9	1155	0.0197	11.16	
500	57.0	40	0.487	28.6	1248	0.0171	10.42	
300	63.0	40	0.393	18.9	1007	0.0208	10.23	
300	50.0	10	0.246	15.0	2522	0.0164	20.21	
400	50.0	10	0.322	20.0	3296	0.0161	25.88	
500	53.0	10	0.403	26.6	4130	0.0152	30.67	
600	56.0	10	0.417	33.7	4271	0.0124	25.87	0.14

Table B.19 X-7 thruster performance data

Hollow cathode - with flow, HC1-F2
0.476 cm cavity, L_g = 0.845 cm

Arc current (A)	Arc voltage (V)	NH_3 flow rate (mg/sec)	Thrust (N)	Power (kW)	Specific impulse (sec)	Thrust power (N/kW)	Thrust efficiency (%)	Magnetic field (tesla)
300	53.0	4	0.212	15.9	4719	0.0132	30.69	0.10
350	55.0	4	0.237	19.3	5287	0.0123	31.82	↓
400	57.0	4	0.279	22.9	6204	0.0122	37.00	
400	41.0	10	0.295	16.4	3025	0.0179	26.58	
500	41.0	10	0.374	20.6	3829	0.0181	34.07	
600	41.0	10	0.420	24.7	4301	0.0170	35.83	
700	46.0	10	0.442	32.3	4532	0.0137	30.39	
400	42.0	20	0.336	16.8	1723	0.0200	16.85	
500	43.0	20	0.405	21.6	2075	0.0188	19.08	
600	42.0	20	0.428	25.3	2190	0.0170	18.15	
400	44.0	30	0.375	17.6	1279	0.0213	13.30	
500	42.0	30	0.431	21.1	1473	0.0205	14.78	
600	42.0	30	0.494	25.3	1688	0.0196	16.16	
400	46.0	40	0.382	18.4	977	0.0207	9.89	0.10

Table B.20 X-7 thruster performance data

Hollow cathode - with flow, HC1-F2
0.476 cm cavity, L_g = 0.685 cm

Arc current (A)	Arc voltage (V)	NH_3 flow rate (mg/sec)	Thrust (N)	Power (kW)	Specific impulse (sec)	Thrust power (N/kW)	Thrust efficiency (%)	Magnetic field (tesla)
300	41.0	10	0.212	12.3	2170	0.0172	18.25	0.10
400	40.0	10	0.276	16.0	2824	0.0172	23.74	0.10
500	40.0	10	0.323	20.0	3306	0.0161	26.04	0.10
300	41.0	20	0.244	12.3	1251	0.0198	12.12	0.07
400	40.0	20	0.282	16.0	1442	0.0176	12.38	0.07

Table B.21 X-7 thruster performance data

Hollow cathode - with flow, HC1-F2
0.476 cm cavity, L_g = 0.516 cm

Arc current (A)	Arc voltage (V)	NH_3 flow rate (mg/sec)	Thrust (N)	Power (kW)	Specific impulse (sec)	Thrust power (N/kW)	Thrust efficiency (%)	Magnetic field (tesla)
300	40.0	10	0.196	12.0	2009	0.0163	16.04	0.10
400	40.0	10	0.267	16.0	2733	0.0167	22.25	0.10
500	40.0	10	0.331	20.0	3386	0.0165	27.32	0.10
300	44.0	20	0.268	13.2	1371	0.0202	13.58	0.10
400	42.0	20	0.356	16.8	1824	0.0212	18.87	0.10
300	45.0	5	0.169	13.5	3457	0.0125	21.09	0.10
400	46.0	5	0.224	18.4	4582	0.0121	27.19	0.10

Table B.22 X-7 thruster performance data

Hollow cathode - with flow, HC1-F3
0.476 cm cavity, L_g = 0.845 cm

Arc current (A)	Arc voltage (V)	NH_3 flow rate (mg/sec)	Thrust (N)	Power (kW)	Specific impulse (sec)	Thrust power (N/kW)	Thrust efficiency (%)	Magnetic field (tesla)
300	41.0	10	0.194	12.3	1989	0.0157	15.33	0.10
400	40.0	10	0.264	16.0	2703	0.0165	21.76	0.10
500	40.0	10	0.333	20.0	3406	0.0166	27.65	0.10
300	46.0	20	0.230	13.8	1175	0.0166	9.54	0.10
400	44.0	20	0.324	17.6	1658	0.0183	14.88	0.10
500	41.0	20	0.412	20.6	2110	0.0200	20.70	0.10

Table B.23 X-7 thruster performance data

HC600 cathode

Arc current (A)	Arc voltage (V)	NH_3 flow rate (mg/sec)	Thrust (N)	Power (kW)	Specific impulse (sec)	Thrust power (N/kW)	Thrust efficiency (%)	Magnetic field (tesla)
200	53.0	20	0.169	10.6	864	0.0159	6.71	0.1
300	47.0	20	0.177	14.1	904	0.0125	5.52	↓
400	46.0	20	0.186	18.4	954	0.0101	4.72	↓
500	45.0	20	0.346	22.6	1773	0.0153	13.32	0.1

Table B24 X-7 thruster performance data

HC600 cathode

Arc current (A)	Arc voltage (V)	NH_3 flow rate (mg/sec)	Thrust (N)	Power (kW)	Specific impulse (sec)	Thrust power (N/kW)	Thrust efficiency (%)	Magnetic field (tesla)
200	49.0	4.6	0.114	9.8	2534	0.0116	14.36	0.10
300	40.0	4.6	0.188	12.0	4172	0.0156	31.80	
400	39.0	4.6	0.255	15.6	5680	0.0163	45.33	
500	38.0	4.6	0.288	19.0	6423	0.0151	47.59	
300	48.0	20.0	0.198	14.4	1015	0.0137	6.81	
400	44.0	20.0	0.263	17.6	1346	0.0149	9.81	
500	38.0	20.0	0.293	19.0	1502	0.0154	11.32	
300	49.0	40.0	0.236	14.7	605	0.0160	4.75	
400	44.0	38.0	0.269	17.6	724	0.0152	5.40	0.10

Table B.25 X-7 thruster performance data

HC6-F2 cathode, 0.319 cm cavity, L_g = 0.406 cm

Arc current (A)	Arc voltage (V)	NH_3 flow rate (mg/sec)	Thrust (N)	Power (kW)	Specific impulse (sec)	Thrust power (N/kW)	Thrust efficiency (%)	Magnetic field (tesla)
200	75.0	20	0.216	15.0	1105	0.0143	7.76	0.10
300	64.0	20	0.333	19.2	1703	0.0173	14.40	
400	61.0	20	0.418	24.5	2145	0.0172	17.98	
200	75.0	4	0.190	15.0	4238	0.0127	26.24	
300	64.0	4	0.281	19.2	6189	0.0146	44.30	
400	57.0	4	0.357	22.9	7952	0.0156	60.79	
500	50.0	4	0.434	25.1	9656	0.0173	81.75	
600	53.0	4	0.455	31.9	10137	0.0142	70.82	0.10

Table B.26 X-7 thruster performance data

HC6-F2 cathode, 0.476 cm cavity, L_g = 0.595 cm

Arc current (A)	Arc voltage (V)	NH_3 flow rate (mg/sec)	Thrust (N)	Power (kW)	Specific impulse (sec)	Thrust power (N/kW)	Thrust efficiency (%)	Magnetic field (tesla)
200	76.0	20	0.210	15.2	1075	0.0137	7.24	0.10
300	67.0	20	0.300	20.2	1538	0.0149	11.21	↓
400	57.0	20	0.396	22.9	2030	0.0174	17.22	
200	73.0	10	0.198	14.6	2030	0.0135	13.44	
300	59.0	10	0.268	17.7	2743	0.0151	20.26	
400	52.0	10	0.357	20.9	3658	0.0172	30.65	
500	55.0	10	0.426	27.6	4361	0.0154	32.96	
600	46.0	10	0.498	27.7	5105	0.0180	44.90	
300	55.0	4	0.240	16.5	5352	0.0145	38.05	
400	47.0	4	0.320	18.8	7122	0.0170	59.14	
500	55.0	4	0.398	27.6	8870	0.0144	62.70	
600	55.0	4	0.513	33.1	11426	0.0155	86.71	
200	77.0	10	0.188	15.4	1929	0.0122	11.51	
300	70.0	10	0.288	21.1	2954	0.0137	19.80	
400	62.0	10	0.359	24.9	3678	0.0144	25.99	0.10

Table B.27 X-7 thruster performance data

HC6-F2 cathode, 0.476 cm cavity, L_g = 0.714

Arc current (A)	Arc voltage (V)	NH_3 flow rate (mg/sec)	Thrust (N)	Power (kW)	Specific impulse (sec)	Thrust power (N/kW)	Thrust efficiency (%)	Magnetic field (tesla)
200	69.0	10	0.166	13.8	1698	0.0120	9.95	0.10
300	59.0	10	0.254	17.7	2602	0.0143	18.23	↓
400	51.0	10	0.343	20.5	3517	0.0168	28.89	0.10

Table B.28 X-7 thruster performance data
HC9 cathode

Arc current (A)	Arc voltage (V)	NH_3 flow rate (mg/sec)	Thrust (N)	Power (kW)	Specific impulse (sec)	Thrust power (N/kW)	Thrust efficiency (%)	Magnetic field (tesla)
300	47.0	14	0.207	14.1	1442	0.0146	10.33	0.10
400	46.0	14	0.301	18.4	2098	0.0163	16.76	
500	47.0	14	0.382	23.6	2666	0.0162	21.18	
300	49.0	10	0.218	14.7	2231	0.0148	16.13	
400	51.0	10	0.267	20.5	2733	0.0130	17.45	
500	51.0	10	0.284	25.6	2914	0.0111	15.87	
200	61.0	4.6	0.119	12.2	2650	0.0097	12.70	
300	61.0	4.6	0.209	18.3	3980	0.0114	19.10	0.10

Table B.29 X-7 thruster performance data
HC9 cathode

Arc current (A)	Arc voltage (V)	NH_3 flow rate (mg/sec)	Thrust (N)	Power (kW)	Specific impulse (sec)	Thrust power (N/kW)	Thrust efficiency (%)	Magnetic field (tesla)
300	50.0	10	0.226	15.0	2311	0.0150	16.97	0.10
400	53.0	10	0.289	21.3	2964	0.0136	19.75	
500	56.0	10	0.324	28.1	3316	0.0115	18.71	
300	53.0	10	0.230	15.9	2351	0.0144	16.57	
400	56.0	10	0.332	22.5	3396	0.0147	24.54	
500	55.0	10	0.361	27.6	3698	0.0130	23.69	
300	71.0	5	0.204	21.4	4180	0.0095	19.54	
400	83.0	5	0.263	33.3	5386	0.0078	20.82	
300	72.0	5	0.259	21.7	5306	0.0120	31.05	
300	74.0	5	0.204	22.3	4180	0.0091	18.75	
400	84.0	5	0.333	33.7	6833	0.0099	33.11	
500	90.0	5	0.404	45.2	8281	0.0089	36.30	
300	52.0	14	0.242	15.6	1688	0.0155	12.80	
400	53.0	14	0.317	21.3	2208	0.0149	16.11	
500	53.0	14	0.312	26.6	2174	0.0118	12.49	
600	46.0	14	0.273	27.7	1900	0.0098	9.16	
600	47.0	14	0.300	28.3	2092	0.0106	10.87	
400	84.0	5	0.278	33.7	5688	0.0082	22.94	
500	90.0	5	0.263	45.2	5386	0.0058	15.36	
450	83.0	4.6	0.276	37.5	6139	0.0073	22.11	
450	83.0	4.6	0.309	37.5	6882	0.0082	27.79	
450	84.0	4.6	0.261	37.9	5811	0.0068	19.58	
475	87.0	4.6	0.238	41.5	5309	0.0057	14.94	
475	89.0	4.6	0.250	42.4	5571	0.0059	16.09	0.10

Table B.30 X-7 thruster performance data

HC9-A cathode

Arc current (A)	Arc voltage (V)	NH_3 flow rate (mg/sec)	Thrust (N)	Power (kW)	Specific impulse (sec)	Thrust power (N/kW)	Thrust efficiency (%)	Magnetic field (tesla)
300	52.0	10	0.249	15.6	2542	0.0159	19.74	0.10
400	52.0	10	0.368	20.9	3768	0.0177	32.53	0.10
450	53.0	10	0.414	23.9	4241	0.0173	35.93	0.10
500	55.0	10	0.479	27.6	4904	0.0174	41.67	0.10
550	52.0	20	0.504	28.7	2582	0.0176	22.22	0.10
300	54.0	10	0.252	16.2	2582	0.0155	19.62	0.14
400	66.0	10	0.462	26.5	4733	0.0175	40.43	0.14
500	68.0	10	0.367	34.1	3758	0.0108	19.79	0.14
400	56.0	15	0.370	22.5	2525	0.0166	20.35	0.14
500	52.0	15	0.392	26.1	2679	0.0150	19.74	0.14

Table B.31 X-7 thruster performance data

HC9-A cathode

Arc current (A)	Arc voltage (V)	NH_3 flow rate (mg/sec)	Thrust (N)	Power (kW)	Specific impulse (sec)	Thrust power (N/kW)	Thrust efficiency (%)	Magnetic field (tesla)
300	50.0	10	0.228	15.0	2331	0.0151	17.26	0.10
400	54.0	10	0.311	21.7	3185	0.0143	22.38	
500	57.0	10	0.404	28.6	4140	0.0141	28.66	
500	57.0	10	0.420	28.6	4301	0.0147	30.93	
600	59.0	10	0.465	35.5	4763	0.0130	30.54	
400	55.0	10	0.325	22.1	3326	0.0147	23.96	
400	58.0	10	0.341	23.3	3497	0.0147	25.12	
500	60.0	10	0.377	30.1	3859	0.0126	23.65	0.10

Table B.32 X-7 thruster performance data

HC9-A cathode - 10 hour test

Arc current (A)	Arc voltage (V)	NH_3 flow rate (mg/sec)	Thrust (N)	Power (kW)	Specific impulse (sec)	Thrust power (N/kW)	Thrust efficiency (%)	Magnetic field (tesla)
300	56.0	10	0.250	16.8	2562	0.0148	18.62	0.10
400	58.0	10	0.360	23.3	3688	0.0155	27.93	↓
400	58.0	10	0.331	23.3	3386	0.0142	23.55	
400	58.0	10	0.341	23.3	3497	0.0147	25.12	
400	58.0	10	0.350	23.3	3587	0.0150	26.43	
400	56.0	10	0.316	22.5	3236	0.0140	22.27	
400	57.0	10	0.328	22.9	3356	0.0143	23.54	
400	57.0	10	0.333	22.9	3416	0.0146	24.39	
400	57.0	10	0.306	22.9	3135	0.0133	20.54	
400	56.0	10	0.313	22.5	3205	0.0139	21.86	
400	56.0	10	0.341	22.5	3497	0.0152	26.01	
400	55.0	10	0.321	22.1	3286	0.0145	23.39	0.10

Table B.33 X-7 thruster performance data

HC9-A cathode

Arc current (A)	Arc voltage (V)	NH_3 flow rate (mg/sec)	Thrust (N)	Power (kW)	Specific impulse (sec)	Thrust power (N/kW)	Thrust efficiency (%)	Magnetic field (tesla)
500	50.0	10	0.359	25.1	3678	0.0143	25.78	0.10
400	74.0	4	0.220	29.7	4893	0.0073	17.73	↓
300	65.0	4	0.193	19.5	4304	0.0099	20.82	
400	50.0	10	0.349	20.0	3577	0.0175	30.49	
500	53.0	10	0.399	26.6	4090	0.0150	30.08	
400	52.0	20	0.377	20.9	1929	0.0180	17.05	
500	53.0	20	0.451	26.6	2311	0.0170	19.21	
400	53.0	30	0.409	21.3	1396	0.0192	13.15	
500	53.0	30	0.423	26.6	1443	0.0159	11.24	
300	45.0	10	0.230	13.5	2351	0.0170	19.41	
400	50.0	10	0.306	20.0	3135	0.0153	23.42	
500	53.0	10	0.371	26.6	3798	0.0139	25.94	
400	54.0	20	0.376	21.7	1924	0.0174	16.34	
450	55.0	20	0.377	24.8	1929	0.0152	14.33	
400	54.0	30	0.425	21.7	1450	0.0196	13.92	
450	54.0	30	0.444	24.4	1517	0.0182	13.54	
300	65.0	4	0.194	19.5	4325	0.0099	21.03	
400	72.0	4	0.264	28.9	5877	0.0091	26.28	
500	80.0	4	0.337	40.1	7515	0.0084	30.95	
300	46.0	10	0.226	13.8	2311	0.0163	18.44	
400	46.0	10	0.294	18.4	3014	0.0160	23.53	
500	49.0	10	0.347	24.6	3557	0.0141	24.61	
400	52.0	20	0.343	20.9	1758	0.0165	14.17	
300	63.0	4	0.197	18.9	4391	0.0104	22.36	
400	72.0	4	0.249	28.9	5549	0.0086	23.43	
450	80.0	4	0.333	36.1	7406	0.0092	33.39	0.10

Table B.34 X-7 thruster performance data

10 hour duration test
HC9-A cathode

Arc current (A)	Arc voltage (V)	NH_3 flow rate (mg/sec)	Thrust (N)	Power (kW)	Specific impulse (sec)	Thrust power (N/kW)	Thrust efficiency (%)	Magnetic field (tesla)
300	63.0	4.6	0.185	18.9	4981	0.0118	28.77	0.10
375	66.0	4.6	0.243	24.8	4566	0.0082	18.46	0.08
375	54.0	7.0	0.199	20.3	3115	0.0105	15.98	0.08
400	50.0	7.0	0.196	20.0	2699	0.0092	12.14	0.08
350	63.0	4.6	0.217	22.1	3430	0.0069	11.69	0.08
350	52.0	4.6	0.179	18.2	3495	0.0085	14.71	0.07
350	60.0	4.6	0.208	21.2	3932	0.0083	16.14	0.07
350	57.0	4.6	0.196	20.0	3648	0.0081	14.62	0.07
350	56.0	4.6	0.192	19.6	3451	0.0078	13.32	0.07
350	60.0	4.6	0.207	21.1	3561	0.0075	13.23	0.07

Table B.35 X-7 thruster performance data

10 hour duration test
HC9-A cathode

Arc current (A)	Arc voltage (V)	NH_3 flow rate (mg/sec)	Thrust (N)	Power (kW)	Specific impulse (sec)	Thrust power (N/kW)	Thrust efficiency (%)	Magnetic field (tesla)
450	26.0	53.4	0.184	11.7	351	0.0156	2.69	0.10
500	25.0	75.5	0.212	12.5	287	0.0169	2.37	0.10
500	31.0	75.5	0.288	15.5	391	0.0185	3.55	0.14
550	39.0	75.5	0.449	21.5	609	0.0209	6.23	0.14
550	40.0	75.5	0.464	22.1	629	0.0211	6.48	0.14
550	41.0	75.5	0.411	22.6	557	0.0181	4.96	0.14
550	43.0	75.5	0.405	23.7	549	0.0171	4.59	0.14
550	43.0	75.5	0.450	23.7	610	0.0190	5.67	0.14
550	42.0	75.5	0.459	23.2	622	0.0198	6.04	0.15
550	42.0	75.5	0.436	23.2	591	0.0188	5.43	0.15

Table B.36 X-7 thruster performance data

HC9-B cathode

Arc current (A)	Arc voltage (V)	NH_3 flow rate (mg/sec)	Thrust (N)	Power (kW)	Specific impulse (sec)	Thrust power (N/kW)	Thrust efficiency (%)	Magnetic field (tesla)
300	66.0	4	0.182	19.8	4041	0.0091	18.08	0.10
400	82.0	4	0.310	32.9	6903	0.0094	31.84	
350	64.0	7	0.227	22.5	3316	0.0101	16.37	
400	69.0	7	0.266	27.7	3890	0.0096	18.29	
450	74.0	7	0.407	33.4	5958	0.0122	35.55	
300	75.0	4	0.189	22.6	4216	0.0083	17.31	
400	51.0	10	0.298	20.5	3055	0.0146	21.80	
300	65.0	4	0.139	19.5	3102	0.0070	10.81	
300	56.0	7	0.130	16.8	1895	0.0076	7.13	
400	60.0	7	0.271	24.1	3962	0.0113	21.82	0.10

Table B.37 X-7 thruster performance data

HC9-E cathode

Arc current (A)	Arc voltage (V)	NH_3 flow rate (mg/sec)	Thrust (N)	Power (kW)	Specific impulse (sec)	Thrust power (N/kW)	Thrust efficiency (%)	Magnetic field (tesla)
300	47.0	6	0.162	14.1	2512	0.0115	14.07	0.10
400	47.0	6	0.238	18.8	3684	0.0126	22.71	0.10
450	46.0	6	0.263	20.8	4080	0.0127	25.29	0.10
300	37.0	6	0.139	11.1	2162	0.0125	13.24	0.06
400	39.0	6	0.181	15.6	2801	0.0115	15.82	0.06
500	41.0	6	0.236	20.6	3654	0.0115	20.48	0.06
300	51.0	10	0.247	15.3	2532	0.0161	19.97	0.10
400	42.0	10	0.247	16.8	2532	0.0147	18.19	0.10
500	47.0	10	0.293	23.6	3004	0.0125	18.30	0.10

Table B.38 X-7 thruster performance data

Hollow cathode - dual flow
0.159 cm cavity, L_g = 0.845 cm

Arc current (A)	Arc voltage (V)	NH_3 flow rate (mg/sec)		Thrust (N)	Power (kW)	Specific impulse (sec)	Thrust power (N/kW)	Thrust efficiency (%)	Magnetic field (tesla)
		P*	S*						
300	59.0	4.6	0	0.248	17.7	5527	0.0139	37.83	0.10
400	70.0	4.6	0	0.338	28.1	7537	0.0121	44.47	0.10
400	67.0	4.6	0	0.326	26.9	7253	0.0121	43.02	0.10
500	92.0	4.6	0	0.460	46.2	10246	0.0099	50.02	0.10

*P - primary
S - secondary

Table B.39 X-7 thruster performance data

Hollow cathode - dual flow
HC1-F1, 0.159 cm cavity
3 injection ports omitted

Arc current (A)	Arc voltage (V)	NH_3 flow rate (mg/sec)		Thrust (N)	Power (kW)	Specific impulse (sec)	Thrust power (N/kW)	Thrust efficiency (%)	Magnetic field (tesla)
		P*	S*						
300	46.0	10	0	0.243	13.8	2492	0.0176	21.44	0.1
400	46.0	10	0	0.298	18.4	3055	0.0162	24.17	
500	48.0	10	0	0.366	24.1	3748	0.0152	27.89	
300	48.0	15	0	0.264	14.4	1802	0.0182	16.12	
300	50.0	4	0	0.194	15.0	4325	0.0129	27.34	
400	58.0	4	0	0.297	23.3	6619	0.0127	41.40	
400	44.0	20	0	0.315	17.6	1613	0.0178	14.08	
300	46.0	20	0	0.239	13.8	1226	0.0173	10.38	
400	44.0	20	0	0.320	17.6	1638	0.0181	14.52	
300	43.0	10	0	0.227	12.9	2321	0.0176	19.90	
400	44.0	10	0	0.298	17.6	3055	0.0169	25.26	
500	45.0	10	0	0.360	22.6	3688	0.0160	28.80	0.1

*P - primary
S - secondary

Table B.40 X-7 thruster performance data

Hollow cathode - dual flow
HC1-F1, 0.476 cm cavity
3 injection ports, L_g = 0.845 cm

Arc current (A)	Arc voltage (V)	NH_3 flow rate (mg/sec)		Thrust (N)	Power (kW)	Specific impulse (sec)	Thrust power (N/kW)	Thrust efficiency (%)	Magnetic field (tesla)
		P*	S*						
300	41.0	10	0	0.186	12.3	1899	0.0150	13.97	0.10
400	40.0	10	0	0.256	16.0	2623	0.0160	20.48	
300	41.0	10	10	0.205	12.3	1050	0.0166	8.54	
400	39.0	10	10	0.286	15.6	1467	0.0183	13.15	
500	39.0	10	10	0.359	19.5	1839	0.0183	16.52	
600	39.0	10	10	0.441	23.5	2261	0.0188	20.82	
300	42.0	0	10	0.148	12.6	1517	0.0117	8.70	
400	42.0	0	10	0.218	16.8	2231	0.0129	14.11	
500	36.0	0	10	0.265	18.0	2713	0.0147	19.49	
300	42.0	20	0	0.235	12.6	1205	0.0186	10.99	
400	40.0	20	0	0.310	16.0	1587	0.0193	15.01	
500	38.0	20	0	0.402	19.0	2060	0.0211	21.28	
300	46.0	20	5	0.264	13.8	1351	0.0190	12.61	
400	41.0	20	5	0.422	16.4	1756	0.0257	22.05	
500	39.0	20	5	0.290	19.5	1209	0.0148	8.78	
300	49.0	20	10	0.368	14.7	1256	0.0250	15.34	
300	51.0	20	10	0.309	15.3	1055	0.0201	10.40	
400	45.0	20	15	0.389	18.0	1139	0.0216	12.03	
500	43.0	20	15	0.473	21.6	1384	0.0220	14.85	
300	52.0	20	20	0.332	15.6	849	0.0212	8.81	
400	46.0	20	20	0.390	18.4	999	0.0212	10.35	
300	51.0	15	20	0.306	15.3	895	0.0199	8.74	
400	45.0	15	20	0.383	18.0	1119	0.0212	11.61	
500	43.0	15	20	0.447	21.6	1309	0.0208	13.29	
300	49.0	10	20	0.285	14.7	974	0.0193	9.24	
400	44.0	10	20	0.363	17.6	1239	0.0206	12.47	
300	45.0	5	20	0.233	13.5	952	0.0172	8.00	
400	40.0	5	20	0.307	16.0	1258	0.0191	11.78	
500	40.0	5	20	0.377	20.0	1543	0.0188	14.19	
300	44.0	0	20	0.182	13.2	929	0.0136	6.23	
400	39.0	0	20	0.273	15.6	1396	0.0175	11.92	
500	38.0	0	20	0.337	19.0	1713	0.0176	14.72	
600	39.0	0	20	0.390	23.5	1994	0.0166	16.20	0.10
300	49.0	0	20	0.195	14.7	999	0.0132	6.48	0.14
400	46.0	0	20	0.253	18.4	1296	0.0137	8.70	0.14

Table B.40 X-7 thruster performance data (cont'd)

Hollow cathode - dual flow
HC1-F1, 0.476 cm cavity
3 injection ports, L_g = 0.845 cm

Arc current (A)	Arc voltage (V)	NH_3 flow rate (mg/sec)		Thrust (N)	Power (kW)	Specific impulse (sec)	Thrust power (N/kW)	Thrust efficiency (%)	Magnetic field (tesla)
		P*	S*						
300	49.0	0	20	0.204	14.7	1045	0.0138	7.08	0.14
500	38.0	0	20	0.296	19.0	1517	0.0155	11.55	
300	50.0	4.6	20	0.249	15.0	1037	0.0166	8.41	
400	46.0	4.6	20	0.324	18.4	1348	0.0176	11.57	
500	44.0	4.6	20	0.410	22.1	1707	0.0186	15.53	
300	52.0	10	20	0.302	15.6	1031	0.0193	9.75	
400	48.0	10	20	0.390	19.2	1333	0.0203	13.23	
500	46.0	10	20	0.447	23.1	1527	0.0194	14.50	
300	56.0	15	20	0.345	16.8	1010	0.0205	10.14	
400	54.0	15	20	0.478	21.7	1398	0.0221	15.09	
300	66.0	20	20	0.412	19.8	1055	0.0208	10.71	
400	56.0	20	20	0.407	22.5	1042	0.0181	9.25	0.14
300	46.0	4.6	0	0.143	13.8	3189	0.0103	16.15	0.08
400	48.0	4.6	0	0.215	19.2	4784	0.0112	26.13	
500	36.0	4.6	0	0.196	18.0	4369	0.0109	23.24	
300	38.0	10	0	0.190	11.4	1949	0.0167	15.88	
400	38.0	10	0	0.249	15.2	2552	0.0164	20.42	
500	38.0	10	0	0.309	19.0	3165	0.0162	25.13	
300	38.0	15	0	0.224	11.4	1527	0.0196	14.62	
400	37.0	15	0	0.286	14.8	1956	0.0193	18.48	
500	37.0	15	0	0.353	18.5	2411	0.0190	22.47	
300	42.0	20	0	0.126	12.6	648	0.0100	3.17	
400	42.0	20	0	0.317	16.8	1623	0.0188	14.94	
300	46.0	20	5	0.186	13.8	759	0.0133	4.98	
400	44.0	20	5	0.359	17.6	1471	0.0203	14.65	
500	40.0	20	5	0.433	20.0	1772	0.0216	18.71	
300	49.0	20	10	0.339	14.7	1159	0.0230	13.06	
400	43.0	20	10	0.406	17.2	1386	0.0235	15.98	
500	40.0	20	10	0.456	20.0	1557	0.0228	17.34	
300	49.0	20	15	0.354	14.7	1036	0.0240	12.18	
400	47.0	20	15	0.435	18.8	1272	0.0230	14.35	
500	42.0	20	15	0.461	21.1	1349	0.0219	14.46	
300	52.0	20	20	0.373	15.6	954	0.0238	11.13	
400	46.0	20	20	0.444	18.4	1138	0.0241	13.41	0.08

Table B.40 X-7 thruster performance data (cont'd)

Hollow cathode - dual flow
HC1-F1-0.476 cm cavity
3 injection ports, Lg = 0.845 cm

Arc current (A)	Arc voltage (V)	NH_3 flow rate (mg/sec)		Thrust (N)	Power (kW)	Specific impulse (sec)	Thrust power (N/kW)	Thrust efficiency (%)	Magnetic field (tesla)
		P*	S*						
500	43.0	20	20	0.493	21.6	1263	0.0228	14.15	0.08
300	48.0	15	10	0.248	14.4	1057	0.0178	9.24	0.08
300	53.0	15	10	0.288	15.9	1181	0.0180	10.46	0.10
400	46.0	15	10	0.356	18.4	1459	0.0193	13.78	0.10
300	49.0	15	10	0.252	14.7	1033	0.0171	8.64	0.08
300	53.0	20	10	0.293	15.9	1001	0.0184	9.01	↓
400	51.0	20	10	0.369	20.5	1259	0.0180	11.11	↓
500	44.0	20	10	0.440	22.1	1500	0.0199	14.63	↓
300	52.0	20	5	0.273	15.6	1117	0.0175	9.53	↓
400	51.0	20	5	0.353	20.5	1447	0.0173	12.22	↓
500	45.0	20	5	0.434	22.6	1776	0.0192	16.71	0.08

*P - primary
S - secondary

Table B.41 X-7 thruster performance data

Hollow cathode - dual flow
HC1-F2, 0.476 cm cavity
3 injection ports, L_g = 0.845 cm

Arc current (A)	Arc voltage (V)	NH_3 flow rate (mg/sec)		Thrust (N)	Power (kW)	Specific impulse (sec)	Thrust power (N/kW)	Thrust efficiency (%)	Magnetic field (tesla)
		P*	S*						
300	40.0	10	0	0.202	12.0	2070	0.0168	17.01	0.10
400	40.0	10	0	0.268	16.0	2743	0.0167	22.41	↓
500	40.0	10	0	0.312	20.0	3195	0.0156	24.33	↓
400	45.0	15	20	0.411	18.0	1203	0.0227	13.41	↓
300	52.0	20	20	0.335	15.6	859	0.0215	9.02	↓
400	52.0	20	20	0.427	20.9	1092	0.0205	10.94	0.10

*P - primary
S - secondary

Table B.42 X-7 thruster performance data

Hollow cathode - dual flow
HC1-F1, 0.476 cm cavity
3 injection ports omitted

Arc current (A)	Arc voltage (V)	NH_3 flow rate (mg/sec)		Thrust (N)	Power (kW)	Specific impulse (sec)	Thrust power (N/kW)	Thrust efficiency (%)	Magnetic field (tesla)
		P*	S*						
400	46.0	10	0	0.292	18.4	2994	0.0158	23.22	0.1
500	47.0	10	0	0.368	23.6	3768	0.0156	28.79	
300	46.0	10	0	0.226	13.8	2311	0.0163	18.44	
400	40.5	15	0	0.382	16.2	2606	0.0235	29.96	
500	40.0	15	0	0.402	20.0	2746	0.0201	26.96	
500	40.0	20	0	0.420	20.0	2150	0.0210	22.03	
400	41.0	20	0	0.337	16.4	1728	0.0205	17.36	
300	44.0	20	0	0.250	13.2	1281	0.0189	11.85	
300	44.0	30	0	0.253	13.2	864	0.0191	8.08	
400	40.0	30	0	0.324	16.0	1105	0.0202	10.91	
300	46.5	20	5	0.271	14.0	1109	0.0193	10.51	
400	43.0	20	5	0.342	17.2	1402	0.0188	13.63	
500	33.0	20	10	0.276	16.5	941	0.0167	7.67	
500	36.0	20	15	0.312	18.0	913	0.0173	7.72	
400	40.0	20	15	0.274	16.0	801	0.0171	6.68	
300	45.0	20	15	0.218	13.5	637	0.0161	5.01	
300	45.0	20	20	0.229	13.5	585	0.0169	4.83	
400	42.0	20	20	0.283	16.8	723	0.0168	5.93	
500	40.0	20	20	0.343	20.0	879	0.0172	7.36	0.1

*P - primary
S - secondary

Table B.43 X-7 thruster performance data

Hollow cathode - dual flow

HC4-F1

Arc current (A)	Arc voltage (V)	NH_3 flow rate (mg/sec)		Thrust (N)	Power (kW)	Specific impulse (sec)	Thrust power (N/kW)	Thrust efficiency (%)	Magnetic field (tesla)
		P*	S*						
300	49.0	20	0	0.277	14.7	1417	0.0187	13.01	0.1
400	48.0	20	0	0.359	19.2	1839	0.0186	16.78	
500	48.0	20	0	0.436	24.1	2231	0.0181	19.76	
300	50.0	30	0	0.288	15.0	984	0.0192	9.24	
400	48.0	30	0	0.384	19.2	1313	0.0200	12.83	
500	47.0	30	0	0.480	23.6	1638	0.0204	16.32	
300	52.5	40	0	0.313	15.8	801	0.0198	7.77	
400	49.0	40	0	0.388	19.6	994	0.0198	9.62	
500	46.0	40	0	0.469	23.1	1200	0.0203	11.95	
300	53.0	50	0	0.319	15.9	653	0.0200	6.39	
400	47.0	50	0	0.382	18.8	781	0.0202	7.74	
300	48.0	20	10	0.319	14.4	1088	0.0221	11.76	
400	47.0	20	10	0.303	18.8	1035	0.0161	8.14	0.1

*P - primary

S - secondary

Table B.44 X-7 thruster performance data

Hollow cathode - dual flow

HC4-F2

Arc current (A)	Arc voltage (V)	NH_3 flow rate (mg/sec)		Thrust (N)	Power (kW)	Specific impulse (sec)	Thrust power (N/kW)	Thrust efficiency (%)	Magnetic field (tesla)
		P*	S*						
400	45.0	20	0	0.347	18.0	1778	0.0192	16.75	0.1
500	48.0	20	0	0.407	24.1	2085	0.0169	17.26	
600	43.0	20	0	0.484	25.9	2482	0.0188	22.75	
700	44.0	20	0	0.548	30.9	2808	0.0179	24.41	
300	52.0	30	0	0.288	15.6	984	0.0184	8.88	
400	42.0	30	0	0.407	20.9	1390	0.0195	13.28	
500	50.0	30	0	0.479	25.1	1634	0.0191	15.28	
300	50.0	20	10	0.306	15.0	1045	0.0204	10.41	
400	49.0	20	10	0.397	19.6	1356	0.0202	13.42	0.1

*P - primary

S - secondary

Table B.45 X-7 thruster performance data

Hollow cathode - dual flow
HC4-F3

Arc current (A)	Arc voltage (V)	NH_3 flow rate (mg/sec)		Thrust (N)	Power (kW)	Specific impulse (sec)	Thrust power (N/kW)	Thrust efficiency (%)	Magnetic field (tesla)
		P*	S*						
300	47.0	10	0	0.236	14.1	2422	0.0167	19.82	0.1
300	52.0	20	0	0.271	15.6	1386	0.0173	11.74	
400	51.0	20	0	0.375	20.5	1919	0.0183	17.21	
500	51.0	20	0	0.464	25.6	2376	0.0181	21.11	
600	51.0	20	0	0.556	30.7	2849	0.0181	25.27	
300	53.0	30	0	0.313	15.9	1068	0.0196	10.26	
400	52.0	30	0	0.410	20.9	1400	0.0196	13.47	
500	50.0	30	0	0.481	25.1	1641	0.0192	15.40	
300	49.0	10	0	0.240	14.7	2462	0.0163	19.65	
400	50.0	10	0	0.316	20.0	3236	0.0158	24.94	
500	52.0	10	0	0.410	26.1	4200	0.0157	32.34	
300	48.0	10	10	0.282	14.4	1442	0.0195	13.76	
400	47.0	10	10	0.365	18.8	1869	0.0193	17.71	0.1

*P - primary
S - secondary

Table B.46 X-7 thruster performance data

HC9-A cathode nitrogen propellant

Arc current (A)	Arc voltage (V)	N_2 flow rate (mg/sec)	Thrust (N)	Power (kW)	Specific impulse (sec)	Thrust power (N/kW)	Thrust efficiency (%)	Magnetic field (tesla)
300	41.0	13.0	0.226	12.3	1751	0.0183	15.67	0.10
400	42.0	13.0	0.294	16.8	2284	0.0175	19.53	
500	47.0	13.0	0.370	23.6	2870	0.0157	22.04	
500	38.0	20.0	0.392	19.0	1960	0.0206	19.76	
400	37.0	20.0	0.336	14.8	1681	0.0227	18.66	
300	36.0	20.0	0.278	10.8	1387	0.0256	17.40	
300	49.0	7.0	0.209	14.7	2816	0.0141	19.54	
400	59.0	7.0	0.281	23.7	3781	0.0119	21.94	0.10

Table B.47 X-7 thruster performance data

HC9-A cathode nitrogen propellant

Arc current (A)	Arc voltage (V)	N_2 flow rate (mg/sec)	Thrust (N)	Power (kW)	Specific impulse (sec)	Thrust power (N/kW)	Thrust efficiency (%)	Magnetic field (tesla)
300	39.0	13.0	0.206	11.7	1598	0.0176	13.74	0.10
400	39.0	13.0	0.267	15.6	2070	0.0171	17.29	
500	43.0	13.0	0.332	21.6	2573	0.0154	19.37	
500	37.0	20.0	0.363	18.5	1813	0.0196	17.37	
400	36.0	20.0	0.308	14.4	1539	0.0214	16.07	
300	38.0	20.0	0.244	11.4	1220	0.0214	12.76	
300	34.0	27.0	0.265	10.2	976	0.0258	12.37	
400	34.0	27.0	0.328	13.6	1207	0.0240	14.19	
500	35.0	27.0	0.395	17.5	1456	0.0226	16.06	
600	37.0	27.0	0.467	22.3	1720	0.0210	17.66	
700	37.0	27.0	0.491	26.0	1811	0.0189	16.77	
700	35.0	35.0	0.519	24.6	1510	0.0211	15.61	
600	34.0	35.0	0.461	20.5	1341	0.0226	14.80	
500	33.0	35.0	0.391	16.5	1139	0.0236	13.19	
400	33.0	35.0	0.324	13.2	942	0.0245	11.27	
300	33.0	35.0	0.252	9.9	733	0.0254	9.12	
300	40.0	13.0	0.216	12.0	1674	0.0179	14.70	
400	39.0	13.0	0.273	15.6	2116	0.0175	18.06	
500	42.0	13.0	0.325	21.1	2520	0.0154	19.02	
500	38.0	20.0	0.349	19.0	1745	0.0183	15.65	
600	39.0	20.0	0.407	23.5	2034	0.0174	17.27	0.10

Table B.48 X-7 thruster performance data

HC9-A cathode, hydrogen-nitrogen propellant

Arc current (A)	Arc voltage (V)	Flow rate (mg/sec)		Thrust (N)	Power (kW)	Specific impulse (sec)	Thrust power (N/kW)	Thrust efficiency (%)	Magnetic field (tesla)
		N_2	H_2						
300	40.0	12.3	0.0	0.221	12.0	1838	0.0183	16.50	0.10
400	41.0	12.3	0.0	0.288	16.4	2402	0.0176	20.62	
500	46.0	12.3	0.0	0.370	23.1	3080	0.0160	24.17	
300	41.0	24.7	0.0	0.250	12.3	1037	0.0203	10.30	
400	40.0	24.7	0.0	0.318	16.0	1318	0.0198	12.78	
500	40.0	24.7	0.0	0.394	20.0	1635	0.0197	15.74	
600	42.0	24.7	0.0	0.447	25.3	1855	0.0177	16.07	
700	43.0	24.7	0.0	0.482	30.2	2001	0.0160	15.66	
300	50.0	24.7	0.9	0.285	15.0	1142	0.0190	10.61	
400	43.0	24.7	0.9	0.335	17.2	1342	0.0194	12.78	
500	42.0	24.7	0.9	0.386	21.1	1546	0.0183	13.89	
300	46.0	24.7	0.9	0.272	13.8	1087	0.0196	10.45	
400	45.0	24.7	0.9	0.335	18.0	1342	0.0186	12.21	
500	43.0	24.7	0.9	0.382	21.6	1527	0.0177	13.23	
300	58.0	24.7	1.7	0.279	17.4	1081	0.0160	8.44	
400	55.0	24.7	1.7	0.323	22.1	1252	0.0146	8.96	
500	50.0	24.7	1.7	0.355	25.1	1378	0.0141	9.55	
300	64.0	24.7	2.6	0.272	19.2	1019	0.0141	7.04	
400	56.0	24.7	2.6	0.309	22.5	1159	0.0137	7.80	
500	51.0	24.7	2.6	0.345	25.6	1295	0.0135	8.56	
300	63.0	24.7	3.5	0.269	18.9	976	0.0141	6.77	
400	58.0	24.7	3.5	0.327	23.3	1186	0.0140	8.15	
500	52.0	24.7	3.5	0.353	26.1	1281	0.0135	8.50	
300	64.0	24.7	4.4	0.281	19.2	987	0.0145	7.04	
400	58.0	24.7	4.4	0.328	23.3	1153	0.0140	7.95	
500	53.0	24.7	4.4	0.375	26.6	1319	0.0141	9.10	
300	65.0	24.7	5.3	0.283	19.5	968	0.0145	6.87	
400	58.0	24.7	5.3	0.335	23.3	1145	0.0144	8.08	
500	53.0	24.7	5.3	0.281	26.6	961	0.0106	4.98	
300	66.0	22.7	3.2	0.274	19.8	1082	0.0137	7.30	
400	59.0	22.7	3.2	0.334	23.7	1323	0.0141	9.15	0.10

Table B.49 X-7 thruster performance data

HC9-A cathode, nitrogen propellant

Arc current (A)	Arc voltage (V)	N_2 flow rate (mg/sec)	Thrust (N)	Power (kW)	Specific impulse (sec)	Thrust power (N/kW)	Thrust efficiency (%)	Magnetic field (tesla)
300	42.0	15.0	0.236	12.6	1614	0.0187	14.78	0.10
300	40.0	15.0	0.226	12.0	1547	0.0188	14.26	
300	42.0	20.0	0.252	12.6	1291	0.0199	12.61	
400	42.0	20.0	0.330	16.8	1688	0.0196	16.16	
500	43.0	20.0	0.388	21.6	1989	0.0180	17.55	
300	40.0	25.0	0.277	12.0	1133	0.0230	12.75	
400	38.0	25.0	0.252	15.2	1443	0.0231	16.32	
500	39.0	25.0	0.414	19.5	1696	0.0212	17.57	
600	40.0	25.0	0.466	24.1	1909	0.0193	18.09	
300	43.0	30.0	0.277	12.9	944	0.0214	9.88	
400	43.0	30.0	0.326	17.2	1112	0.0189	10.27	
500	43.0	30.0	0.384	21.6	1313	0.0178	11.46	
600	41.0	30.0	0.421	24.7	1437	0.0171	12.00	
300	42.0	35.0	0.259	12.6	758	0.0205	7.60	
400	42.0	35.0	0.322	16.8	941	0.0191	8.80	
500	42.0	35.0	0.381	21.2	1114	0.0180	9.85	
600	40.0	35.0	0.425	24.1	1243	0.0177	10.74	
300	43.0	15.0	0.228	12.9	1554	0.0176	13.38	
300	40.0	20.0	0.252	12.0	1291	0.0210	13.24	
400	40.0	20.0	0.349	16.0	1788	0.0218	19.05	
500	41.0	20.0	0.419	20.6	2145	0.0204	21.40	
300	40.0	20.0	0.248	12.0	1321	0.0215	13.86	
400	41.0	20.0	0.313	16.4	1602	0.0190	14.93	
500	43.0	20.0	0.389	21.6	1994	0.0180	17.63	
300	44.0	15.0	0.235	13.2	1601	0.0178	13.88	
400	45.0	15.0	0.332	18.0	2264	0.0183	20.36	
500	45.0	15.0	0.374	22.6	2552	0.0166	20.69	
300	49.0	10.0	0.224	14.7	2291	0.0152	17.02	
400	50.0	10.0	0.304	20.0	3115	0.0152	23.12	
500	54.0	10.0	0.372	27.1	3808	0.0137	25.60	
300	52.0	8.0	0.225	15.6	2876	0.0143	20.22	
400	59.0	8.0	0.259	23.7	3316	0.0109	17.76	
500	62.0	8.0	0.335	31.1	4296	0.0108	22.69	
300	58.0	6.0	0.225	17.4	3835	0.0128	24.17	
400	67.0	6.0	0.220	26.9	3751	0.0081	15.01	
300	75.0	4.0	0.162	22.6	4145	0.0072	14.55	
300	83.0	4.0	0.273	25.0	6984	0.0109	37.34	0.10

Table B.50 X-7 thruster performance data

HC9-A cathode, nitrogen propellant

Arc current (A)	Arc voltage (V)	N_2 flow rate (mg/sec)	Thrust (N)	Power (kW)	Specific impulse (sec)	Thrust power (N/kW)	Thrust efficiency (%)	Magnetic field (tesla)
300	36.0	13.0	0.177	10.8	1375	0.0165	11.09	0.10
400	34.0	13.0	0.224	13.6	1722	0.0164	13.83	
500	37.0	13.0	0.266	18.5	2047	0.0143	14.36	
300	32.0	15.0	0.189	9.6	1293	0.0197	12.44	
400	33.0	15.0	0.234	13.2	1594	0.0177	13.76	
500	34.0	15.0	0.264	17.0	1802	0.0155	13.65	
300	36.0	10.0	0.189	10.8	1939	0.0175	16.59	
400	39.0	10.0	0.221	15.6	2261	0.0141	15.61	
500	40.0	10.0	0.220	20.0	2251	0.0110	12.07	
300	40.0	8.0	0.173	12.0	2210	0.0143	15.52	
400	43.0	8.0	0.194	17.2	2487	0.0113	13.71	
500	44.0	8.0	0.188	22.1	2411	0.0085	10.07	
300	46.0	6.0	0.160	13.8	2730	0.0116	15.44	
400	48.0	6.0	0.183	19.2	3115	0.0094	14.45	
500	47.0	6.0	0.205	23.6	3500	0.0086	14.90	
300	48.0	5.0	0.153	14.4	3135	0.0106	16.26	
300	47.0	5.0	0.150	14.1	3075	0.0106	15.97	
300	34.0	10.0	0.156	10.2	1597	0.0152	11.92	
400	34.0	10.0	0.171	13.6	1748	0.0125	10.71	
500	36.0	10.0	0.202	18.0	2070	0.0112	11.34	
300	40.0	8.0	0.144	12.0	1846	0.0120	10.83	
400	40.0	8.0	0.173	16.0	2210	0.0108	11.64	
500	42.0	8.0	0.202	21.1	2587	0.0096	12.15	
300	46.0	6.0	0.157	13.8	2679	0.0113	14.87	
400	48.0	6.0	0.157	19.2	2679	0.0081	10.69	
400	48.0	6.0	0.199	19.2	3400	0.0103	17.21	
500	41.0	6.0	0.176	20.6	2998	0.0085	12.53	
300	42.0	5.0	0.120	12.6	2452	0.0094	11.36	
400	42.0	5.0	0.144	16.8	2954	0.0085	12.37	0.10

Table B.51 X-7 thruster performance data

HC9-A cathode, helium propellant

Arc current (A)	Arc voltage (V)	Helium flow rate (mg/sec)	Thrust (N)	Power (kW)	Specific impulse (sec)	Thrust power (N/kW)	Thrust efficiency (%)	Magnetic field (tesla)
400	59.0	15	0.329	23.7	2244	0.0138	15.25	0.10
500	66.0	15	0.543	33.1	3711	0.0164	29.83	
300	54.0	15	0.277	16.2	1889	0.0171	15.74	
300	50.0	20	0.281	15.0	1437	0.0186	13.12	
400	50.0	20	0.372	20.0	1904	0.0185	17.28	
500	54.0	20	0.444	27.1	2276	0.0164	18.28	
300	47.0	25	0.391	14.1	1603	0.0277	21.73	
400	47.0	25	0.465	18.8	1905	0.0247	23.00	
500	50.0	25	0.527	25.1	2162	0.0211	22.28	
300	48.0	25	0.352	14.4	1443	0.0244	17.22	
300	48.0	25	0.449	14.4	1841	0.0312	28.04	
300	90.0	10	0.225	27.1	2301	0.0082	9.34	
300	90.0	10	0.222	27.1	2271	0.0081	9.10	
300	61.0	15	0.160	18.3	1092	0.0087	4.65	
400	59.0	15	0.301	23.7	2056	0.0127	12.81	
500	64.0	15	0.490	32.1	3349	0.0153	25.06	0.10

Table B.52 X-7 thruster performance data

HC9-A cathode, helium propellant

Arc current (A)	Arc voltage (V)	Helium flow rate (mg/sec)	Thrust (N)	Power (kW)	Specific impulse (sec)	Thrust power (N/kW)	Thrust efficiency (%)	Magnetic field (tesla)
300	56.0	15	0.288	16.8	1969	0.0172	16.50	0.10
400	60.0	15	0.407	24.1	2780	0.0169	23.02	
500	68.0	15	0.533	34.1	3651	0.0157	28.02	
300	59.0	15	0.285	17.7	1949	0.0161	15.34	
400	59.0	15	0.413	23.7	2820	0.0175	24.09	
500	64.0	15	0.546	32.1	3738	0.0171	31.21	
300	80.0	10	0.317	24.1	3246	0.0131	20.91	
300	76.0	10	0.315	22.9	3226	0.0137	21.74	
400	82.0	10	0.402	32.9	4120	0.0123	24.66	0.10

Table B.53 X-7 thruster performance data

HC9-A cathode, neon propellant

Arc current (A)	Arc voltage (V)	Neon flow rate (mg/sec)	Thrust (N)	Power (kW)	Specific impulse (sec)	Thrust power (N/kW)	Thrust efficiency (%)	Magnetic field (tesla)
300	90.0	10	0.194	27.1	1989	0.0071	6.98	0.10
300	90.0	10	0.301	27.1	3085	0.0111	16.79	↓
300	90.0	10	0.331	27.1	3386	0.0122	20.24	
300	75.0	15	0.322	22.6	2197	0.0142	15.34	
300	83.0	10	0.316	25.0	3236	0.0127	20.03	
300	95.0	5	0.308	28.6	6311	0.0108	33.29	0.10

Table B.54 X-7 thruster performance data

HC9-A cathode, xenon propellant

Arc current (A)	Arc voltage (V)	Xenon flow rate (mg/sec)	Thrust (N)	Power (kW)	Specific impulse (sec)	Thrust power (N/kW)	Thrust efficiency (%)	Magnetic field (tesla)
300	49.0	10	0.193	14.7	1979	0.0131	12.70	0.10
350	56.0	10	0.246	19.6	2522	0.0126	15.46	↓
400	60.0	10	0.292	24.1	2994	0.0122	17.80	
300	73.0	5	0.123	22.0	2532	0.0056	6.97	
350	76.0	5	0.177	26.7	3617	0.0066	11.72	
300	54.0	10	0.204	16.2	2090	0.0126	12.85	
350	57.0	10	0.263	20.0	2693	0.0131	17.32	
400	62.0	10	0.299	24.9	3065	0.0120	18.05	
450	64.0	10	0.322	28.9	3296	0.0111	17.97	
300	53.0	15	0.209	15.9	1427	0.0130	9.15	
350	55.0	15	0.250	19.3	1708	0.0129	10.83	
400	55.0	15	0.289	22.1	1976	0.0131	12.69	
450	57.0	15	0.323	25.7	2204	0.0125	13.53	
500	60.0	15	0.374	30.1	2552	0.0124	15.52	
550	62.0	15	0.389	34.2	2659	0.0114	14.82	
300	58.0	20	0.237	17.4	1210	0.0136	8.10	
350	59.0	20	0.264	20.7	1351	0.0127	8.43	
400	60.0	20	0.293	24.1	1502	0.0122	8.96	
450	60.0	20	0.312	27.1	1597	0.0115	9.01	
500	58.0	20	0.348	29.1	1783	0.0120	10.45	
300	52.0	10	0.211	15.6	2160	0.0134	14.25	
350	56.0	10	0.251	19.6	2572	0.0127	16.09	
300	58.0	5	0.135	17.4	2773	0.0077	10.53	
300	67.0	5	0.239	20.2	4884	0.0118	28.27	↓
350	74.0	5	0.308	26.0	6311	0.0119	36.63	0.10
300	60.0	10	0.226	18.0	2311	0.0125	14.14	0.14

Table B.54 X-7 thruster performance data (cont'd)

HC9-A cathode, xenon propellant

Arc current (A)	Arc voltage (V)	Xenon flow rate (mg/sec)	Thrust (N)	Power (kW)	Specific impulse (sec)	Thrust power (N/kW)	Thrust efficiency (%)	Magnetic field (tesla)
350	57.0	10	0.171	20.0	1748	0.0085	7.30	0.10
300	59.0	20	0.237	17.7	1211	0.0133	7.89	
350	62.0	20	0.260	21.8	1331	0.0120	7.78	
400	64.0	20	0.285	25.7	1462	0.0112	7.95	
450	64.0	20	0.295	28.9	1507	0.0102	7.51	
500	64.0	20	0.377	32.1	1929	0.0118	11.08	0.10
300	59.0	20	0.280	17.7	1437	0.0158	11.11	0.14
350	60.0	20	0.315	21.1	1613	0.149	11.80	
400	61.0	20	0.290	24.5	1487	0.0119	8.64	
450	61.0	20	0.309	27.5	1582	0.0112	8.69	
500	60.0	20	0.341	30.1	1748	0.0114	9.71	
550	62.0	20	0.356	34.2	1824	0.0104	9;29	
300	60.0	20	0.280	18.0	1437	0.0155	10.93	
300	60.0	20	0.304	18.0	1557	0.0169	12.84	0.14
300	51.0	10	0.204	15.3	2090	0.0132	13.60	0.10
350	54.0	10	0.180	18.9	1849	0.0095	8.62	
400	57.0	10	0.192	22.9	1969	0.0083	8.10	
300	56.0	18	0.235	16.8	1339	0.0139	9.16	
300	52.0	5	0.144	15.6	2954	0.0092	13.33	
300	52.0	5	0.202	15.6	4140	0.0129	26.18	
350	61.0	5	0.274	21.4	5607	0.0127	35.09	
400	72.0	5	0.163	28.9	3336	0.0056	9.20	
300	64.0	5	0.187	19.2	3839	0.0097	18.28	
350	71.0	5	0.304	24.9	6230	0.0122	37.22	
400	77.0	5	0.353	30.9	7235	0.0114	40.49	
300	74.0	5	0.246	22.3	5045	0.0111	27.31	
350	81.0	5	0.151	28.4	3095	0.0053	8.05	
300	65.0	10	0.205	19.5	2100	0.0105	10.78	
350	62.0	10	0.284	21.8	2914	0.0130	18.65	
400	63.0	10	0.318	25.3	3256	0.0126	20.04	
450	64.0	10	0.356	28.9	3648	0.0124	22.01	0.10
500	63.0	10	0.397	31.6	4070	0.0126	25.05	0.14
300	57.0	10	0.230	17.1	2351	0.0133	15.40	
350	61.0	10	0.297	21.4	3045	0.0138	20.69	
400	64.0	10	0.328	25.7	3356	0.0127	20.97	
300	83.0	5	0.292	25.0	5989	0.0117	34.32	
300	56.0	15	0.255	16.8	1741	0.0151	12.90	
300	55.0	10	0.239	16.5	2442	0.0144	17.22	
350	58.0	10	0.215	20.4	2200	0.0105	11.36	
300	60.0	5	0.263	18.0	5386	0.0145	38.40	
300	71.0	5	0.271	21.4	5547	0.0127	34.42	0.14

9 References

1. *Burkhart, J.A., "Segmented Anode, CO_2-H_2 Performance and Hollow Cathode Erosion Tests on a Low Power MPD Arc Thruster," AIAA Paper 69-242 (March 1969).*

2. *Esker, D.W., Kroutil, J.C., and Checkley, R.J., "Radiation Cooled MPD Arc Thruster," McDonnell Douglas Report H296, NASA CR 72557 (June 1969).*

3. *Jones, R.E., and Walker, E.L., "Status of Large Vacuum Facility Tests of MPD Arc Thrusters," NASA TMX-52155, (January 1966).*

4. *Connolly, D.J., and Sovie, R.J., "The Effect of Background Pressure and Magnetic Field Shape on MPD Thruster Performance," AIAA Paper 69-243 (March 1969).*

5. *Fradkin, D.B., Blackstock, A.W., Roehling, D.J., Stratton, T.F., Williams, M., and Liewer, K.W., "Experiments Using a 25 kW Hollow Cathode Lithium Vapor MPD Arc Jet," AIAA Paper 69-241 (March 1967).*

6. *Hoell, J.M., and Brooks, D.R., "Effects of Propellant Injection Through Electrodes on Potential Distribution in an MPD Arc," AIAA Paper 67-49 (March 1967).*

10 Distribution list

NASA Lewis Research Center (1)
21000 Brookpark Road
Attention: Research Support Procurement Section,
MS 500-312

NASA Lewis Research Center (1)
21000 Brookpark Road
Attention: Technology Utilization Office, MS 3-19

NASA Lewis Research Center (1)
21000 Brookpark Road
Attention: Technical Information Division, MS 5-5

NASA Lewis Research Center (2)
21000 Brookpark Road
Attention: Library, MS 60-3

NASA Lewis Research Center (1)
21000 Brookpark Road
Attention: Report Control Office, MS 5-5

NASA Lewis Research Center (1)
21000 Brookpark Road
Attention: C.C. Conger, MS 54-1

NASA Lewis Research Center (1)
21000 Brookpark Road
Attention: H. Hunczak, MS 54-3

NASA Lewis Research Center (1)
21000 Brookpark Road
Attention: S. Domitz, MS 54-3

NASA Lewis Research Center (1)
21000 Brookpark Road
Attention: E.W. Otto, MS 54-1

NASA Lewis Research Center (1)
21000 Brookpark Road
Attention: W. Moeckel, MS 301-1

NASA Lewis Research Center (1)
21000 Brookpark Road
Attention: G. Seikel, MS 301-2

NASA Lewis Research Center (62)
21000 Brookpark Road
Attention: D. Connolly, MS 301-2

National Aeronautics and Space Administration (1)
Washington, D.C. 20546
Attention: RNT/James Lazar

National Aeronautics and Space Administration (1)
Washington, D.C. 20546
Attention: RRP/Dr. K.H. Thom

National Aeronautics and Space Administration (1)
Washington, D.C. 20546
Attention: RNT/J. Mullin

NASA Scientific and Technical Information Facility (6)
P.O. Box 33
College Park, Maryland 20740
Attention: NASA Representative RQT-2448

NASA Marshall Space Flight Center (1)
Huntsville, Alabama 35812
Attention: Ernest Stuhlinger (M-RP-DIR)

NASA Langley Research Center (1)
Langley Field Station
Hampton, Virginia 23365
Attention: M. Ellis

Research and Technology Division (1)
Wright-Patterson AFB, Ohio 45433
Attention: AFAPL (APIE-1)/David Fritts

United States Air Force (1)
Office of Scientific Research
Washington, D.C. 20025
Attention: M. Slawsky

Case Institute of Technology (1)
10900 Euclid Avenue
Cleveland, Ohio 44106
Attention: Dr. Eli Reshotko

Princeton University (1)
Forrestal Research Center
Princeton, New Jersey 08540
Attention: Dr. R.G. Jahn

Aerospace Corporation (1)
P.O. Box 95085
Los Angeles, California 90045
Attention: Library/Technical Documents Group

Giannini Scientific Corporation (1)
3839 South Main Street
Santa Ana, California 92702
Attention: Adriano Ducati

NASA Marshall Space Flight Center (1)
Huntsville, Alabama 35812
Attention: G. Heller

Air Force Weapons Laboratory (1)
Kirtland AFB, New Mexico 87417
Attention: WLPC/Capt. C.F. Ellis

Case Institute of Technology (1)
10900 Euclid Avenue
Cleveland, Ohio 44106
Attention: Professor O.K. Mawardi

Catholic University of America (1)
Department of Space Sciences and Applied Physics
Washington, D.C. 20017
Attention: Professor C.C. Chang

University of Minnesota (1)
Department of Mechanical Engineering
Heat Transfer Laboratory
Minneapolis, Minnesota 55435
Attention: Dr. E. Pfender

Avco Everett Research Laboratory (1)
A Division of Avco Corporation
2385 Revere Beach Parkway
Attention: Dr. R.M. Patrick

Jet Propulsion Laboratory (1)
4800 Oak Grove Drive
Pasadena, California 91103
Attention: N.M. Nerheim

Los Alamos Scientific Laboratories (1)
P.O. Box 1663
Los Alamos, New Mexico 87544
Attention: Dr. Stratton

Westinghouse Astronuclear Laboratories (1)
Electric Propulsion Laboratories
Pittsburgh, Pennsylvania 15234

Avco Corporation (1)
Research and Advanced Development Division
201 Lowell Street
Wilmington, Massachusetts 01887
Attention: S. Bennett

Avco Corporation (1)
Research and Advanced Development Division
201 Lowell Street
Wilmington, Massachusetts 01887
Attention: A.C. Malliaris

University of California, San Diego (1)
La Jolla, California 92037
Attention: Professor R. Lovberg

TRW Systems Incorporated (1)
One Space Park
Redondo Beach, California 90278
Attention: Dr. J.M. Sellen

Ion Physics Department (1)
Hughes Research Laboratories
301 Malibu Canyon Road
Malibu, California
Attention: Jerome H. Molitar

Department of Mechanical and Aerospace Engineering (1)
North Carolina State University
Raleigh, North Carolina 27607
Attention: Professor H.A. Hassan

Institut fur Plasmadynamic (1)
Deutsche Versuchsanstalt fur
Luft-und Raumfahrt e.v.
West Germany
Attention: Dr. W.L. Bohn

Comsat Laboratories (1)
Positioning and Orientation Branch
Washington, D.C.
Attention: Bernard Free

NASA Mission Analysis Division OART (1)
Moffett Field, California 94035
Attention: Dr. Frederico G. Cassal

NASA Goddard Space Flight Center (1)
Systems Analysis and Electric Propulsion Section
Greenbelt, Maryland 20771
Attention: Mr. William C. Isley

Jet Propulsion Laboratory (1)
4800 Oak Grove Drive
Pasadena, California 91109
Attention: Mr. Daniel J. Kerrisk

NASA Marshall Space Flight Center (1)
Nuclear and Plasma Physics Branch
Huntsville, Alabama 35812
Attention: Mr. Russell D. Shelton

Princeton University (1)
Guggenheim Laboratories
James Forrestal Campus
Princeton, Jew Jersey
Attention: Woldemar J. von Jaskowsky

TRW Systems Incorporated (1)
One Space Park
Redondo Beach, California 90278
Attention: Dr. C.L. Dailey

Institut fuer Plasma-dynamik (1)
Deutsche Versuchsanstalt fuer Luft-und Raumfahrt,
Stuttgart, German Federal Republic
West Germany
Attention: G. Kruelle

Institute for Jet Propulsion (1)
Deutsche Farschungsanstalt fur
Luft-und Raumfahrt
DFL, Braunschwieg
West Germany
Attention: Gunther F. Au
Head, Electric Propulsion Section

Electro-Optical Systems Incorporated (1)
Electric Propulsion Applications Office
306 North Halsted Street
Pasadena, California 91109
Attention: Mr. Ronald S.H. Toms

Republic Aviation (1)
Farmingdale, Long Island, New York 11735
Attention: Mr. William J. Guman
Head, Electric Propulsion Power
Conversion Division

Electrogasdynamics Branch (FDM) (1)
Mr. J. Doyle
Flight Dynamics Laboratory
Wright-Patterson AFB, Ohio 45433

Plasmadynamics and Laser Branch (1)
Dr. R. Hess
NASA Langley Research Center
Hampton, Virginia 23365

Magnetogasdynamics Branch (1)
Dr. H. Stine
NASA Ames Research Center
Moffett Field, California 94035

Arnold Engineering Development Center (1)
Mr. D. Eastman (AEGT)
Arnold Air Force Station
Tullahoma, Tennessee

Department of Mechanical and Electrical Engineering (1)
Dr. D. Benenson
State University of New York at Buffalo
Buffalo, New York

Mechanical Engineering Department (1)
Dr. C. Cremers
University of Kentucky
Lexington, Kentucky

Mechanical Engineering Department (1)
Dr. J. Fay
Massachusetts Institute of Technology
Cambridge, Massachusetts

School of Mechanical Engineering (1)
Dr. F.P. Incopera
Purdue University
LaFayette, Indiana

Department of Aero-Astronautics (1)
Dr. R.S. Devoto
Stanford University
Stanford, California

Department of Aerospace Engineering (1)
Dr. R.L. Phillips
University of Michigan
Ann Arbor, Michigan

Space Physics Division (1)
Mr. J. Morris
Avco Corporation
Wilmington, Massachusetts

AVCO (1)
Everett Research Laboratory
Dr. J. Klepeis
Everett, Massachusetts

Arc Heater and Lamp Department (1)
Electro Optical Systems, Inc.
Mr. R. Richter
Pasadena, California

Westinghouse Research Laboratory (1)
Dr. Emmerich
Pittsburgh, Pennsylvania

Greyrad Corporation (1)
Dr. J. Grey
Twelve Station Drive
Princeton, New Jersey

Mr. E. Soehngen, Project Officer (1)
Director, Thermomechanics Research Laboratory
Aerospace Research Laboratory
Wright-Patterson AFB, Ohio 45433

AFSC European Field Office (AFSC/EFO) (1)
Box 410
APO New York 09080

Bundesminister der Verteidigung (1)
Unterabteilung T II
53 Bonn 1
Postfach 161

Institut fuer Plasmadynamik der Deutschen (1)
Versuchsanstalt f. Luft-und Raumfahrt e.v.
Dr. Th. Peters
Stuttgart, Vaihingen

Institut fuer Energiewandlung und Elektrische Antriebe (1)
DFVLR
Stuttgart Vaihingen
Pfaffenwaldring 38-40

Institut fuer Tech. Physik Kernforschungsanlage (1)
Dr. T. Bohn
Juelich

Institut fuer Elektrophysik (1)
Prof. Dr. H. Maecker
Techn. Hochschule Muenchen

Institut fuer Raumfahrt (1)
Prof. Dr. G. Ecker
Universitaet Bochum

I Physikalisches Institut (1)
Prof. Dr. H. Uhlenbusch
Technische Hockschule Aachen
Templergraben 55

Dr. Karl-Heinz Gronau, Project Officer (1)
Bundesministerium der Verteidigung
Referat T II 5
53 Bonn 1
Schliessfach 161

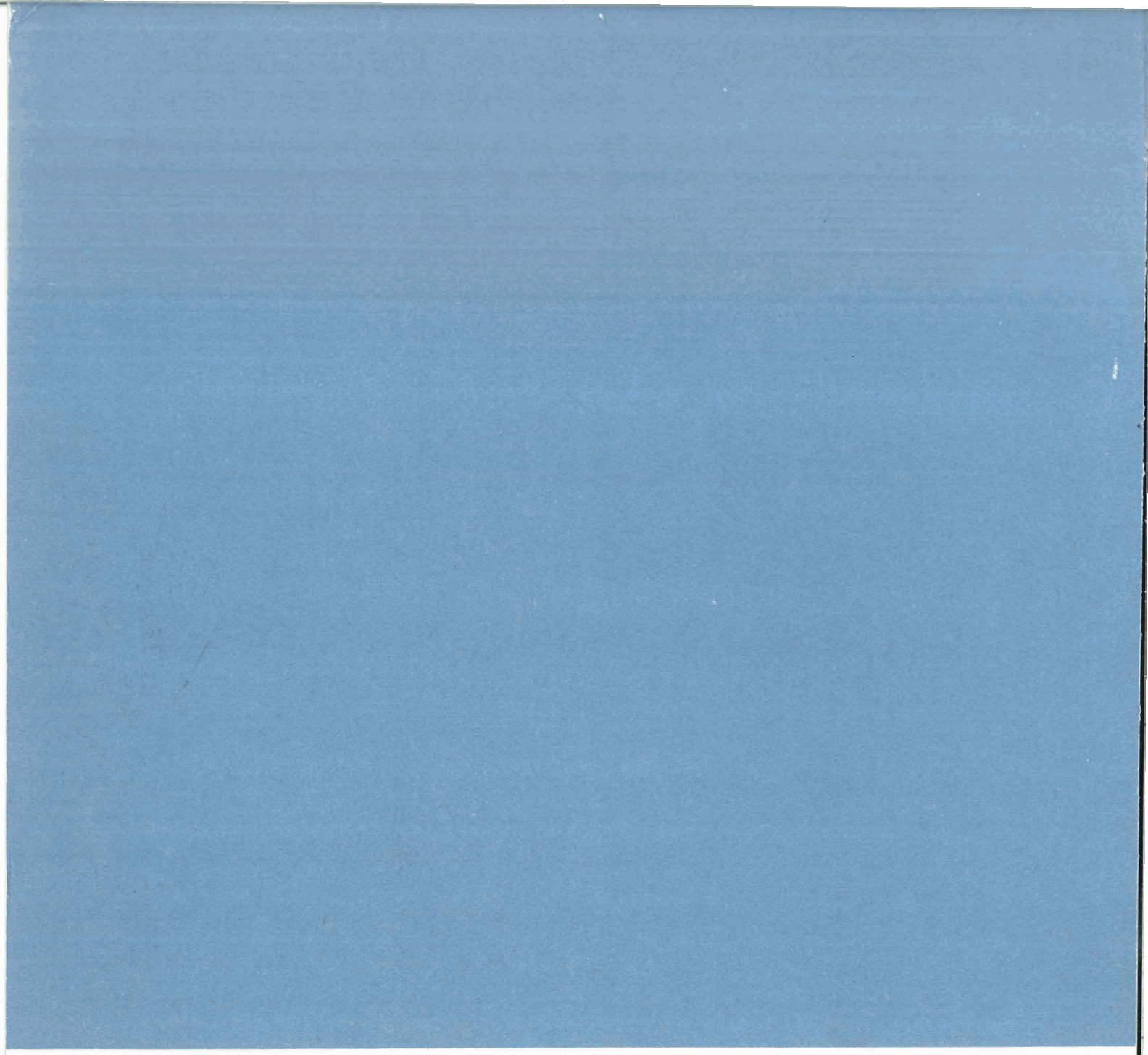

MCDONNELL DOUGLAS RESEARCH LABORATORIES

Saint Louis, Missouri 63166